MATHEMATICAL AND COMPUTATIONAL MODELLING OF CHEMICAL HEAT PUMPS

A THESIS SUBMITTED TO
THE GRADUATE SCHOOL OF NATURAL AND APPLIED SCIENCES
OF
MIDDLE EAST TECHNICAL UNIVERSITY

BY

TALHA GÜNEŞ

IN PARTIAL FULFILLMENT OF THE REQUIREMENTS
FOR
THE DEGREE OF MASTER OF SCIENCE
IN
CHEMICAL ENGINEERING

NOVEMBER 2018

Approval of the thesis:

MATHEMATICAL AND COMPUTATIONAL MODELLING OF CHEMICAL HEAT PUMPS

submitted by **TALHA GÜNEŞ** in partial fulfillment of the requirements for the degree of **Master of Science in Chemical Engineering Department, Middle East Technical University** by,

Prof. Dr. Halil Kalıpçılar
Dean, Graduate School of **Natural and Applied Sciences** _____

Prof. Dr. Pınar Çalık
Head of Department, **Chemical Engineering** _____

Prof. Dr. Yusuf Uludağ
Supervisor, **Chemical Engineering, METU** _____

Prof. Dr. Gürkan Karakaş
Co-Supervisor, **Chemical Engineering, METU** _____

Examining Committee Members:

Prof. Dr. Halil Kalıpçılar
Chemical Engineering Dept., METU _____

Prof. Dr. Yusuf Uludağ
Chemical Engineering Dept., METU _____

Prof. Dr. Gürkan Karakaş
Chemical Engineering Dept., METU _____

Prof. Dr. Nihal Aydoğan
Chemical Engineering Dept., Hacettepe University _____

Assoc. Prof. Dr. Erhan Bat
Chemical Engineering Dept., METU _____

Date: 29.11.2018

I hereby declare that all information in this document has been obtained and presented in accordance with academic rules and ethical conduct. I also declare that, as required by these rules and conduct, I have fully cited and referenced all material and results that are not original to this work.

Name, Surname: Talha Güneş

Signature:

ABSTRACT

MATHEMATICAL AND COMPUTATIONAL MODELLING OF CHEMICAL HEAT PUMPS

Güneş, Talha
Master of Science, Chemical Engineering
Supervisor : Prof. Dr. Yusuf Uludağ
Co-Supervisor : Prof. Dr. Gürkan Karakaş

November 2018, 133 pages

Chemical heat pumps are valuable alternatives to conventional heat pumps when the aim is re-utilizing waste energy that is created from natural or industrial sources. In this study, kinetic data of an activated carbon – ethanol adsorption reactor is modeled and properly implemented into COMSOL Multiphysics software, and the geometry is modified for higher rate of heat transfer with the aim of gaining more performance from the system. On top of that, various cycle times are studied for gaining optimal cooling power from designed reactor bed. The results showed that, providing better heat transfer domain to designed systems drastically increased the efficiency of the bed and although more vapor is adsorbed by extended time period, cooling power value did not expand linearly due to increased operation time.

Keywords: Adsorption heat pump, COMSOL Multiphysics, activated carbon

ÖZ

KİMYASAL ISI POMPALARININ BİLGİSAYAR ORTAMINDA MATEMATİKSEL OLARAK MODELLENMESİ

Güneş, Talha
Yüksek Lisans, Kimya Mühendisliği
Tez Danışmanı : Prof. Dr. Yusuf Uludağ
Ortak Tez Danışmanı : Prof. Dr. Gürkan Karakaş

Kasım 2018, 133 sayfa

Kimyasal ısı pompaları, doğal veya endüstriyel kaynaklardan üretilen atık enerji yeniden kullanılmak istenildiğinde geleneksel olanlara göre değerli alternatiflerdir. Bu çalışmada, aktifleşmiş karbon-etanol adsorsiyon reaktörünün kinetik verileri modellenmiş ve COMSOL Multiphysics yazılımına tümüyle uygulanmıştır. Ardından, daha yüksek ısı transferi oranını sağlamak ve bu yolla sistemden daha yüksek performans elde etmek amacı ile geometri çeşitli yollarla modifiye edilmiştir. Bunun üzerine, tasarlanan reaktör yatağından optimum güç üretimini elde etmek için yatak, çeşitli döngü süreleri ile çalıştırılmaktadır. Elde edilen sonuçlar, tasarlanan sistemlere daha iyi bir ısı transfer alanının sağlanmasının yatağın verimliliğini önemli ölçüde arttırdığını ve daha uzun süre ile beraber daha fazla buharın adsorbe olmasına rağmen, güç üretim değerinin, artan çalışma süresi nedeniyle doğrusal olarak ilerlemediğini göstermiştir.

Anahtar Kelimeler: Adsorsiyon ısı pompası, COMSOL Multiphysics, aktifleşmiş karbon

Dedicated to My Family…

ACKNOWLEDGMENTS

I am particularly grateful for the guidance given by Prof. Dr. Yusuf Uludağ through my entire M.Sc. journey for his advice of proper ways of doing a research, corrections of my mistakes and also for his lead to new and innovative areas in life as well as in the study.

Assistance provided by Prof. Dr. Gürkan Karakaş was greatly appreciated for having constructive recommendations on this project and filling the study with fresh ideas.

I wish to acknowledge the help provided by Arda Yılmaz, Aziz Doğan İlgün and Sohrab Nikazar on the field of finite element analysis and post-processing.

I would also like to extend my thanks to M.Sc. students of METU for keeping me alive and intrigued to academic advancement, as well as Satı Ömercan for her kind services.

Finally, I wish to thank my parents for their support and encouragement throughout my study. Especially my father, who always boosted my morale in times of need and pushed me into completing the project with his precious suggestions.

TABLE OF CONTENTS

LIST OF TABLES

TABLES

LIST OF FIGURES

FIGURES

CHAPTER 1

INTRODUCTION

Cooling processes have always been an important case for the protection of widely varying contents both in domestic use and in industrial environments. Currently, there are numerous methods for cooling or refrigeration, whereas compression heat pumping is the most used one commercially. Regarding the heat pump operating principle, cooling technologies can apply several different physical phenomena for heat transfer from the hot zone to the cold zone, depending on the type of the system.

Compression heat pumps use the energy change arising during phase transformation due to compression or expansion of the material, whereas adsorption heat pumps operate in a completely different method compared to the compression heat pumps, in that they use the adsorption or desorption of the vapor by the adsorbent.

The vacuum effect originating from adsorption cause some stored liquid on the other side to boil, and the heat input for boiling provides the cooling effect. There are also other heat pump systems operating through utilization of a chemical reaction, however, there are limited researches on these types of systems, which are much more complex and more difficult to produce than adsorption heat pumps. In addition, they usually use catalysis and in various approaches, they utilize compressors or other similar equipment (Kawasaki, Kanzawa, & Watanabe, 1998), consequently, here we will not be dealing with such systems within the scope of this research project.

Independent of the preferred method of cooling, a certain amount of energy is required to operate the heat pump, since the heat pump floats the heat from the cold

to the hot zone, which is contrary to the thermodynamics. When the heat pump method or type changes the type of input power also changes.

For a compression heat pump, the operating energy is the mechanical energy provided by the compressor, and for an adsorption heat pump, the work entering the system is in the form of heat energy used for the desorption of the adsorbed material from the adsorbent bed, so no mechanical energy is required. However, regardless of what kind of energy is utilized, heat pumps necessitate additional energy to work.

The performance of heat pumps is measured by the coefficient of performance (COP), defined as the ratio of the useful heat transfer performed by the heat pump to the input energy supplied to the system. COP values change between 2 to 3 for compression heat pumps, whereas it is less than 1 for most of the alternative approaches. These values indicate that the necessary energy for a heat pump is considerably high, whereas it is much higher for the adsorption heat pumps. However, the freedom adsorption heat pumps offer in choosing different sources of energy overcomes the benefit the lower COP values bring. For example, if the system is meeting the requirements for desorption at about 120 ° C; sunlight, one of the most common renewables and free energy sources, might become a possible alternative to the system as an energy source. Similarly, energy sources like exhaust gases which are not originally free but practically have no cost since they are normally disposed of can be considered.

The COP values of adsorption heat pumps are lower compared to the commercial compression type heat pumps. Considering feasibility the comparison of adsorption pumps and compression heat pumps should not be performed based on COP. On the contrary, adsorption heat pumps should be considered as a means for the use waste energy from various operations. But this statement does not necessarily imply that the system will be feasible and beneficent just because it utilizes a free energy resource, discarding other performance criteria.

In any system, various factors such as initial cost, operating and maintenance costs, and equipment size are also important along with the cost of operating power. The

results obtained by comparing all the above criteria should be as satisfactory as possible in order to be able to utilize adsorption heat pumps in industrial practice and commercial markets. Although COP is not considered among the most effective criteria for the chemical heat pumps it can influence a few of the other criteria. For instance; for a heat pump to be operated with solar energy a solar collector area to supply the necessary solar energy for the operation will be required, such that the necessary area of solar collectors would decrease with the increasing value of COP. Consequently, both the cost of the system as well as the necessary area which will be occupied by the system will decrease. Although COP value is not a predominant criterion for an adsorption pump, when considering the size and initial cost of the equipment, the COP value should be kept as high as possible. On the other hand, financial evaluation cannot be the single element determining the use of the heat pump, restrictions on the use of the system are also important in terms of the availability of the system. Attempts to increase the COP value, which increase the minimum temperatures achieved by the system or cause the system to necessitate higher desorption temperatures, limits the practical usability of the system. For instance, adsorption chillers, which do not refrigerate but just cool, generally have higher COP values contrasted with adsorption refrigerators (L. W. Wang, Wang, Wu, Wang, & Wang, 2004). This limits the range of the study, so there is no significant development for technology with such an approach (L. W. Wang et al., 2004).

On the other hand, systems using chemisorption have higher COP values compared to physisorption systems, but in this method, higher desorption temperatures preventing the use of free energy sources such as sunlight are required (L. W. Wang et al., 2004). Considering every single one of these criteria, the utilization of adsorption heat pumps requires an alternative method to get an ideal COP, without trading off from the working range flexibility or the probability to utilize a free heat resource. The operating range of a heat pump is usually determined by the boundary temperature at which cooling or heating is performed. Heat pumps are generally used to maintain temperatures below the freezing temperature of water, which usually

requires cooling below 0 ° C. Here, cooling should be provided by the available free heat source, which usually corresponds to the sunlight the most common and available renewable resource. It is no wonder that the daily needs and practices influence the scientific studies, as expected systems that can work up to freezing temperatures by taking advantage of sunlight have been studied in the literature many times. Such systems usually utilize solar collector plates and activated carbon hydrocarbon pair heat exchangers. Additionally, there are also some other works considering utilization of different heat resources like exhaust heat, but they have been limited to experimental systems built for performance capacity measurements for tested operating conditions. However, if we chose the correct adsorbent, calculate and design the system geometry, especially the adsorbent bed, appropriately, then it is possible to catch a performance improvement for the adsorption heat pump. Actually, there are several studies on the selection of the adsorption pair and on how the material pair affects the performance of the heat pumps. There are few studies on modeling system geometry, but most of them are limited to mass and macroscopic scale studies that use not only the critical error range but also a few simplified models that also limit the applicability of the model to different geometries.

When the concept of the chemical heat pump is considered as a whole, under the light of the above-mentioned problems and requirements; in order to develop flexible and more useful systems with high COP, it is necessary to model with the necessary amount of precision in accordance with the wide system parameters. This raises the need for reliable modeling tools that can successfully predict the behavior of systems of different sizes. This modeling approach should also include the physical adsorption data required for the selected adsorption pair; the main focal point of this study is this type of modeling approach.

CHAPTER 2

LITERATURE REVIEW

Chemical heat pumps and associated cooling processes have been an important field of study and research for many scientists for long years. Commercial applications have generally used the compression heat pumping method, however; scientific works tried the utilization of some other heat pumping methods like compression, chemical reaction, and adsorption. Indeed, chemical heat pumps utilize reversible chemical reactions. This approach has not gained wide attention; there are only a vast number of studies on the subject matter. Kawasaki et al. (1998) are one of these; here the researchers have studied a chemical heat pump utilizing paraldehyde de-polymerization which yielded a cooling rate of 10 kW per unit catalyst weight. The process was based on the application of a high-pressure system continuously polymerizing and depolymerizing a par-aldehyde solution yielding heat which was used in heat transformation, where the forward and reverse reaction balance was supplied with the use of a catalyst (Kawasaki et al., 1998). In 2004 Wang and his colleagues worked on a CaCl2 ammonia heat pump, which could be an example for both adsorption and chemical heat pumps (L. W. Wang et al., 2004).

Adsorption cooling recently has received more attention in terms of research compared to chemical reaction heat pumps. According to researchers, these systems appear to be useful because they necessitate low grades of heat energy which offers the possibility of using cost-free resources like sunlight as well as exhaust gasses. They also indicate that such systems present lower COP values than the commercial systems so that the researches are directed towards system performance and optimization. Although these studies are mostly concerned with the results obtained

using different experimental systems, there are also articles comparing different adsorption material pairs; even articles on modeling such systems are not rare.

Researchers have performed many experiments with adsorption heat pumps in the last decades and published their findings of performance. The source of energy in most of these experimental studies has been the sunlight due to being cost-free as well as having almost no environmentally harmful side effects; however, there are also additional studies on systems utilizing different resources like exhaust gasses. Li and Sumathy's 1999 study focused on a solar-powered ice maker with a pair of activated carbon and methanol using a simple flat ice picker (Li & Sumathy, 1999). Trying three different activated carbon brands produced in China whose performances were measured and compared, they have decided on the use of CHK-3 activated carbon. Using a 0.92 m^2 solar collector area, the researchers could obtain 4-5 kg of ice per day observing COP values between 0.1 and 0.2. Plotting COP versus various system operational parameters including the temperature of evaporation, they concluded that the COP could become better for evaporation at 0 ^oC compared to evaporation below 0 ^oC. According to their results, the optimum desorption temperature with the highest COP for methanol-activated carbon pair was 110 ^oC. They state that although higher desorption temperatures rise the system capacity, the COP value is decreased. Working on adsorption heat pumps, Anyanwu et al. created an experimental model in Nigeria using a system having a plate-type solar collector with a 1.2 m^2 solar collector area and 60 kg of activated carbon operating utilizing a single adsorption bed (Anyanwu & Ezekwe, 2003). This experimental system yielded 200 kJ of cooling performance per day with a COP value of about 0.08 to 0.1. The solar intensity during the experiments has been noted as around 16 MJ/m^2.

Dous and colleagues (Douss, Meunier, & Sun, 1988) studied heat pump with two adsorption cycles making use of a NaX zeolite and water pair. Focusing on both heating and cooling performances they have obtained a COP value of 1.83 for heating. The 2001 dated research of Wang and colleges examined adsorption heat pumps both as freezers as well as chillers (R. . Wang, Wu, Xu, & Wang, 2001). In both freezers and chillers, they have utilized activated carbon-methanol pair for

adsorption where they have used adsorbent beds with bigger volumes and considerably fewer amounts of activated carbon. Changing the time of cycles they have looked for optimum values. The COP values have been found to be 0.15-0.2 and up to 0.4 for freezing and chilling operations respectively. Theoretically, they claimed that in the freezing system it is possible to get ice up to 2.6 kg per kg of adsorbent per day and to achieve a heat of up to 300 W per kg for the cooling system.

Since the COP in adsorption heat pumps is often very low, studies of adsorption heat pumps are generally focused on increasing the COP using different parameters that can be optimized for performance, among which the most commonly worked parameter, is the modification of the adsorption pair. One of these studies was the work of Wang and his friends in 2004 (L. W. Wang et al., 2004); in this study, the performances of the different adsorption pairs to be used in the ice makers for the fishing boats were examined and three different adsorption pairs; activated carbon-methanol, $CaCl_2$ - ammonia and composite adsorbent – methanol were comparatively examined. For the determination of the performance of activated carbon-methanol system, a model system was formed, and adsorption data was used to predict the performance of the adsorption pair as a heat pump for the other pairs. $CaCl_2$-ammonia pair yielded the highest cooling power; around 20 kW, but on the other hand; it was noticed that utilization of chemical adsorbents necessitates higher amounts of energy, and this amount of energy is not possible to be driven from renewable and cost-free resources like sunlight. This means that obtaining a high cooling power density and COP brings about the need for high-temperature resources like exhaust gasses (Ziegler, 1971).

In 2008 San and Lin examined the use of three different adsorption pairs utilized in adsorption heat pumps (San & Lin, 2008). In this study, San and Lin used a four-bed adsorber heat exchanger applying a solid side residence model and compared activated carbon-methanol, zeolite - water and 13X molecular sieve-water adsorption pair alternatives. Among the three couples, the activated carbon-methanol pair showed the highest efficiency and specific cooling power results, where 13Xsieve-

water pair displayed very close results compared to the winning pair. Also, the heat effects in the adsorbent bed during the process were investigated and it was found that neglecting the effect of the increase in temperature in the adsorption bed would cause the system performance to be estimated at higher values. Additionally, the researchers have concluded that when the flow rate of adsorbate through the bed increases, the effect of temperature increase on system performance decreases. But increasing the adsorbate flow rate responded positively just up to a certain level, after that point increasing the adsorbate flow rate did not help for increasing thermal conductivity. Along with the above findings, it has been claimed that increased desorption temperature will support system performance and thus increase COP; however, it has been stated that a certain desorption temperature giving the highest COP depending on the type of adsorption pair exists and a further increase in the desorption temperature, will decrease the COP, even though this increases the performance (Ziegler, 1971).

In 2005 dated study of Wang et al. adsorption heat pumps were studied once more comparing different adsorbent adsorbate pairs, namely; activated carbon-methanol, activated carbon-ammonia, and activated carbon-$CaCl_2$ cement composite. In this study, the composite adsorbent showed the best adsorbent performance and when used as a physical adsorbent with methanol, it yielded a 0.125 COP and 32.6 W / kg-adsorbent specific cooling power. On the other hand, when this consolidated adsorbent was used in combination with ammonia in the adsorbent chemical adsorption system, it was reported that the COP increased by 1.8 times to 0.35 and the specific corrosion power reached to 492 W / kg by 14 times (L. W. Wang et al., 2006).

To increase the performance of adsorption heat pumps, many parameters need to be optimized, and one of these parameters is the power of the heat resource. In 2007, Gonzales and Rodrigues worked on an adsorption heat pump using a parabolic solar collector instead of planar one. They have used solar collectors at angles of 45 ° C and 90 ° C. They claimed that they reached COPs of about 0.078 to 0.096 and that they were able to cool the system from 23 ° C to 2 ° C per unit area of 9 kg of the

collector. Consequently, they argued that half angles of the collectors should be optimized for better COP values (González & Rodríguez, 2007). In 2004, Wang and colleagues in their work on ice machines for fishing boats suggested that the engine's exhaust gas be used as the heat source in the system (L. W. Wang et al., 2004). The proposed system was able to use chemical adsorbents such as CaCl2 and thus had higher COP values and cooling power than physical adsorption systems (Ziegler, 1971).

In order to optimize the performance of the adsorption heat pump, although the selection of the adsorption pair is the first and basic decision, the design of the adsorption bed is also important, whereas the design of a system requires adequate and accurate modeling to predict the results obtainable from particular geometries. In 2007, Anyanwu and Oquege reviewed the interim analysis and performance estimates of the adsorption solar refrigerator. They utilized a test system with a 1.2 m^2 solar collector area and compared the results of the temporary model with the experimental data. In the study, shell type microscopic energy balance was used for the adsorbent bed and the temperature profile was modeled. The system used activated carbon and methanol. Anyanwu and Oquege claimed that they predicted the required temperatures at some acceptable error range, 5%, and 9% error intervals, and estimated the COP. In addition, they have drawn the heat histogram of the system during the cooling and regeneration cycles and modeled the surfaces of the system temperature as well as the temperature changes in the cooling water with respect to time (Anyanwu & Ogueke, 2005).

In 1998, Dous et al. in their research with two adsorption cycles using the NaX zeolite-water pair, modeled the adsorption heat pump as what they termed the white box, where they have taken the heat and mass transfer restrictions and inner structure was taken into account (Douss et al., 1988). With the correct design and modeling of the system, they claimed that such systems can have valuable COP values that enable them to have better COPs than compression pumps (Ziegler, 1971).

2002 dated study of Miltkau and Dawout examined the adsorption and heat transfer effects on the adsorption and desorption processes for an adsorption heat pump. Their main concentration point was the zeolite-water adsorption pair. The model was based on discrete methods helped by package programs, and one dimensional. The Knudsen diffusion theory for diffusion coefficient, the ideal gas law for gas densities, and the general mixture rules for liquid uptake and the density of the zeolite were utilized for modeling. Consequently, Miltkau and Dawout draw the temperature profiles versus position and time for zeolite layers in the adsorber bed (Miltkau & Dawoud, 2002).

One of the most important disadvantages and the most undesirable behavior of adsorption heat pumps is the inexorable non-continuous operation. Some researchers have suggested systems that can work almost continuously. In 2006, San examined the performance analysis of a multi-bed adsorption heat pump using a solid side residence model. Unlike many other studies, San proposed a four-bed heat pump in this study and claimed that using four beds at different stages would cause almost continuous operation. Here San's adsorption pair was activated carbon-methanol pair. With the help of a mathematical model, San estimated the system performance with respect to different variables like heat and mass transfer resistances of the system. According to the findings of the self-developed mathematical model San stated that increased cycle time would increase the COP value but this increase would be significant only up to 10 minutes. Additionally, San concluded that lowering the temperature inside the bed would bring about better COP values, which also could be obtained by reducing the grain size of the active carbon similarly. The evaporation temperature was found to be directly proportional to COP value which was also found to be directly proportional to the degree of heat transfer. Finally, as the regeneration temperature increases, COP was found to rise up to 100 ° C reaching a maximum value at this point (San, 2006). In 1998, Dous and colleagues proposed a two-bed system as a system with two-cycle rotation, not just as two different systems operating in opposite phases. In this way, they claimed that they

achieved a system with a COP of 1.56, higher than 1.38, which can only be achieved by a single-stage heat pump, as well as a longer-lasting system (Douss et al., 1988).

Although not only required for heat pumps, studies on adsorption processes for activated carbon and organic liquids are important and may help in designing better adsorption heat pumps. For example, Menard and Mazet in 2005 focused on the adsorption behavior of active carbon for CO_2, particularly the effect of temperature changes, the carbon capacity, and the effect of the adsorption process on temperature. Additionally, in their work, they developed the graph of the heat profile within the CO2 adsorbing activated carbon bed. Menard and Mazet, who studied both the adsorption capacity and the temperature profile of the effect of the monolithic addition of active carbon, have found that the addition of high conductive materials increases the thermal conductivity and overall performance of the bed by comparing the added activated carbon with ordinary granular carbon. In their next work, the researchers have focused on the regeneration process, which takes the effect of conductivity on the total duration of regeneration and its effect on efficiency into account(Menard, Py, & Mazet, 2005).

In recent years, researchers focused more on modeling tools to compose better systems. For example, TeGrotenhuis et al. studied on simplified lumped parameter model in detailed finite element analysis, where they simulated multi-bed adsorption heat pump in 2012. In their simulated model, they transferred heat from beds that are being cooled to beds being heated. By using this method with ammonia-carbon pair, they attained the COP value of 1.24 (TeGrotenhuis, Humble, & Sweeney, 2012).

Another model derived by C.Y.Tso in year 2012 utilized a composite adsorbent of activated carbon for the purpuse of achieving better heat and mass transfer. In their model, the reactor bed has reached a COP value of 0.65 where the source temperature was 85 °C and the target temperature was 30°C and 14°C in turn. The optimum cycle time is for the best efficiency found as 360 seconds (Tso, Chao, & Fu, 2012).

In 2012 Onur et Al. derived the adsorption-desorption rate expression from experimental data of their activated carbon – ethanol pair, and by using this data, they created their own model with different bed sizes with the purpose of increasing maximum adsorption capacity. They also worked on varying cycle times to find optimum COP and cooling power values.The COP values they found, varied from 0.49 to 0.65 depending on both cycle time and geometry (Yurtsever, Karakas, & Uludag, 2013).

In order to increase overall thermal performance, in 2017, Askany et Al used metallic additives on their reactor bed for purpose of having high thermal conductivity values of reactor bed instead of altering geometry. In their findings, they discovered that the cycle time can be reduced significantly which would result in high work generation. In short, specific cooling power is increased by 100% by adding 30% weight of metallic additives (Askalany, Henninger, Ghazy, & Saha, 2017).

In 2016, Chekirou et Al added a heat recovery cycle to activated carbon-methanol pair in a basic adsorption system simulation. They found out that in the analyzed system, COP has reached 0.483 without added heat recovery cycle and 0.682 with added heat recovery cycle. They also pointed out that these values were strongly dependent on operating temperatures which was 125 °C in their case (Chekirou, Boukheit, & Karaali, 2016).

Jribi et Al. Constructed a CFD simulation of ethanol-activated carbon pair by using different adsorption rate models in year 2016. In fickian diffusion based model that they built, the simulation didn't converge and in their Isothermal linear driving force based adsorption kinetics model, it under-estimated the kinetic data. Later, they imported the adsorbent temperature dataset by the purpose of switching to non-isothermal model. Their simulation results matched the obtained experimental ones with uptake value of 0.86 kg adsorbate/kg adsorbent (Jribi et al., 2016).

When we evaluate the studies about adsorption heat pumps, although the COP values cannot be compared with the ones of commercial compression heat pumps,

adsorption heat pumps are a more attractive research topic recently because of environmental issues and sustainable energy necessities. Unfortunately, most of the above-mentioned studies resulted in low COP values and cooling power results indicating the handicaps in using these systems commercially. On the other hand, there are various studies on water-zeolite systems aiming to increase the performance, which has observed COP values up to 0.4. Unfortunately, this choice restricts the use of water only for chilling since temperatures below 0 ° C are not achievable with water. Although the use of chemical adsorbents such as $CaCl_2$ has yielded better results, this method has limitations with respect to the heating sources, moreover, adsorbents such as ammonia are generally toxic (L. W. Wang et al., 2006). Although activated carbon-methanol pair is the most studied couple, methanol can also be limiting safety due to its toxicity potential. For this reason, safer materials with a lower melting point such as ethanol should be recommended, and in order to bring the COP to a significant level, high-precision modeling taking heat and mass transfer limitations into account should be performed.

CHAPTER 3

THEORETICAL BACKGROUND

3.1 Significant Design Concepts

3.1.1 Operation Principles

Heat pumps differ in their internal construction depending on the type that results from different operating principles. Differently from compression heat pumps, adsorption heat pumps use adsorption and desorption in conjunction with the evaporation of the adsorbed liquid by the refrigerant to affect heat transfer. In its simplest form, an adsorption heat pump consists of an adsorption bed, an evaporator and a condenser, three of which are connected by a pipe and emptied so that only the liquid and vapor are absorbed in the system. Schematically, the simplest approach for a chemical heat pump can be seen in Figure 1.

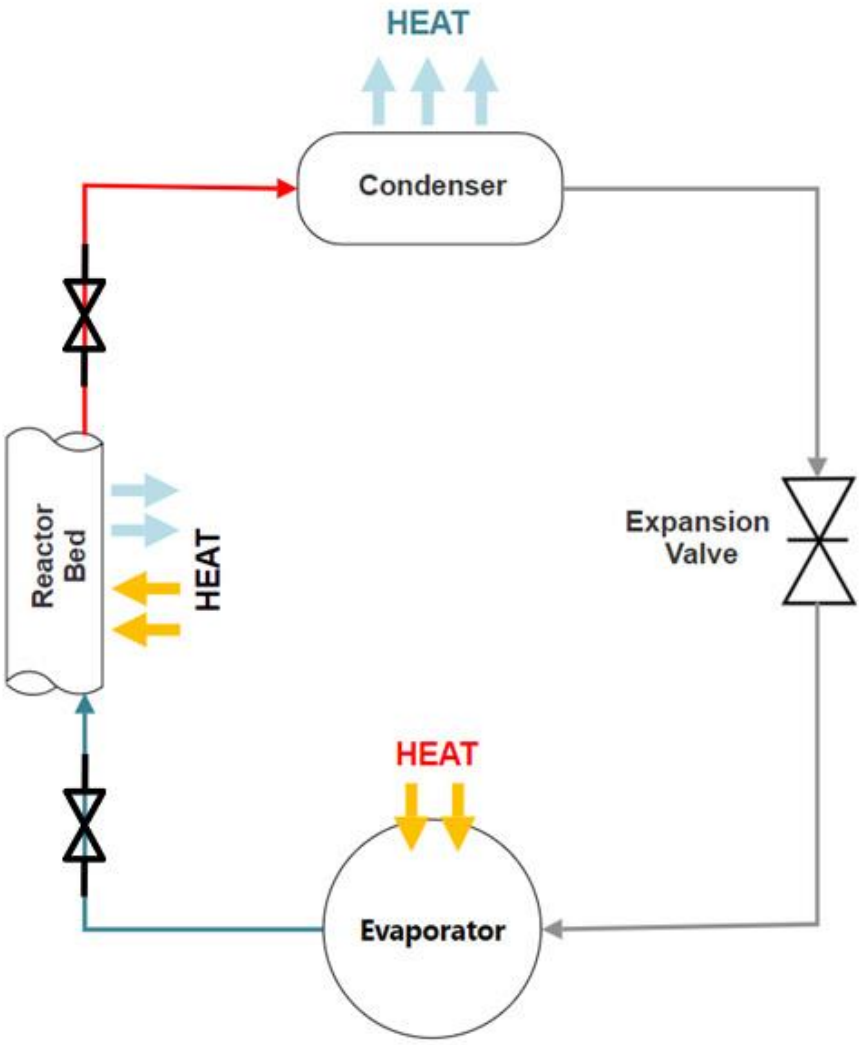

Figure 1. Operation scheme of adsorption heat pump built with single reactor bed. Blue line represents the adsorption step, whereas the red line represents the regeneration step.

The single adsorption bed heat pump shown in Figure 1 operates cyclically in two steps; in the first cycle, the adsorption promoting heat transfer, particularly the cooling effect, is carried out, when the adsorption is complete, the system goes through the second order; no cooling is done here, but instead the regeneration process which prepares the system for the next cycle. If the heat pump is mostly used for actual state cooling, stages can be called cooling and regeneration. Throughout the cooling cycle, the vapor in the system is adsorbed by the adsorbent material,

consequently causing the pressure inside the system to decrease, which in turn boils the liquid in the evaporator due to the low pressure. While the evaporating liquid fills the system, the boiling is continuously supported by the adsorption of the vapor obtained with the adsorbate material. Adsorption is an exothermic reaction; therefore the adsorption bed needs to be cooled continuously as long as this step continues. As the adsorption process goes on and the bed becomes more and more saturated with the adsorbate material reaching a saturation point eventually, the adsorption process stops or slows down. Here the cooling phase is completed and the regeneration starts. During the regeneration process, the system is prepared for the next cycle; the adsorption bed is heated, thereby releasing the adsorbate content. At this step, the steam does not flow directly into the evaporator. Instead, it is cooled and liquefied in the cooler. The liquefied vapor consequently is preserved in the evaporator until the next refrigeration step.

Like almost all systems, there is a need for a continuous, cyclic process also for heat pumps, and the use of two adsorption beds appears to be an effective solution to this problem. In a pair of adsorbed bed heat pumps schematically illustrated in Figure 2, one adsorption bed is in adsorption and the other is in regeneration step within the cycle. When the step is complete, the roles of adsorption beds are reversed. In this way, a continuous cooling is achieved compared to the single adsorption bed system. In addition to the presence of an inactive step in single adsorption bed systems, the adsorption, hence the cooling rate is not constant during the adsorption step since the adsorbed concentration changes slowing down the adsorption process. In other words, the cooling power is higher at the beginning of each step and gradually decreases as the adsorption progresses, i.e.; the bearing approaches the saturation point. It is a problem that a variable cooling rate is observed even in the bed's usable adsorption period. Although the double adsorption heat pump does not have an idle stage, the cooling rate slows towards the end of each step and the cooling power is varying. This problem can be overcome by using multiple adsorption beds and almost continuous heat transfer ratios can be obtained similarly to the applications in compression heat pumps.

A target heat source present in adsorption heat pumps as well as conventional compression heat pumps. This target should be cooled or heated depending on the system through a medium where the heat is disposed off or taken in via an energy input. In a cycle, evaporator is placed where the cooling is wanted and heat is disposed off through a cooler which is open to an environment. Analogous to work input of compression heat pumps, process energy of heating should be supplied in desorption stage and cooling should be done in adsorption stage over adsorption heat pump.

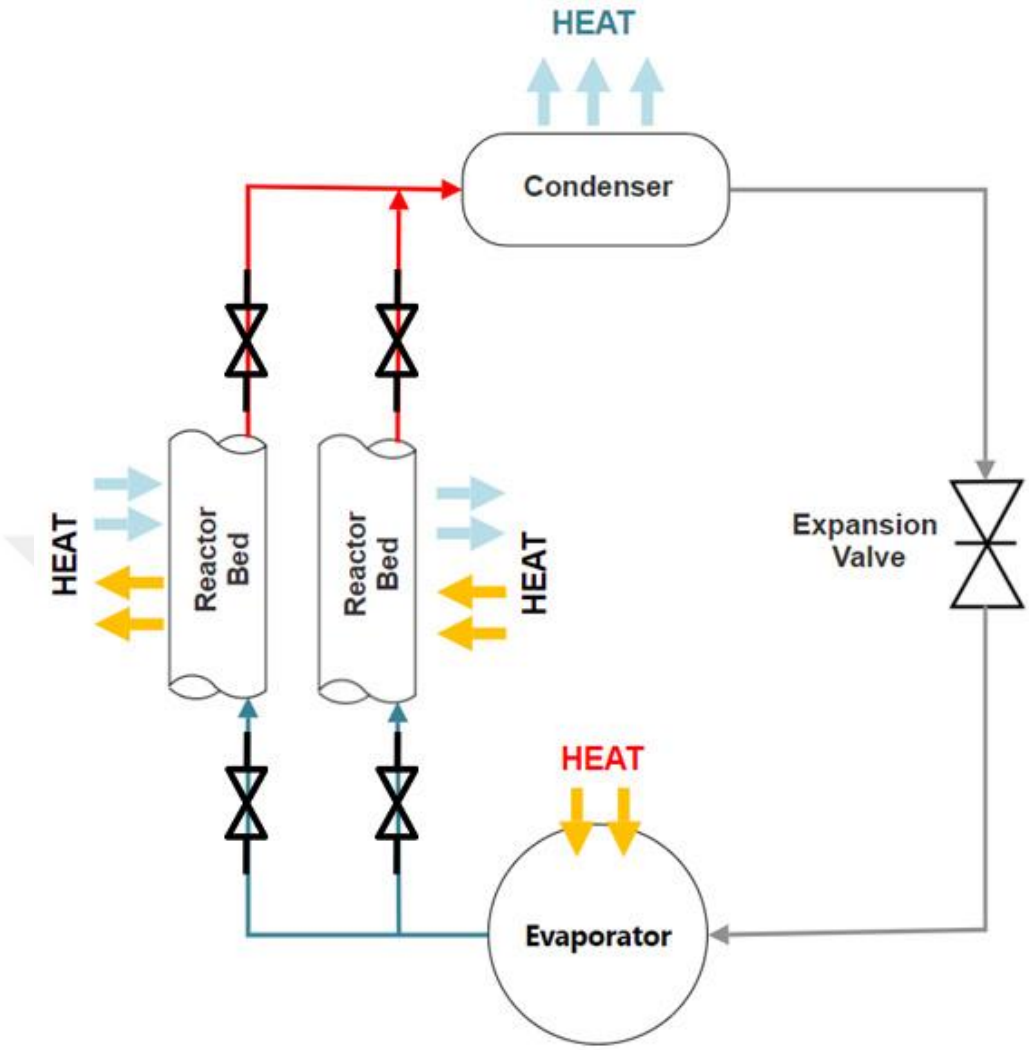

Figure 2. Operation scheme of adsorption heat pump built with double reactor bed. Blue line represents the adsorption step, the red line represents the regeneration step.

In order for an adsorption heat pump to possess the most efficient system performance value, the latent heat of the adsorbate should be kept high to deposit more energy inside before phase change, and the heat of adsorption must be as low as possible for better regeneration of the bed in desorption stage. These two properties are the most important factors for efficiency, but adsorption heat and latent heat are usually similar in degree. Since these two factors are alike, other options should be considered for gaining more COP value.

Other than the adsorption and latent heat of adsorbing materials, there are other factors that are important for the adsorption bed performance. Adsorption or desorption in the adsorption bed is a highly thermal process in which significant quantities of heat must be supplied to the bed during adsorption or heat must be removed from the bed during desorption steps. For this reason, due to the three-dimensional structure of the bed, the heat must be transmitted through the bed during operation leading to the problem of thermal conduction. If there is no proper heat transfer in the adsorbent bed, the temperature inside the bed will not be homogeneous and this will bring about two problems: First, the inhomogeneous temperature profile causes the excessive temperature in the inner regions, adsorbing and adsorbent material might become damaged. Secondly, due to the hot zones in the bed, more heat should be given to the bed, which will reduce the COP due to the increase in the observed desorption heat. Consequently, in order to obtain better system performances, high thermal conductivity adsorbents should be preferred. In order to obtain better conductivity generally non-porous solids should be preferred, however; since adsorption is a surface related phenomenon, adsorbate materials must possess larger surface areas and porous materials should be preferred as adsorbates. Increasing the performance necessitates minimization of the heat transfer resistances without endangering the adsorption capacity, which may be possible by changing the geometry or particle size. In finer particles, as the contact between the particles increases, the thermal conductivity will also increase, but this will also reduce the mass permeability of the medium. Unluckily, the adsorbent permeability is another significant parameter in the design of adsorption bed. If the equation 1 is used the mass transfer resistance or the adsorbent material permeability would not change the value of COP. Poor mass permeability increases the necessary time for adsorption or desorption, but as adsorption or desorption times increase, the cooling over time decreases reducing the system's power. To overcome this specific power loss, larger adsorption beds should be used, which leads to larger systems and higher capital costs.

A successful adsorption heat pump design should maximize both heat and mass transfer. For better mass transfer or high permeability, the particles should not be kept too small; however, this is conflicting with the heat transfer performance. Heat transfer can be enhanced with the help of thermally conductive materials, such as metal fins, without altering the thermal conductivity of the material. This will reduce the total length of the heat path along the adsorbate, which will reduce the thermal resistance and prevent excessive temperature gradients. The bed design includes a decision on the shape and size of the adsorption bed with conductive inputs. To find the optimal shape and size of the bed, the temperature and concentration changes within the bed during adsorption or desorption must be estimated.

The adsorption rate for any possible temperature and concentration in the adsorption bed should also be provided. Due to the temperature, pressure and composition dependent properties and coupled governing heat and mass transfer model equations, it is not possible to use analytical methods to get the solution. Hence, governing differential equations should be solved by numerical methods.

A successful system modeling demands knowledge of the thermo-physical properties of the adsorbent adsorbate couple together with the adsorption capacities and ratios. The heat and mass transfer properties of activated carbon can be found in the literature for a variety of liquids and vapors, but the adsorption data for activated carbon as well as most of the other adsorbents appear in the forms of isotherms and data of capacity, additionally the relations to the rate of adsorption of vapors by activated carbon and other adsorbents are not widely available. This leads to the problem that the adsorption or desorption ratio of the adsorbent should be known with respect to the temperature, the vapor concentration and the degree of saturation of the adsorbent.

3.2 COMSOL

COMSOL Multiphysics is an interactive environment for problem-solving, modeling and simulation. The Model Builder provides an integrated desktop environment and ease of access where the overview of the model can be accessed with full functionality. Each type of physics can be assigned to domains and can be coupled via multiphysics option.

By utilizing physics packages and built-in material properties, users can easily construct their model just by defining sources, fluxes constraints rather than starting from defining physical equations. After completing the pre-processing part, with the settings provided in the study node, various types of studies could be performed.

Finite-Element Method (FEM) is used by COMSOL when the model is simulated. The software is sufficiently sophisticated in meshing techniques such as adaptive meshing and re-meshing on targeted domains. Also, error tolerance and convergence parameters can be controlled by using various numerical techniques. Additionally, COMSOL supports multiprocessing and cluster computing for faster simulation runs as well as having auxiliary and parametric sweeps for effortless design control. In this thesis, COMSOL version 5.3a is used.

3.3 Specification of Efficiency Valuation

As described in the introductory part, the cooling power applied to reactor bed provides more ethanol to be adsorbed by the adsorbent, which boils down the adsorbate in evaporator due to low pressure. Therefore, the cooling effect is developed in an area that the evaporator is placed. By following this route, the coefficient of performance (COP) can be expressed as

$$COP = \frac{Latent\ heat\ of\ adsorbate}{heat\ of\ desorption} \quad (1)$$

And this expression points out the first and most important principle in the designed system, which is utilized materials. Also, other criteria such as maximum cooling that can be done without surpassing optimal limits or lowest temperature that can be achieved in adsorption stage to further increase the adsorption amount are highly important due to a direct effect on COP value. All the explained criteria have to be considered in order to have a highly effective designed system.

Having a high COP value only is not a good indicator of an efficient heat pump. The reason is, COP value of operating bed can be increased with more time allowed for adsorption in the containment stage. On the other hand, increasing operation time of bed for higher COP values will lower generated power by the reason of more time-consuming in a cycle which will result in a poorly operational heat pump.

CHAPTER 4

PROBLEM DESCRIPTION

4.1 Model Geometry

With the purpose of having high adsorption capacity, cylindrical 2D cross section geometries which consist of a reactor bed, a heat sink that wraps the bed from outside and an inner part of the pipe that allows the flow ethanol vapor freely are drawn in AutoCAD 2016. The model is illustrated in Figure 3.

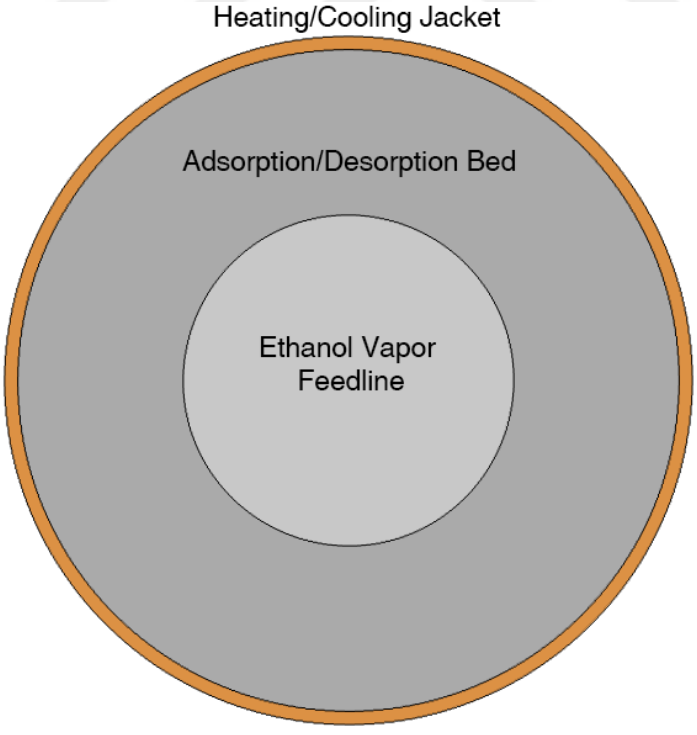

Figure 3. Cross-section view of the studied geometry of finless reactor bed.

4 different geometries are utilized for construction of the model. Initially, a geometry from previous studies is used. Then by using different radii values and by incorporating internal fins different geometries were also investigated. The aim of the geometry modifications was to improve the system performance via enhanced heat transfer characteristics in the reactor. Parameters of created geometries are given in Table 1. Also, the copper tube that is wrapping the reactor bed and fins have thickness value of 1 mm.

Table 1. Parameters of modeled geometries. Unit of all values is mm.

Config No.	r_{in}	r_{out}	h_{fin}	Volume Loss
1	12.5	25	0	-
2	37.5	75	0	-
3	37.5	75	15	2.2%
4	37.5	75	37.5	5.6%

Fins that drawn for improved heat exchange purposes are internal. As a result of this modification, the loss of adsorbent material in Config 3. is 2,2% while in Config. 4 is 5.6%.

Further modifications are applied to benefit from the symmetrical shape of geometries. For this, the work domain is reduced by dividing the geometry to their symmetrical planes. There are 16 fins placed evenly in geometries which are used as a reference for the division process. Finalized geometries and their symmetry lines after the aforementioned modification are given in Figure 4.

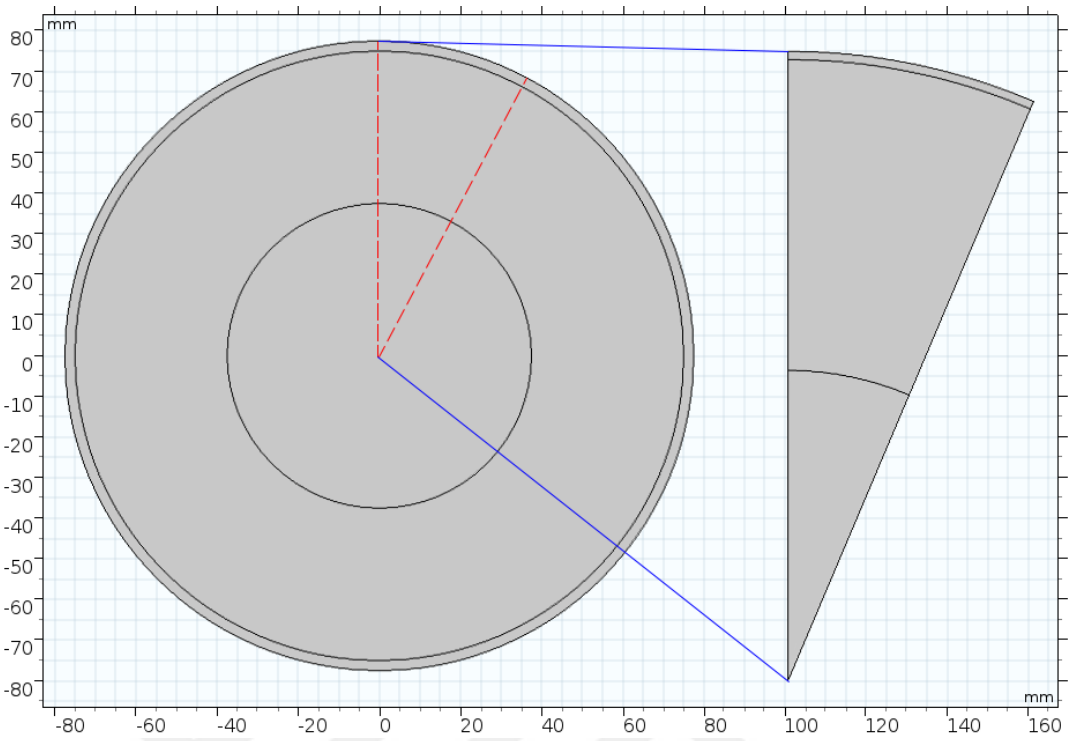
mm
80
70
60
50
40
30
20
10
0
-10
-20
-30
-40
-50
-60
-70
-80
-80
-60
-40
-20
0
20
40
60
80
100
120
140
160
mm

(a)

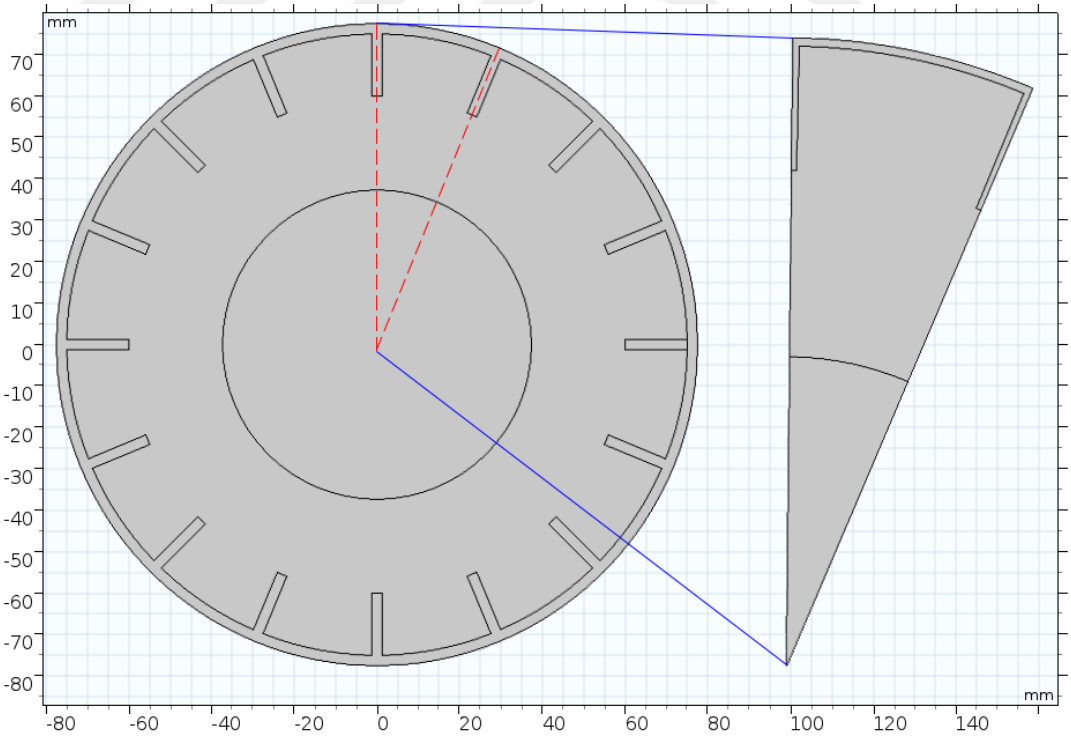
mm
70
60
50
40
30
20
10
0
-10
-20
-30
-40
-50
-60
-70
-80
-80
-60
-40
-20
0
20
40
60
80
100
120
140
mm

(b)

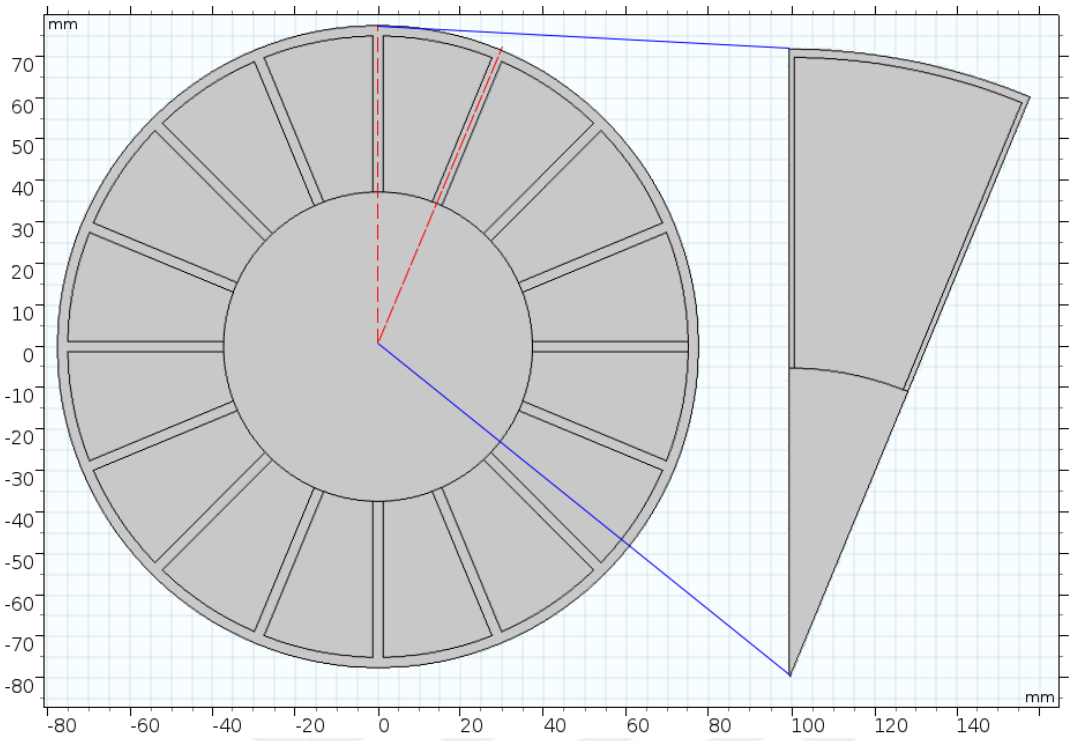

(c)

Figure 4. Geometries of modified reactor beds; (a) Config. 1 and 2, (b) Config. 3, (c) Config. 4. A symmetrical part is taken from each geometry shown in right side of figures and physics are applied on it for faster calculation.

4.2 Model Mesh

In all scientific simulation software, a proper meshing is required depending on physics to reduce numerical errors and increase the resolution on analyzed domains. For this, structured and unstructured meshing can be applied to worked domains depending on the complexity of studied geometry. For simple geometries with a low amount of details such as curves or random shapes, structured meshing should be applied to decrease skewness and eliminate reversed grids as much as possible.

While building the mesh for geometry, COMSOL Mesher is utilized. "Mapped" node, which uses structured quadrilateral mesh on 2D domains, used for meshing operation. Each meshed geometry with its statistics is given in Figure 5.

.When the statistics are analyzed, it is seen that minimum element quality in the worst case (Config. 2) is 0.8735 which indicates that the overall mesh quality is very high and there is no degenerate mesh on the applied domains.

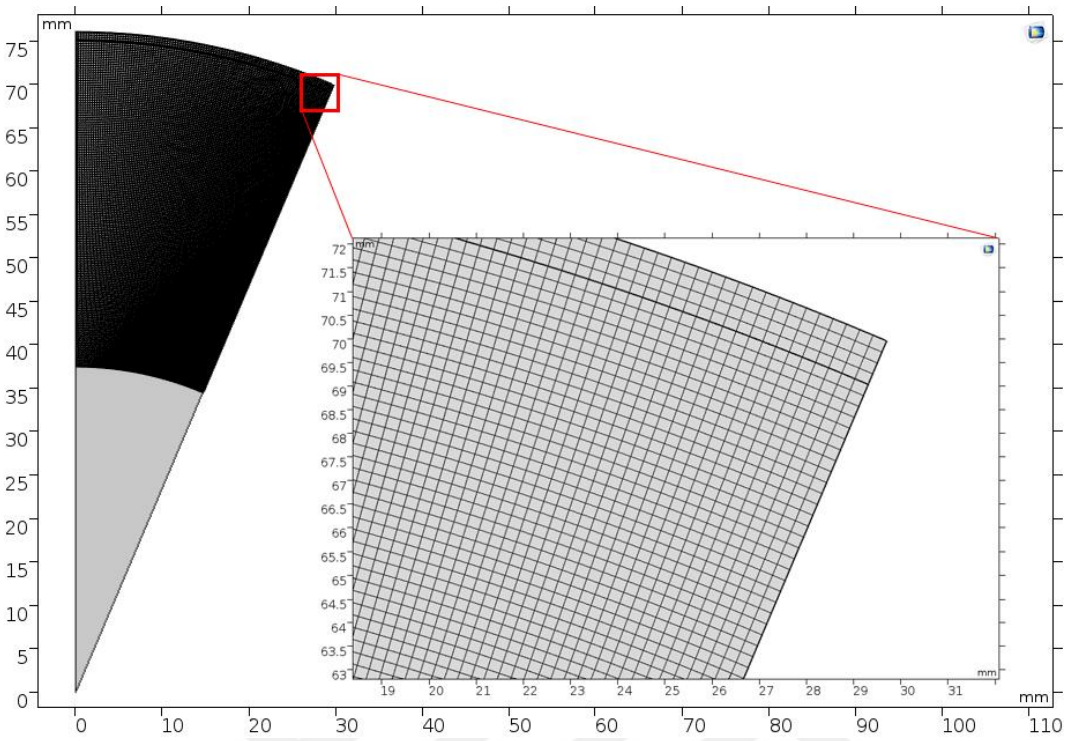

Statistics

Partial mesh

Mesh vertices:	15655
Element type:	All elements
Quads:	15400
Edge elements:	608
Vertex elements:	6

Domain element statistics

Number of elements:	15400
Minimum element quality:	0.9987
Average element quality:	0.9987
Element area ratio:	0.4959
Mesh area:	877.1 mm^2

(a)

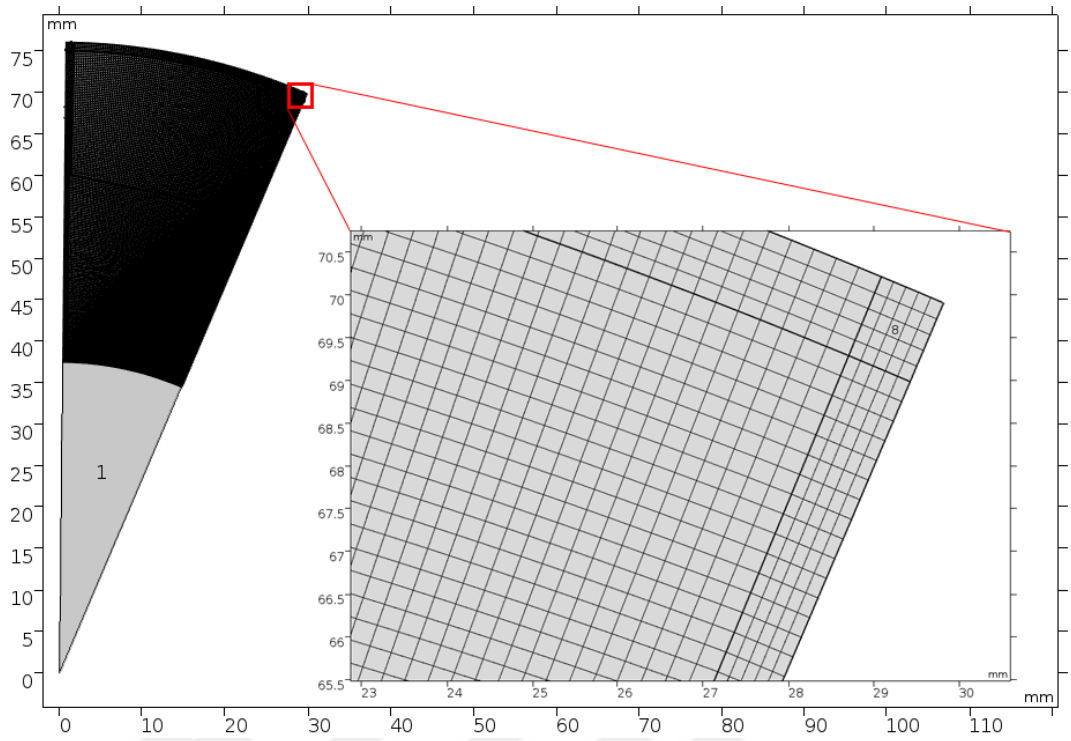

Statistics

Partial mesh

Mesh vertices:	17427
Element type:	All elements
Quads:	17160
Edge elements:	882
Vertex elements:	14

Domain element statistics

Number of elements:	17160
Minimum element quality:	0.8735
Average element quality:	0.9675
Element area ratio:	0.4157
Mesh area:	858.3 mm²

(b)

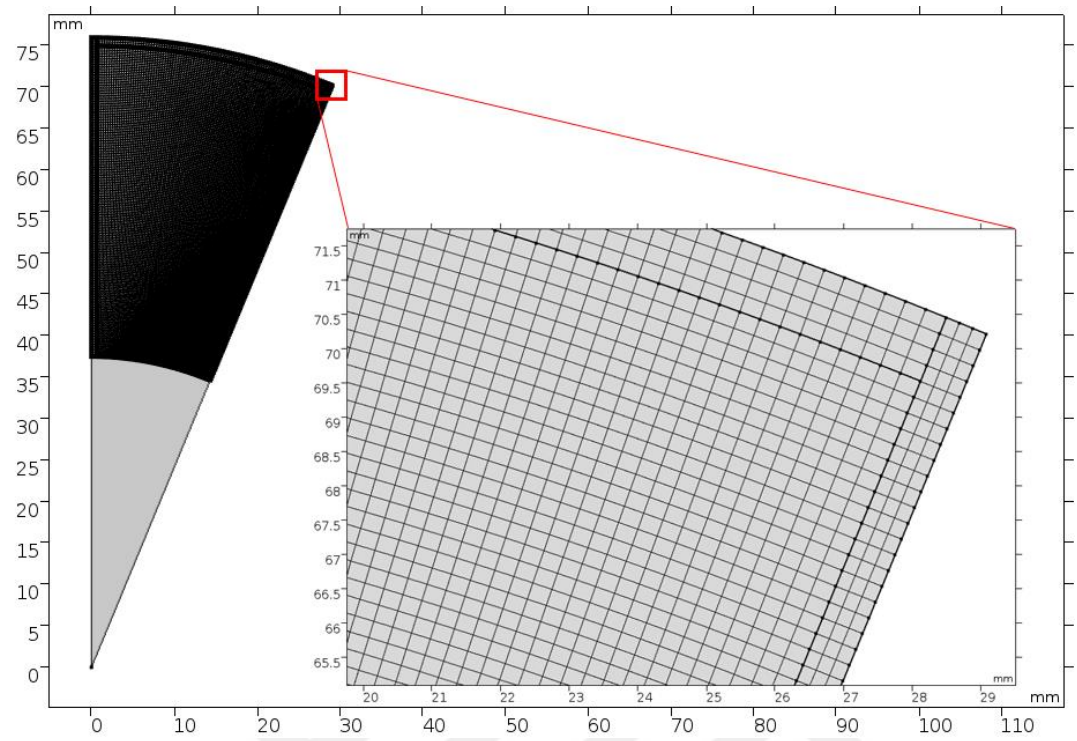

Statistics

Partial mesh

Mesh vertices:	15132
Element type:	All elements
Quads:	14880
Edge elements:	902
Vertex elements:	10

Domain element statistics

Number of elements:	14880
Minimum element quality:	0.9881
Average element quality:	0.9949
Element area ratio:	0.4709
Mesh area:	858 mm²

(c)

Figure 5. Meshing of geometries and their statistics; (a) Config. 1 and 2, (b) Config. 3, (c) Config. 4.

4.3 Condition Selection

A successfully designed heating/cooling systems should have optimally selected evaporation/condensation temperatures. For such inspection, Clausius-Clapeyron curves are used. The Clapeyron graph of a selected pair is given in Figure 6. Having placed the evaporator in a low-temperature environment will provide low pressure of adsorbate material since the pressure of gases increases with temperature, which baffles the adsorption process. Likewise, having the condenser in a very high-temperature domain will increase the pressure of adsorbate gas that prevents desorption to occur appropriately.

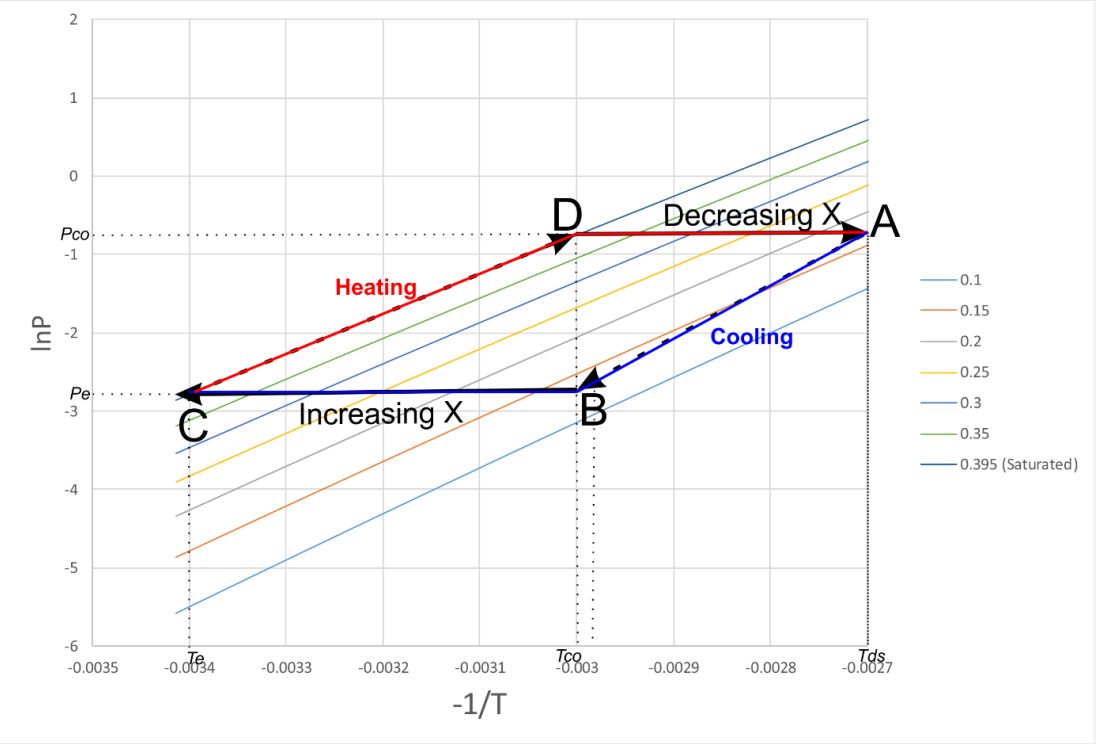

Figure 6. Clasius-Clapeyron curve of selected reactor bed.

The adsorption-desorption system can be described in 4 paths as shown in Figure 6.

A-B path: After the system is stabilized where the adjacent cycles have no difference in the total amount of adsorbate material in reactor bed, first adsorption stage is initiated after desorption stage is ended. The heat removal occurs with supplied cold source and with that the pressure starts to decrease. It is a preparatory path applied for more efficiency to have low overall temperature along the bed, but in our system, this stage is skipped because between stage switches, a sudden change of pressure occurs.

B-C path: Between the points of B and C, the adsorption occurs. In this stage, the temperature will increase due to the nature of adsorption process which prevents more adsorbate to be contained in reactor bed. In order to increase the total adsorbed amount in the bed, the temperature should be kept as low as possible with continuous heat removal. The pressure stays constant during the adsorption process.

C-D path: Another preparatory path where heating is perpetually applied and as a result of this, the temperature and pressure are increased. When the temperature of the bed is equal to the temperature of the condenser, the stage is stopped after having uniform condenser temperature along the bed. This stage is non-existent in the designed system because of a sudden stage switch.

D-A path: The desorption process takes place at this stage. During desorption, the temperature of the bed tends to decrease because of the endothermic nature of physical reaction between adsorbate and adsorbent, and to allow the stage to be completed perfectly, constant heat supply should be applied. With added heat, the temperature of the bed increases while the pressure is kept constant.

In the designed system, the evaporator is placed at 20 °C environment while the condenser is at 60°C where saturation pressures are 0.06 bar and 0.47 bar respectively. The reason of this temperature selections is highly related to ethanol vapor pressure, in very low temperatures the saturated ethanol vapor pressure is considerably low which negatively affects the adsorption rate, likewise, in desorption

process, if the condenser is placed to hotter environment, the system would fail to release its contained vapor due to high vapor pressure.

All the inspected parameters are utilized in boundary conditions section in COMSOL software.

4.4 Adsorbate – Adsorbent Pair Selection

The selection of material pair has vital importance on the performance of the system. Although having high adsorption capacity and the rate is favored, there are other parameters that should be investigated. Selected adsorbate should have (Ahmed, Abd, & Shehata, n.d.);

- Proper pore size and distribution to allow adsorption of vapor fluid
- Shouldn't degrade in varied operating temperature
- Non - corrosive and non – toxic
- High thermal conductivity for easy heat addition/removal
- Possession of low sensible heat compared to the latent heat of adsorption

The parameters that should be considered for adsorbate material;

- Low saturation pressures at a defined operating temperature
- Low specific volume and high latent heat of vaporization
- Low molecular size
- No degradation with use
- Easily producible and low cost
- Non-flammable, non-toxic and non- corrosive

Activated carbon - ethanol pair is used in the light of above-mentioned parameters. Used material properties are given in Table 2.

Table 2. Material properties of activated carbon-ethanol pair.

ρ_s (kg/m^3)	ρ_v (kg/m^3)	Cp_s (J/kg K)	Cp_v (J/mol K)	k_s (W/m K)	ΔH_v (kJ/mol)	ε
750	790	700	78	0.17	38.6	0.25

K value of activated carbon- ethanol pair is taken from a study of Onur et al. Density and heat capacity values of a working pair are calculated with volume average method. Finally, Saturation pressure P_s is calculated with Antoine Eq in the following formula:

$$log_{10}(P_s) = A - \frac{B}{C + T} \quad (2)$$

Where the constants are taken from National Institute of Standarts and Technology webpage. (Ambrose, Sprake, & Townsend, 1975)

The thermal properties of copper which wrap the reactor and provides efficient heat transfer is taken from COMSOL material library (vers. 5.3a).

4.5 Model Physics

A well-specified and precisely described model physics is the main key to have a properly constructed simulation. To define heat and mass transfer interactions in the model, pre-built 'Heat Transfer' and 'Chemical Species Transport' modules are used.

4.5.1 Assumptions

Several assumptions are made to fit the model into the simulation correctly, and those assumptions are;

- Length of the reactor is adequately larger than its diameter, therefore, transfer of mass end energy only occurs in the radial direction.
- No thermal contact resistances between heating/cooling heatsink and reactor bed so the energy flow is uninterrupted.

- The pressure is uniform throughout the entire reactor bed and it is regulated by the temperature of the evaporator in the adsorption stage and temperature of the condenser in the desorption stage.
    - This assumption is verified with Kozeny-Carman equation, switching superficial velocity value that is required by equation with adsorption rate gives very low drop in pressure ($\Delta P < 1$ Pa/m , by Onur et Al.)
- Pressure drop due to adsorption of adsorbate material into adsorbent is negligible.
- The heating/cooling fluid applied for energy exchange application is at a constant temperature during each stage.
- Heat transfer between reactor bed and the inner part where adsorbate material is supplied is negligible.

4.5.2 Transport of Diluted Species

The transport of diluted species interface which is found under chemical species transport subgroup is used for modeling mass transport in targeted domains. The module brings up the following equation:

$$\frac{\partial c_i}{\partial t} + \nabla.(-D_i \nabla c_i) = R_i \tag{3}$$

Here in Eq. 3, the first term is the accumulation of species i that is followed by diffusion and reaction rate terms. The subscript i stands for species that defined in the simulation which is adsorbate material in this model. The adsorption rate term R_i of activated carbon – ethanol pair is studied by Onur et al. (Yurtsever et al., 2013) and determined with employing LDF Equation given in Eq. 4.

$$\frac{k_s a_v}{M} \rho_c (1 - \epsilon)(W - w) = R_{ads} \tag{4}$$

Where the first term $k_s a_v$ is the mass transfer coefficient that heavily depends on temperature by following Arrhenius type relationship which is studied by Saha (Bidyut Baran Saha et al., 2006) in Eq. 5, M is molecular weight of adsorbate fluid, ρ_c is bulk density of the adsorbent material and ϵ being porosity.

$$k_s a_v = 0.58\, e^{-\frac{1970}{T}} \tag{5}$$

T and w are independent variables, temperature (K) and the adsorbed amount in given time (kg ethanol vapor/kg activated carbon) respectively and W is the

adsorption capacity term derived by Dubinin – Radushkevich Equation, given in Eq. 6.

$$W = W_0\, exp\{-D\,[\,T\, ln\left(\frac{P_s}{P}\right)^n\,]\} \tag{6}$$

Here W_0, D and n numbers are constants and calculated from experimental results. Those constants are;

W_0: 0.3955

D: 0.0006049

n: 1.156

Finally, the P term is the pressure of ethanol (bar) either in the evaporator in adsorption stage or condenser in desorption stage and P_s term is saturation pressure of ethanol at the operating temperature. Finalized mass transfer relation is given in Eq. 7. The rate equation is entered to COMSOL by using 'Reactions' interface.

$$\frac{0.58\, e^{-\frac{1970}{T}}}{M}\rho_c(1-\epsilon)(W_0\, exp\{-D\,[\,T\, ln\left(\frac{P_s}{P}\right)^n\,]\} - w) = \frac{\partial c_{ads}}{\partial t} \tag{7}$$

4.5.2.1 Initial Values

The startup of simulation begins with 0 mol/m^3 adsorbed amount of ethanol in reactor bed. For the consequent adsorption/desorption stages, the initial value is taken from the last conditions of the previous stage.

4.5.2.2 Boundary Conditions

4.5.2.2.1 No Flux

In COMSOL, no flux interface is used to cease the mass transfer at external boundaries. The module represents boundaries where no mass flows in or out of the boundaries. Hence, total flux is set to zero. Selected boundaries are given in Figure 7.

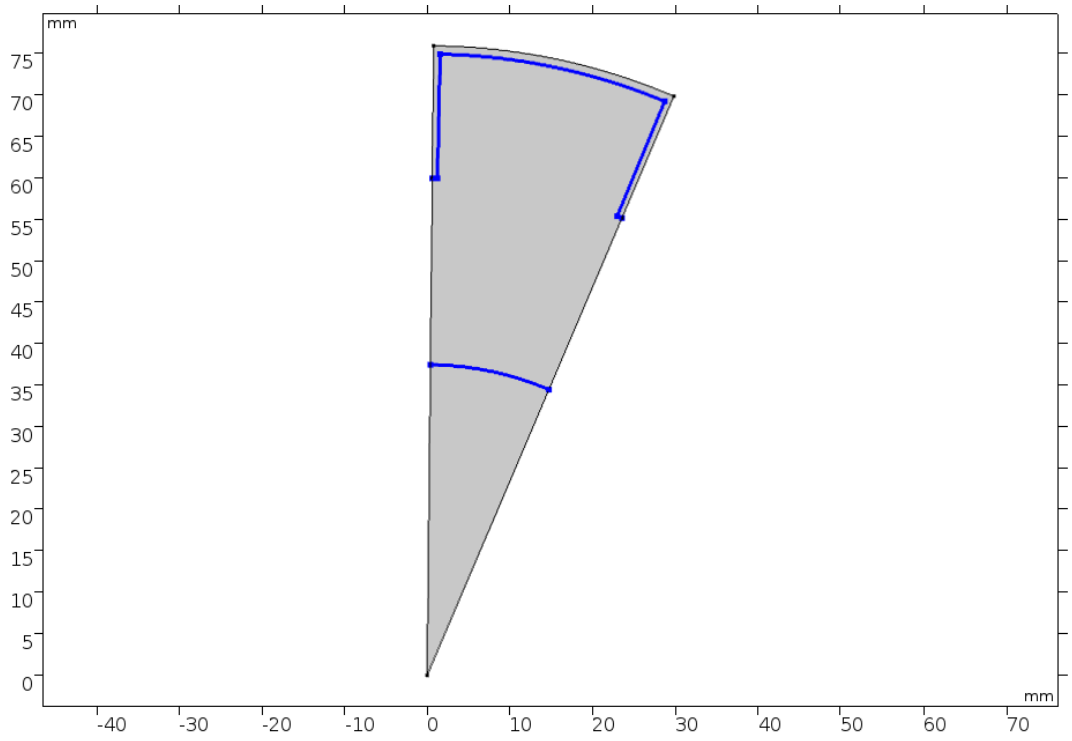

Figure 7. No mass flux boundaries of displayed configuration.

4.5.2.2.2 Symmetry

Symmetry condition can be used to decrease unnecessary operational cost in simulation, and it is used when selected boundaries have symmetric concentration of studied species. A perfect symmetric geometry is required in order to apply this condition. Represented boundaries are given in Figure 8.

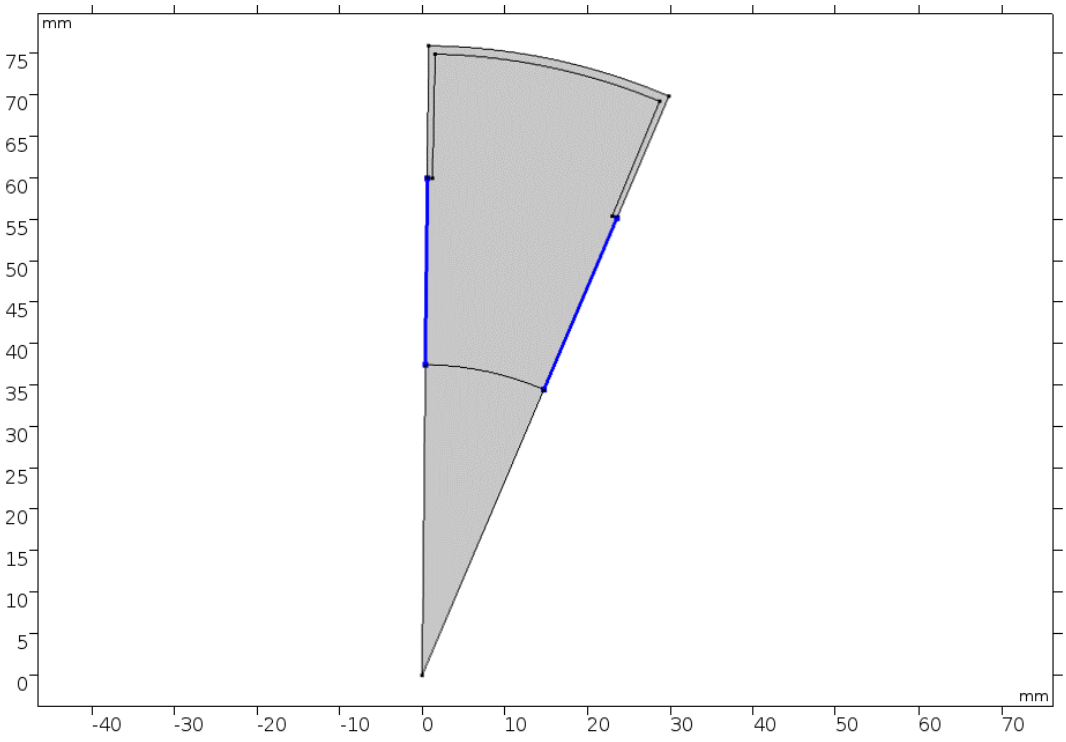

Figure 8. Symmetrical boundaries of displayed configuration in terms of mass transfer.

4.5.3 Heat Transfer in Reactor Bed

In COMSOL, Heat interactions in defined solid domains are calculated with conservation of heat equation, given in Eq. 8;

$$\rho C_{peff} \frac{\partial T}{\partial t} + \nabla.(k\nabla T) = Q \tag{8}$$

where, the first term is energy accumulation, followed by the constitutive equation of Fourier's Law and the heat source term.

Adsorption of ethanol on to activated carbon is an exothermic reaction. Hence, heat source term has a significant impact on temperature profile of the bed. The heat source term is defined as in Eq. 9.

$$R_{ads} * \Delta H_{ads} = Q \tag{9}$$

where R_{ads} is rate of adsorption term and ΔH_{ads} is isosteric heat of adsorption term. ΔH_{ads} is a temperature-dependent value, given in Eq. 10.

$$\Delta H_{ads} = 30 + 0.057 * T(K) \tag{10}$$

In desorption, adsorption rate term will be negative due to decreasing adsorption capacity of reactor bed with increasing temperature. Therefore, the term stays unchanged, but the isosteric heat of adsorption term is switched with heat of vaporization term as in Eq. 11.

$$R_{ads} * \Delta H_{vap} = Q \quad (11)$$

4.5.3.1 Initial Values

Initially, the system temperature is set to 20°C degrees. For consequent stages, initial value data of the solved stage is obtained by last conditions of previous stages.

4.5.3.2 Boundary Conditions

4.5.3.2.1 Heat Flux

The objective of cooling the reactor bed in adsorption stage and heating it in desorption stage is done by heat flux module in COMSOL. This interface adds heat flux to desired boundaries by utilizing Newtons Law of cooling equation, given in Eq. 12;

$$q_0 = h \,.\, (T_{ext} - T) \quad (12)$$

Where q_0 is total heat transferred (W/m^2), h is heat transfer coefficient (W/m^2 K), T_{ext} is heating / cooling fluid temperature. For this simulation, heat transfer coefficient is set to 500 (W/m^2 K), while cooling and heating temperatures are selected as 25°C degrees and 100°C degrees respectively. The applied boundary is given in Figure 9.

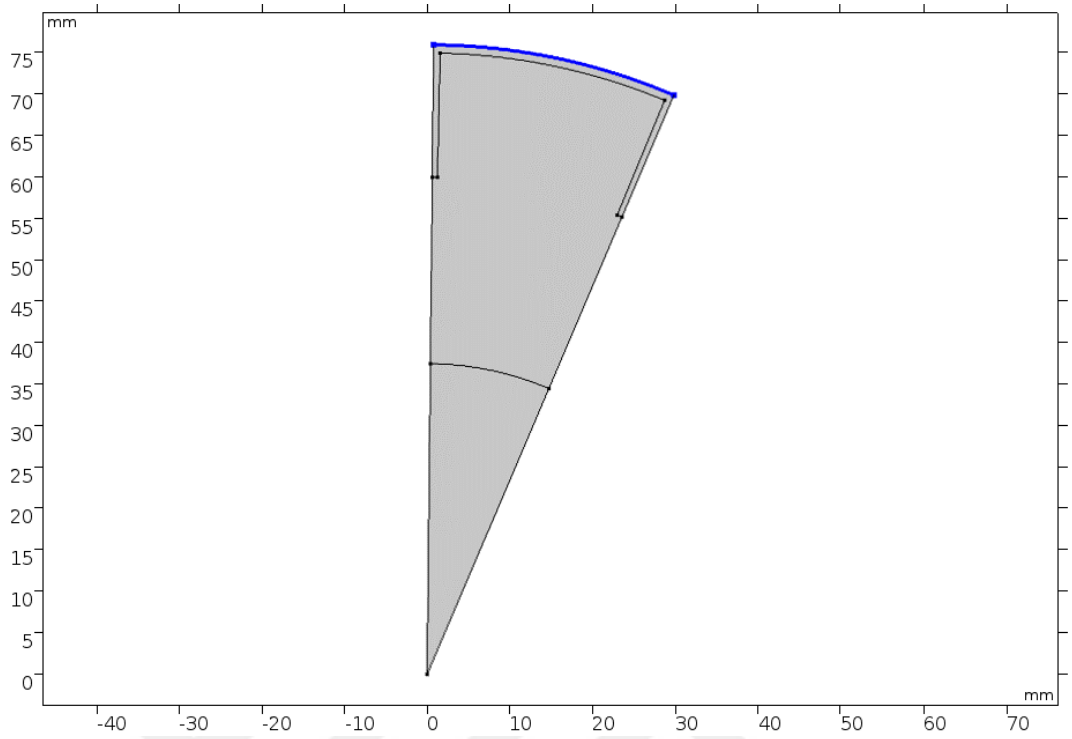

Figure 9. Heat is added/removed from the system in selected boundary for displayed configuration.

4.5.3.2.2 Thermal Insulation

As described in assumptions, the thermal insulation condition which prevents heat flux across to boundary is applied to capture the negligible heat transfer between the ethanol vapor feed line and reactor bed. The boundary that carries this condition is given in Figure 10.

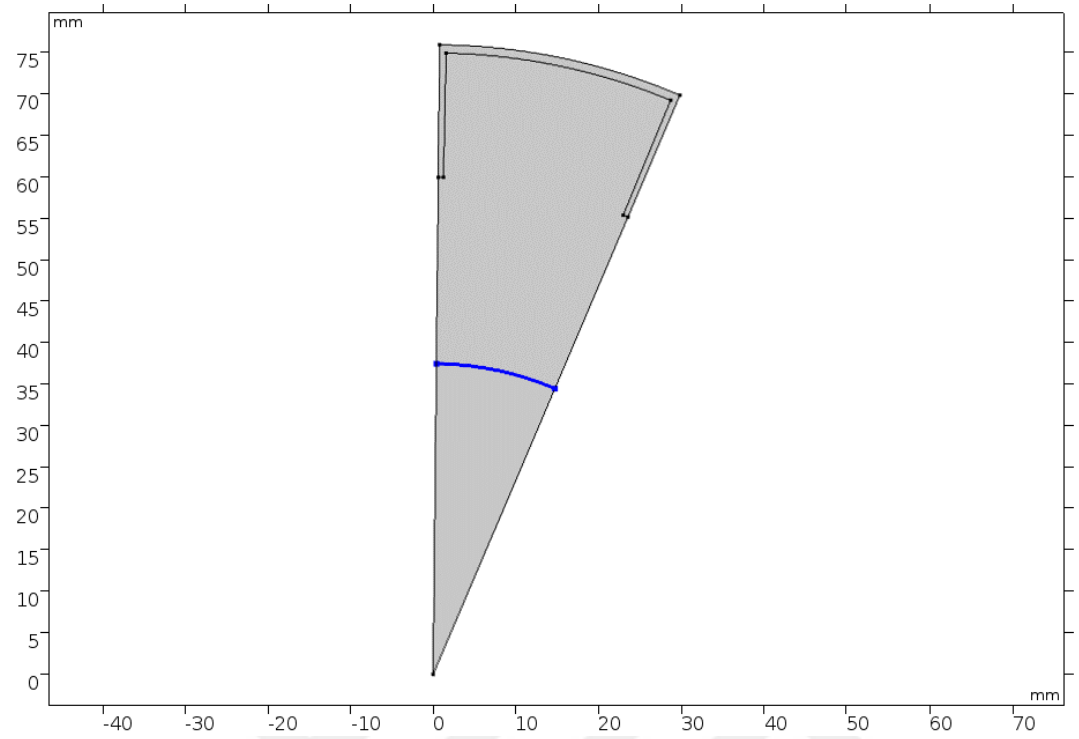

Figure 10. The assumption of thermal insulation is added to the system through the highlighted boundary for displayed configuration.

4.6 Time-Stepping and Solver Settings

In COMSOL, the solver is determined depending on the physics used in simulations, either direct or iterative methods are utilized. The default solver is set by software composers and changing those options are not recommended.

When default solver settings assigned by COMSOL are inspected, it is seen that solving method is selected as PARDISO solver that uses direct method.

For time stepping, an implicit solving method named as Backward Differentiation Formula (BDF) is set. Free selection of time stepping granted the solver to take larger or smaller timesteps as to satisfy the relative set tolerance value of 0.001.

Also, to have separate datasets for uncomplicated post-processing in each stage, the stages are solved with the newly assigned time-dependent solver. For this, initial values of each stage are taken from previous stages last recorded data. With this method, all cycles are chained and individual changes in each stage remained accessible.

4.7 COP Calculation

Unlike other heat pumps, calculation of COP value of adsorption heat pumps requires an alternative approach because of its principle of operation. For this calculation, the following equation (Eqn. 13) is utilized.

$$COP = \frac{\Delta H_v * n_{ads}}{\Delta H_{ads} * n_{ads} + C_{peff} * m_{bed} * \Delta T} \quad (13)$$

where n_{ads} is the total number of moles adsorbed vapor, ΔT is the temperature difference between adsorption and desorption stages, C_{peff} and m_{bed} are the average heat capacity and the mass of the bed (adsorbent + adsorbed vapor), respectively.

The energy accumulation of the bed should be minimized while the adsorbed vapor amount is maximized for high COP values.

4.8 Power Calculation

The energy of environment is withdrawn via evaporator in adsorption heat pump. Hence, total moles of adsorbed vapor which will be removed from evaporator will give power value when multiplied with enthalpy of vaporization and divided with time. Since desorption is only used for regeneration of the bed, the time consumption in desorption stage will be counted as loss time and will be added in total operation time. Following equation is used (Eqn. 14.) for calculation of power values.

$$W_t = \frac{(n_{ads,final} - n_{ads,beginning}) * \Delta H_v}{Total\ Cycle\ Time} \quad (14)$$

Where $n_{ads,final}$ is the adsorbed amount of vapor in the end of adsorption stage and $n_{ads,beginning}$ is in the beginning.

CHAPTER 5

RESULTS AND DISCUSSION

As explained in previous parts, the total adsorbed/desorbed amount of vapor determines the power or performance of the system. Integration of concentration profile of reactor bed with respect to area is done to find the total amount of vapor that is obtained from the designed reactor bed. On the other hand, the distribution of concentration of the bed is mainly led by its temperature profile.

In results, the beds that will operate for 600 seconds are inspected, rest of the cycle times are given in Appendix B. Since it is known that due to low heat conductivity of bed material, the temperature difference between inner and outer parts will be higher as the radius of the bed increases. To have a better view of the effect of bed radius on temperature, the simulation is started with the lowest bed diameter.

5.1 Low Bed Diameter (Config. 1)

For the beginning, simulation runs are started with the lowest diameter since its known that temperature distribution will be more homogenous throughout the bed. The simulation is done with 10 minutes stages with 100 minutes in total time due to fact that the bed started to repeat its profile and got stabilized after the 5^{th} cycle. Adsorbed amount of vapor versus time is given in Figure 11.

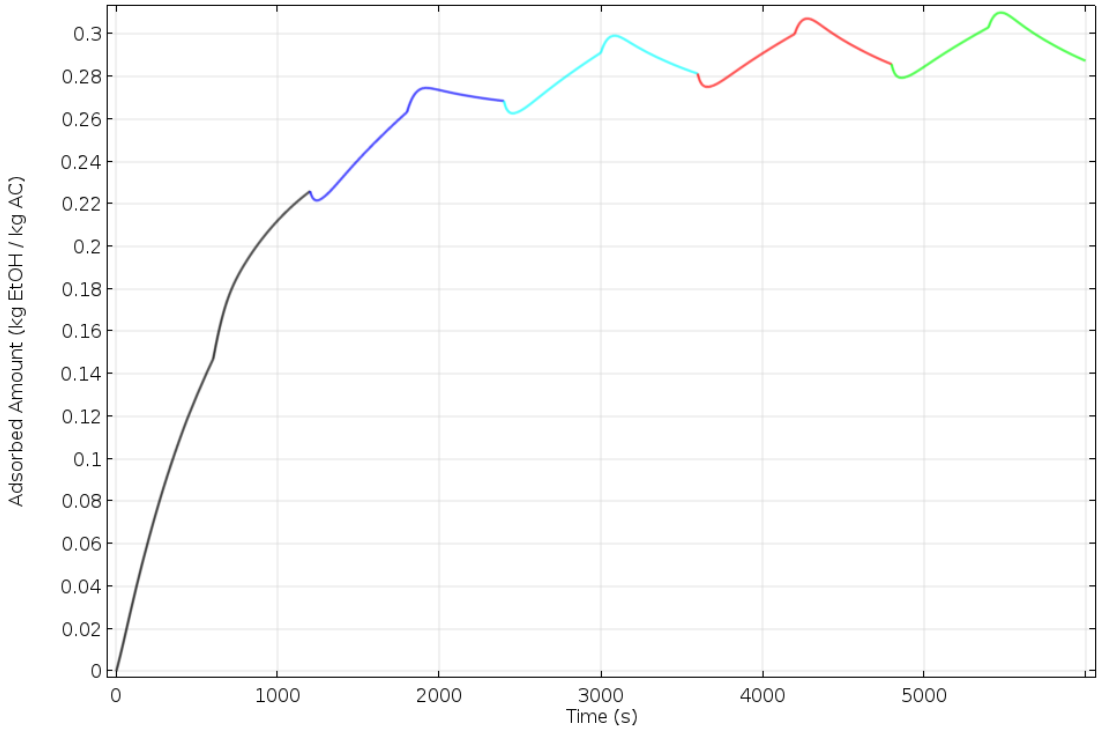

Figure 11. Total adsorbed amount of ethanol(kg/kg) with respect to time for Config. 1. Each color represents a cycle.

As can be seen in Figure 11, Initial effects started vanishing after 3rd cycle due to having low bed diameter which supports homogenous temperature distribution. Only the last cycle will be inspected since the bed will keep repeating itself because the initial effects are completely cleared.

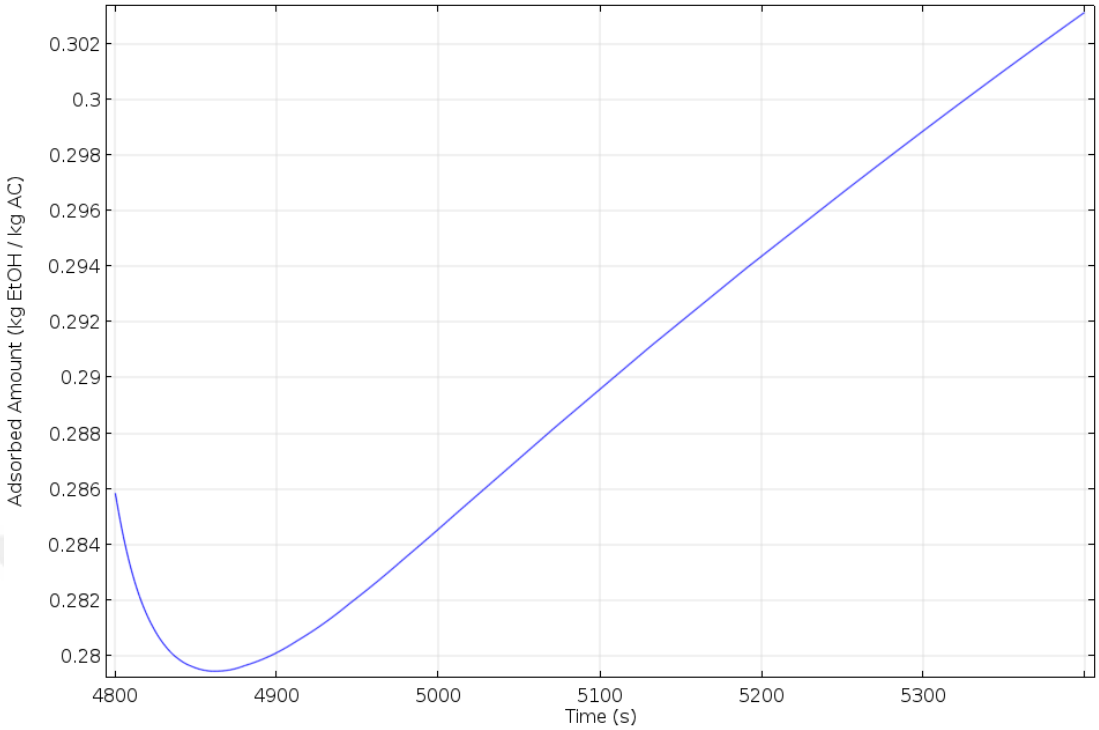

Figure 12. Total adsorbed amount of ethanol(kg/kg) with respect to time in adsorption stage of last cycle.

Adsorption stage of the 5th cycle is given in Figure 12. As illustrated in Figure 12, even though the bed is in the adsorption stage, the first 80 seconds the bed keeps losing its contained vapor, with the reason of residual heat remaining from the previous stage amplified with the sudden switch to the low pressure of evaporator. The pressure of the bed fell instantly with switching to the adsorption stage, but applied cooling still needs time to allow the bed to adsorb. During the adsorption stage, 0.305 mol/m vapor is adsorbed.

The concentration profile of aforementioned stage is given in Figure 13.

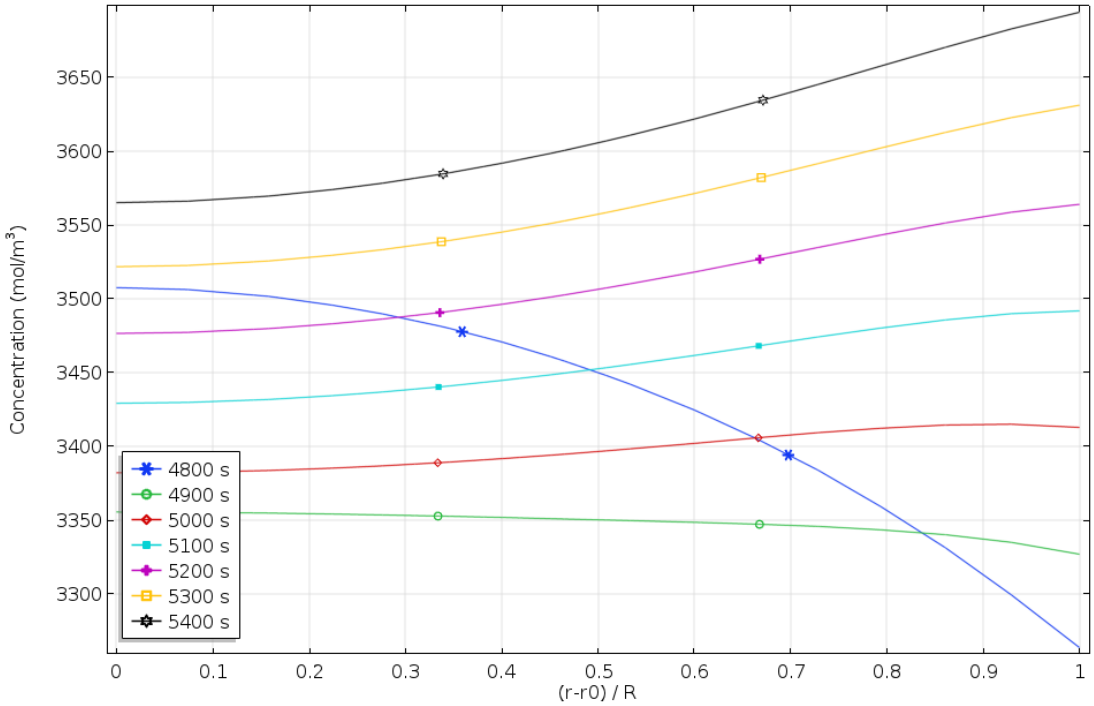

Figure 13. Concentration profile of Config. 1 in the adsorption stage with respect to radial position in the reactor bed and time.

On this graph and in the following position-dependent ones, the x-axis represents bed length where x=0 is at the inner radius, where, x=1 is the inner radius. The blue line is the initiation of the adsorption stage where desorption stage characteristics are inherited. As time progresses, the concentration will decrease due to having the bed in a warm state, but after 100 seconds, the bed will start accumulating vapor and increase its ethanol concentration. The outer part of the bed will have adsorbed more ethanol due to temperature distribution illustrated in Figure 14.

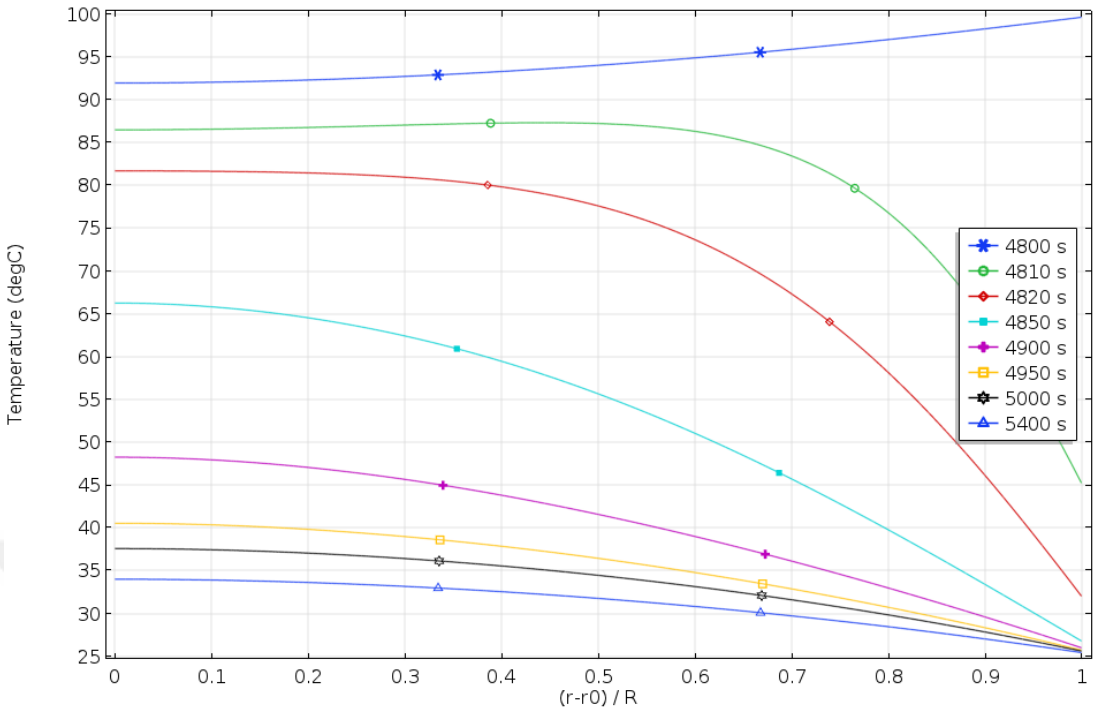

Figure 14. Temperature profile of Config. 1. in the adsorption stage with respect to radial position in the reactor bed and time.

Since the bed is freshly switched from the desorption stage, it was in a high-temperature state. In first 50 seconds, outer parts of bed have responded quickly to heat withdrawal, however, due to low heat conductivity of the bed, the inner parts responded later, and after 400 seconds it almost reached its final temperature for given time. The uniform distribution of temperature in the bed provided homogenous concentration profile which allowed a quick switch from desorption stage and high overall concentration at the end of adsorption stage. When the previous figures are inspected, it can be seen that accumulation of high concentration of vapor favors low temperatures which observed initially at the outer parts of the bed.

In the desorption stage, the process is worked in the opposite way. As shown in Figure 15, the bed kept adsorbing vapor for the first 80 seconds in the beginning, then the desorption process started.

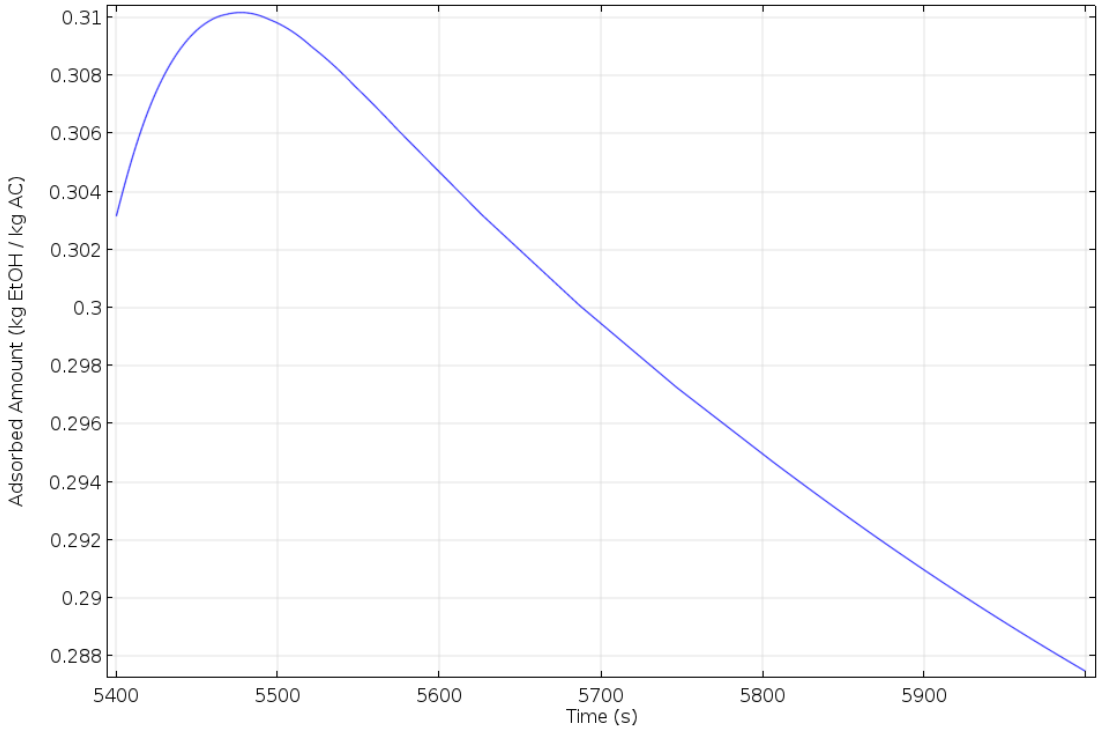

Figure 15. Total adsorbed amount of ethanol(kg/kg) with respect to time in desorption stage of the last cycle.

As described in the previous stage, the bed inherited conditions of the previous adsorption stage so initially, it has a high amount of ethanol vapor contained inside. As time progresses, the bed will be heated from outer parts and likewise, the outer parts will respond quickly.

The concentration profile of desorption stage of config. 1 is given in Figure 16. According to this graph, over time, the outer parts of the bed rapidly released the retained ethanol, but the internal parts continued to accumulate ethanol for some time due to the adsorption effect remained from the previous stage.

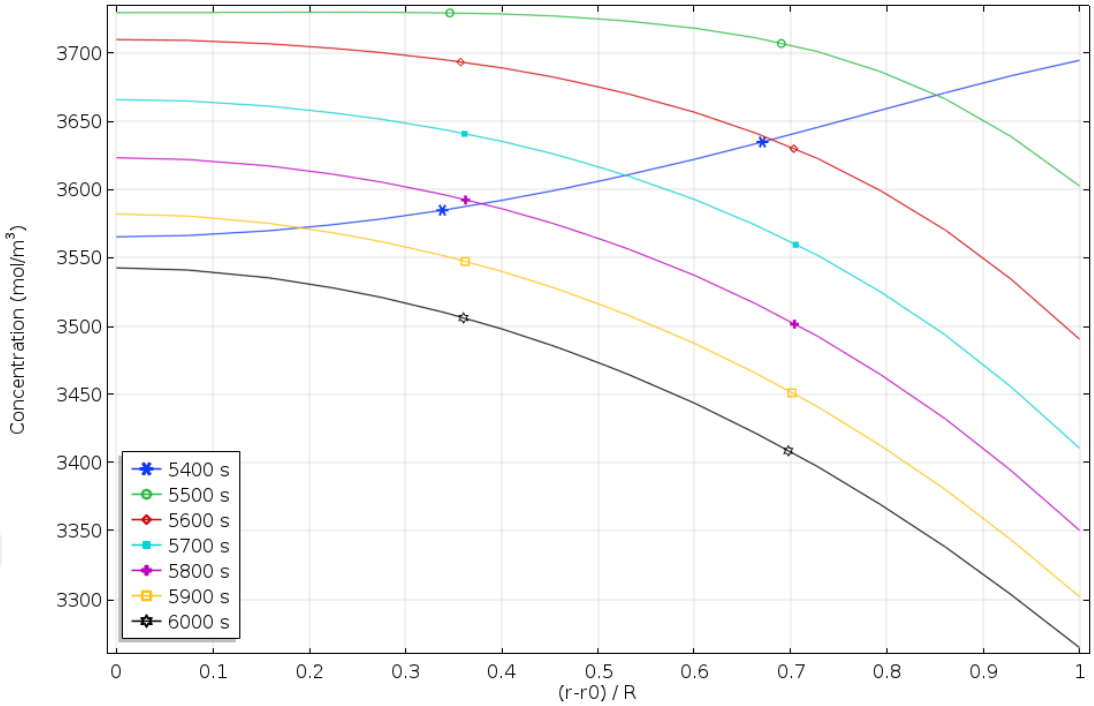

Figure 16. Concentration profile of Config. 1. in desorption stage with respect to radial position in the reactor bed and time.

With the heating effect, the bed kept desorbing the conserved vapor until a new stage is started. The bed in desorption stage has a temperate profile as in Figure 17. In the first 50 seconds, the outer parts have responded to heat load rapidly, but inner parts followed afterward.

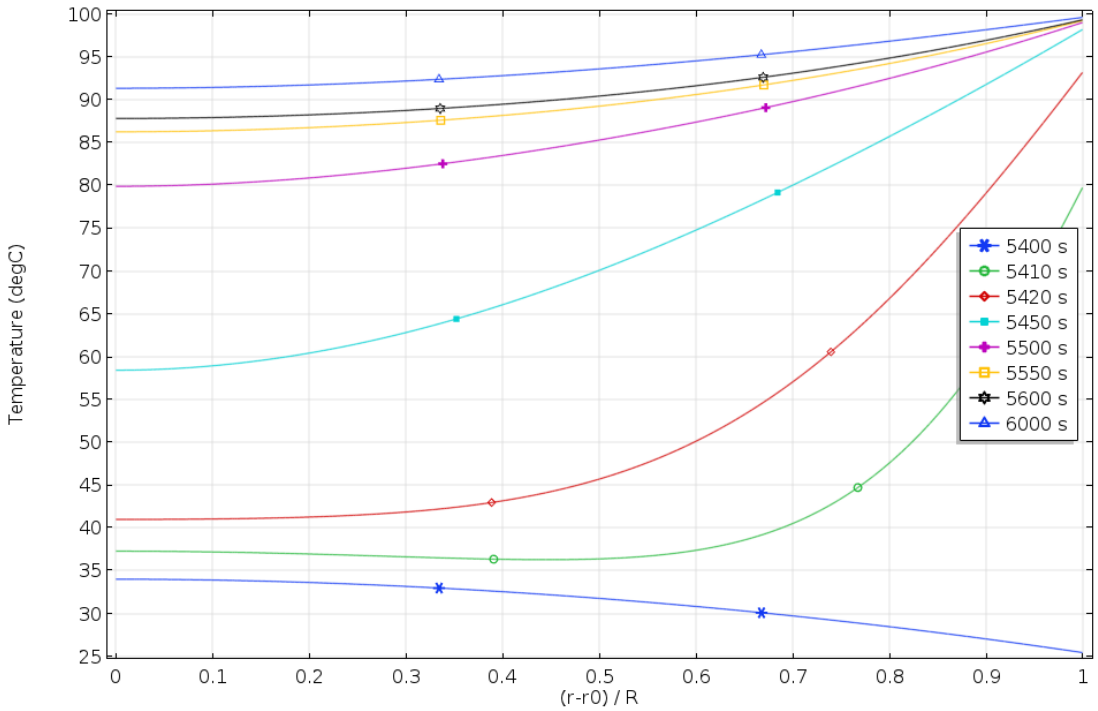

Figure 17. Temperature profile of Config. 1. in desorption stage with respect to radial position in the reactor bed and time.

Since the bed has left the adsorption stage in a cooled state, it was initially warm, as time progressed, the temperature of bed has raised sharply in 50 seconds of its operation time, and again due to low heat conductivity of adsorbent, inner regions started reaching high temperatures after 150 seconds. When both concentration and temperature profiles of this stage are inspected, it is seen that decrease of concentration is observed after temperature load occurs. This relation between temperature and concentration proves that as well as the kinetics of process, the heat transfer also has a great impact on the system.

5.2 High Bed Diameter

5.2.1 Unfinned Configuration (Config.2)

After inspection of low bed diameter, to see the worst-case scenario of low operation time – low heat conduction due to finless geometry is investigated. The bed diameter is tripled in radius and everything else is left as it is. It should be noted that, larger diameter bed means higher adsorption/desorption hence higher energy pumping capacity compared to the smaller diameter beds. From an industrial application point of view, higher capacities have an important advantage over smaller ones.

The adsorption/desorption cycles are repeated until the initial condition of the bed vanishes and concentration and temperature profiles become periodic with respect to the cycles. The adsorbed amount of ethanol through the stabilization cycle is given in Figure 18. As the figure illustrates, the bed has lost the initial load and reached repetition after the 15^{th} cycle. The required amount of cycles before reaching to stabilization is increased dramatically compared to the previous configuration. This phenomenon itself shows that the given stage time was insufficient, and the total process time of cycles terminated prematurely. Additionally, having a bed with higher diameter created these stability issues due to low heat dissipation throughout the bed.

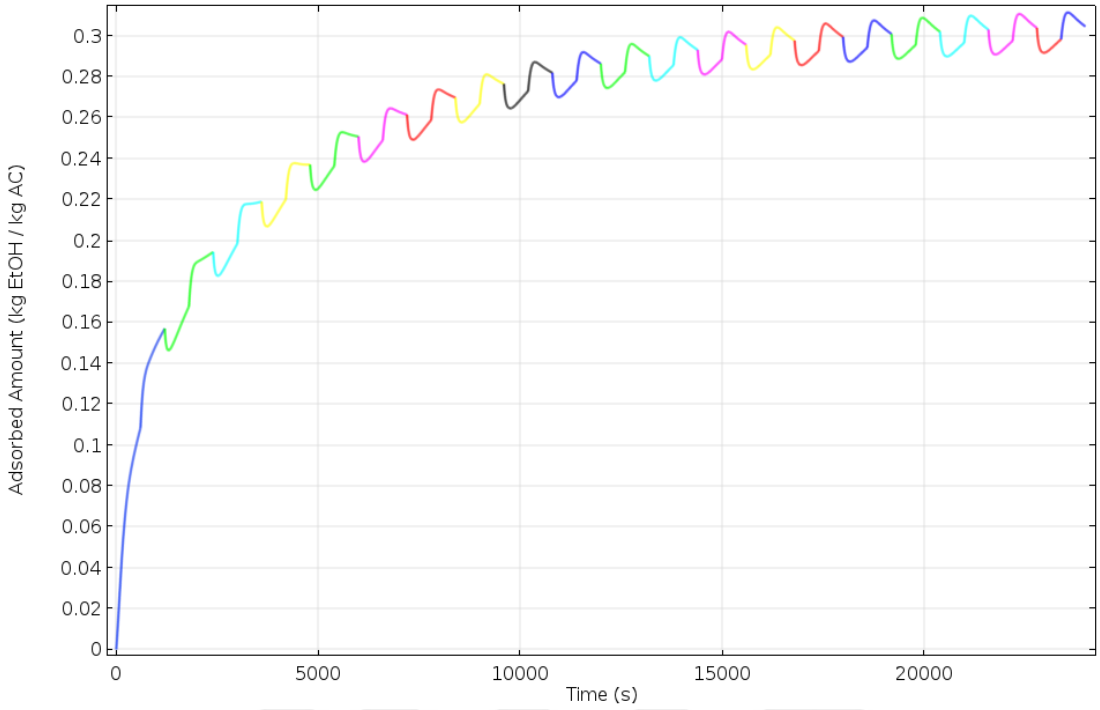

Figure 18. Total adsorbed amount of ethanol(kg/kg) with respect to time for Config. 2. Each color represents a cycle.

The adsorption stage of the bed, which is when it has reached the stability, is given in Figure 19.

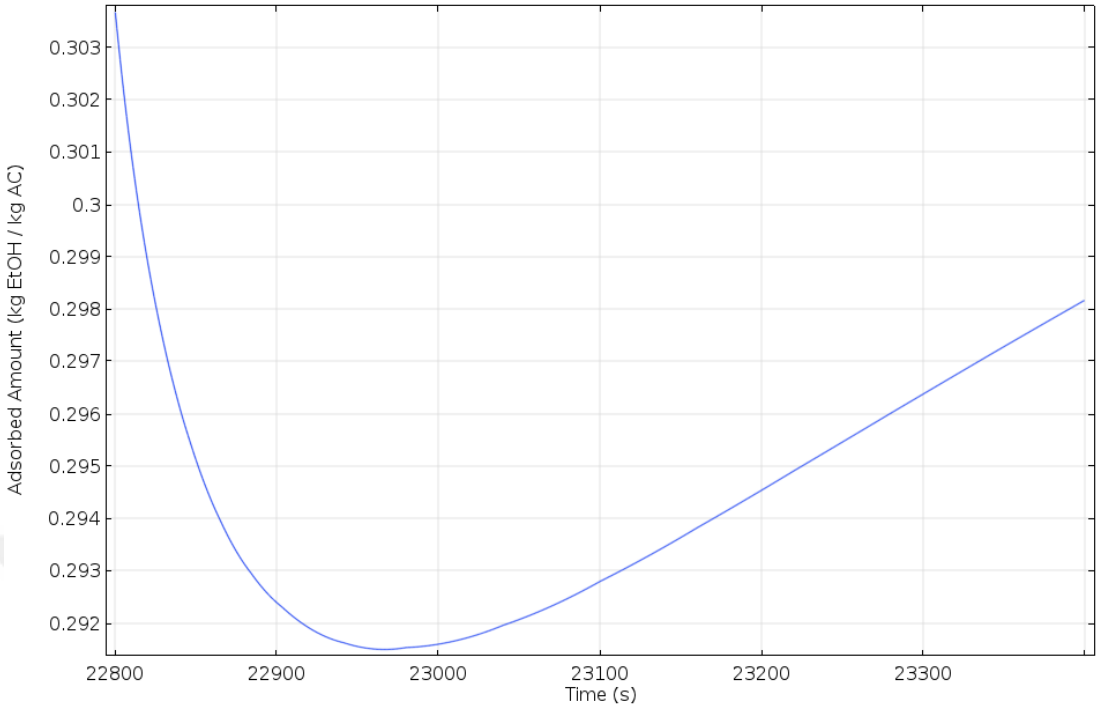

Figure 19. Total adsorbed amount of ethanol(kg/kg) with respect to time in adsorption stage of last cycle.

A sudden change in pressure resulted in a quick drop of the total adsorbed amount of vapor in first 150 seconds, later the bed started adsorbing for the time remaining. After completion of the current stage with 600 seconds passed, the bed couldn't recover its lost amount of ethanol and acted as it is in the desorption stage. The concentration profile during the adsorption stage is investigated in Figure 20.

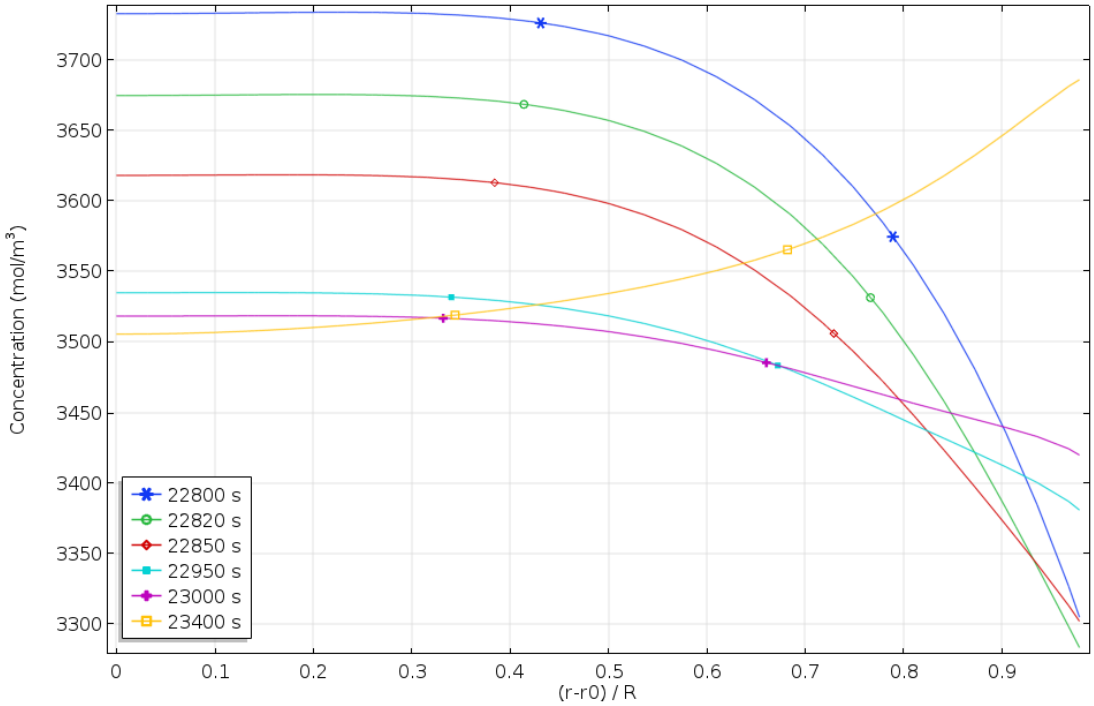

Figure 20. Concentration profile of Config. 2. in adsorption stage with respect to radial position in the reactor bed and time.

Again, due to the sudden pressure change, all parts of the bed lost adsorbed amount for first 150 seconds, but this overall decrease was lower in outer parts because of the applied heat removal from outer walls. In an ongoing process, outer parts of the wall started recovering its lost vapor, but the inner parts remained inactive. For a better understanding of bed concentration profile, a 2D depiction of bed in its corresponding times is given in Figure 21.

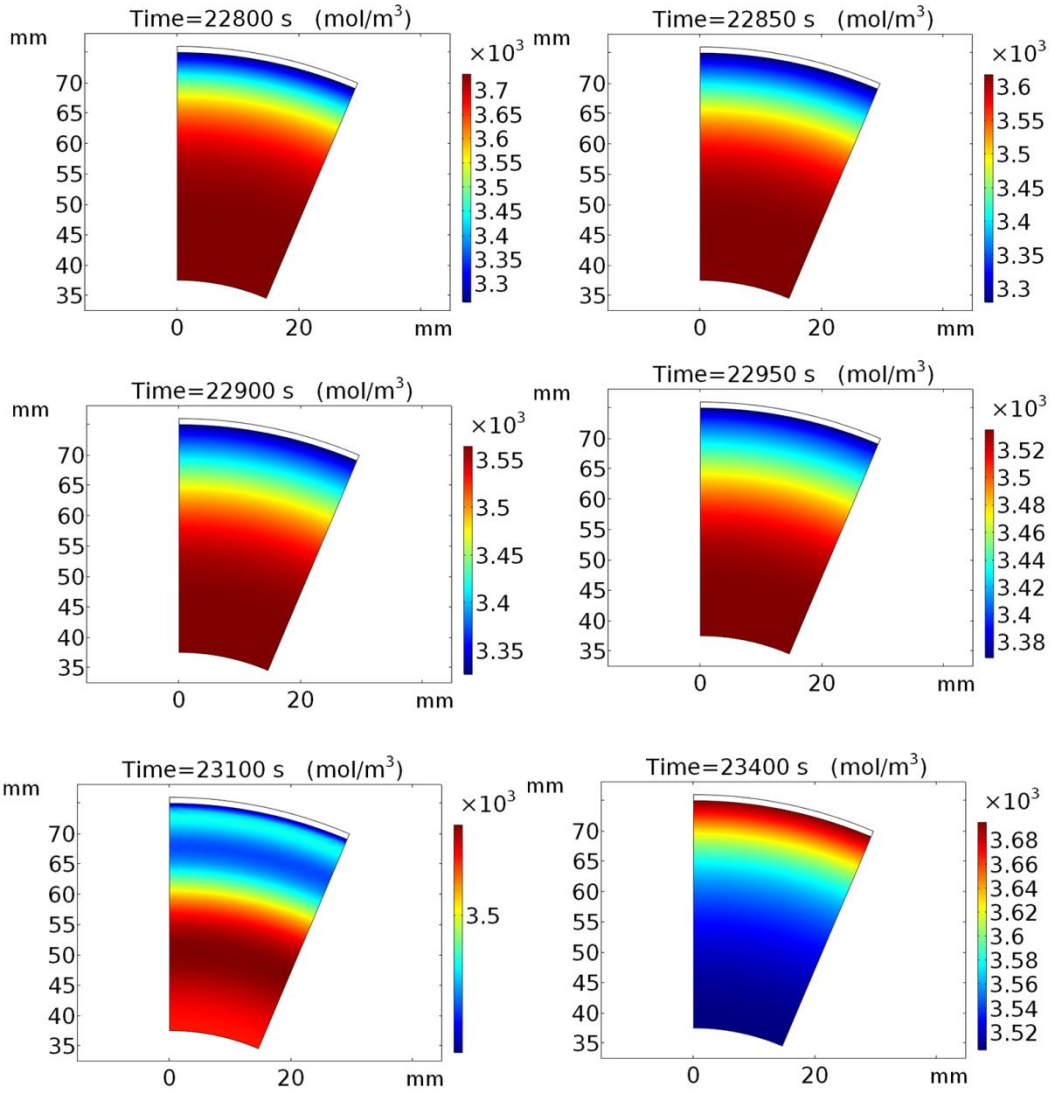

Figure 21. 2D snapshots of concentration profiles of Config. 2 in adsorption stage at their specified time.

Temperature profile of mentioned stage is given in Figure 22. As described previously, concentration of vapor in outer parts are constant in first two illustrations but starts to increase slowly later on, whereas the inner parts keep losing the contained vapor until the last picture.

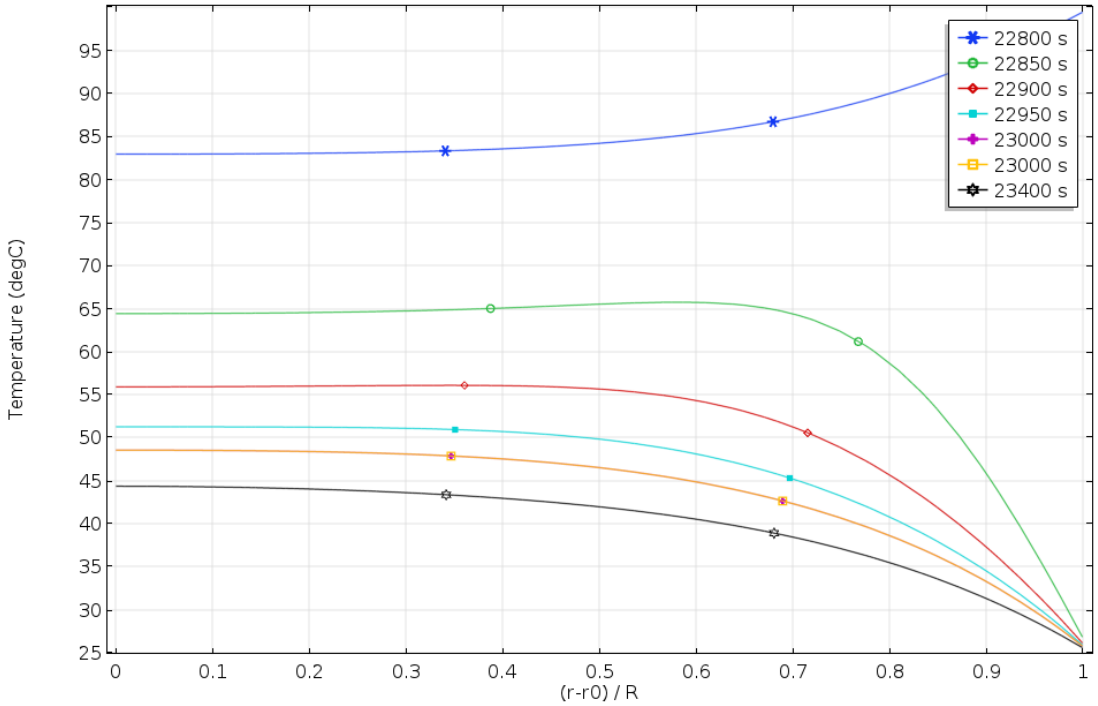

Figure 22. Temperature profile of Config. 2. in adsorption stage with respect to radial position in the reactor bed and time.

When the temperature profile of the adsorption stage is inspected, it is seen that the drop in the value of temperature variable is more in outer parts when compared to inner parts. Even though the inner parts followed the same behavior, the residual temperature was still high in these areas at the end of the adsorption process. The 2D depiction of the reactor bed is given in Figure 23.

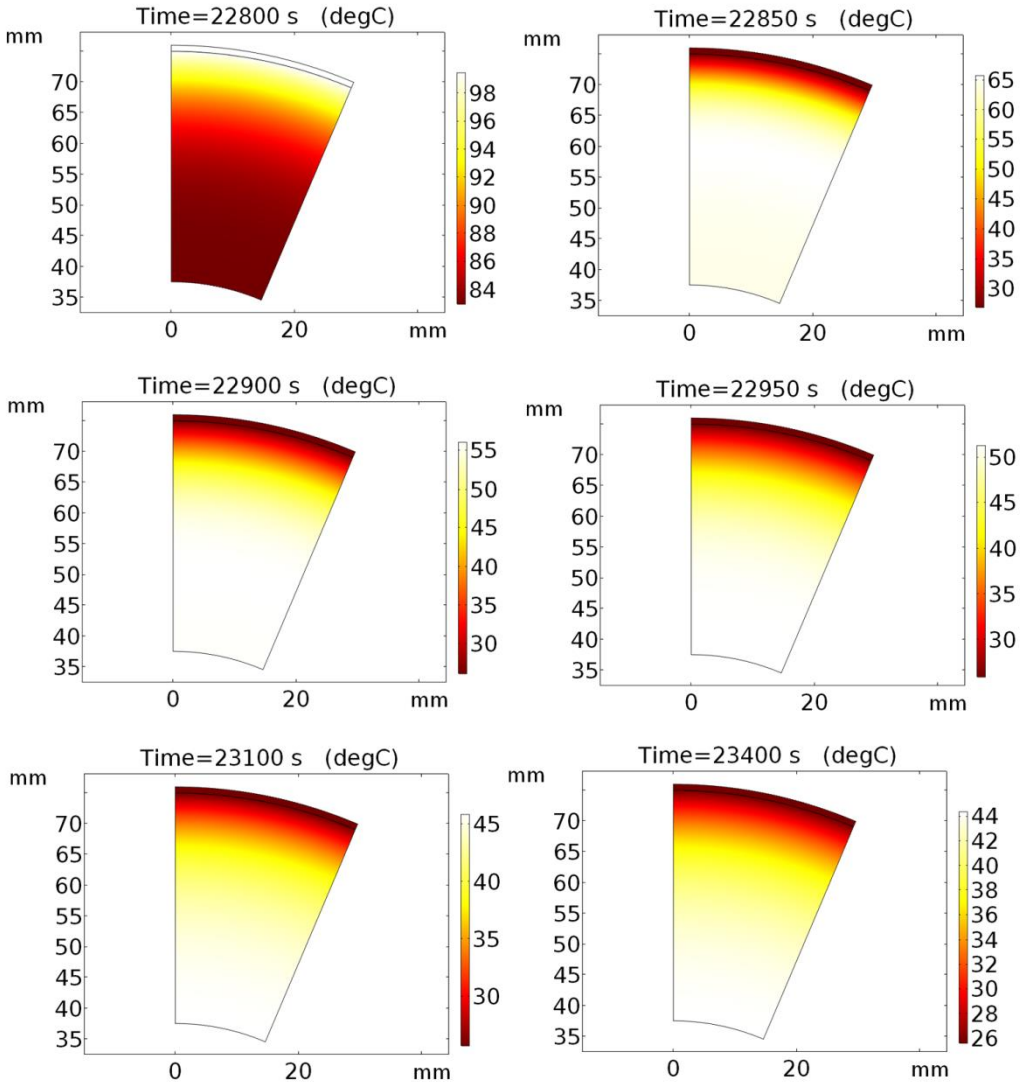

Figure 23. 2D snapshots of temperature profiles of Config. 2 in adsorption stage at their specified time.

The adsorbed amount of vapor in desorption stage is given Figure 24. When the graph is analyzed, it is seen that as the reverse of the adsorption process, the sudden pressure change caused an increment in the adsorbed amount of vapor up to first 160 seconds. As the pressure is equalized and high temperature propagation occurred through the bed, the bed started desorbing the adsorbed ethanol as intended. But the given time wasn't enough for the bed to lose its accumulated vapor and therefore the bed couldn't desorb in its corresponding stage, hence failed to operate as designed.

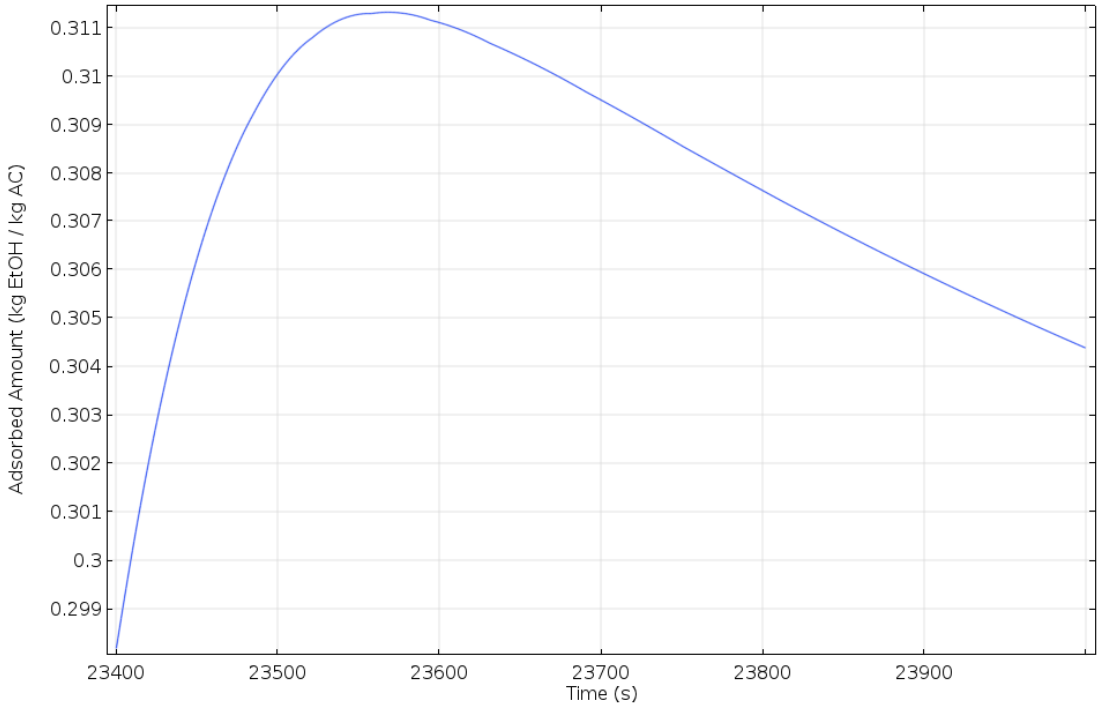

Figure 24. Total adsorbed amount of ethanol(kg/kg) with respect to time in desorption stage of the last cycle.

The concentration profile of bed is given in Figure 25. According to the graph, the outer parts have responded to stage shift slowly but progressively, while inter parts had no influence from the heating process. As time progresses, the outer parts

change behavior and start to desorb, whereas inner parts keep adsorbing vapor from condenser.

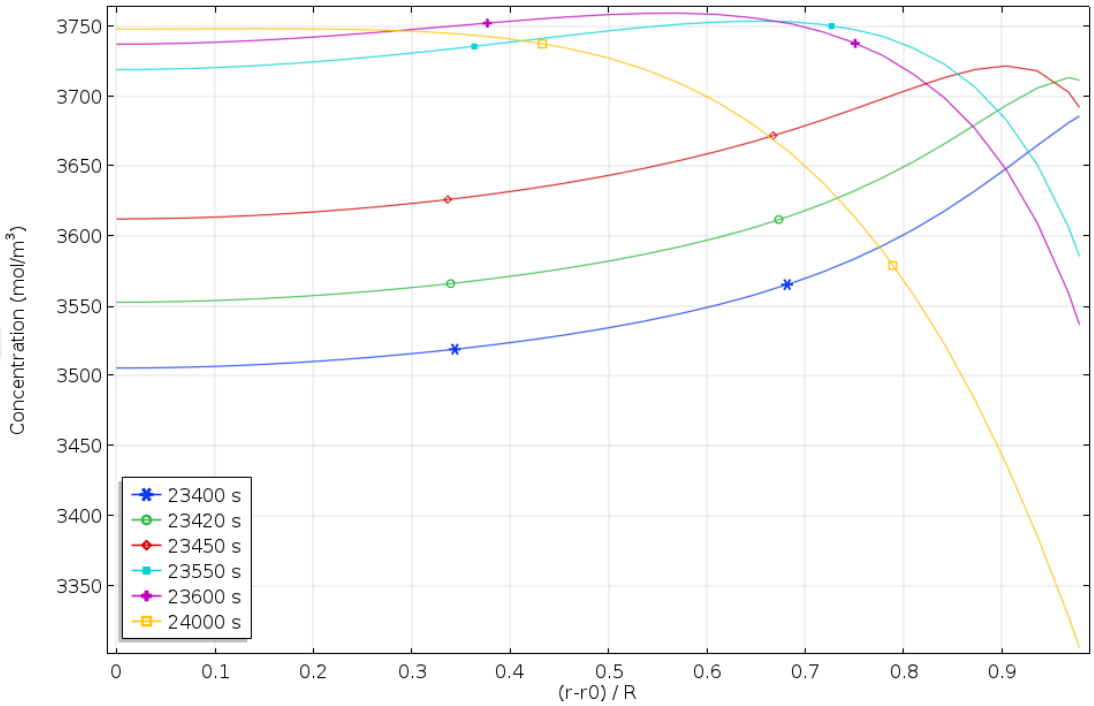

Figure 25. Concentration profile of Config. 2. in desorption stage with respect to radial position in the reactor bed and time.

The 2D visuals of the same reactor bed in corresponding times are given in Figure 26. Excluding the first 160 seconds where the adsorption occurred unintentionally, both inner and outer parts lose its contained vapor, but outer parts were more successful on this due to supplied heat from the heating jacket.

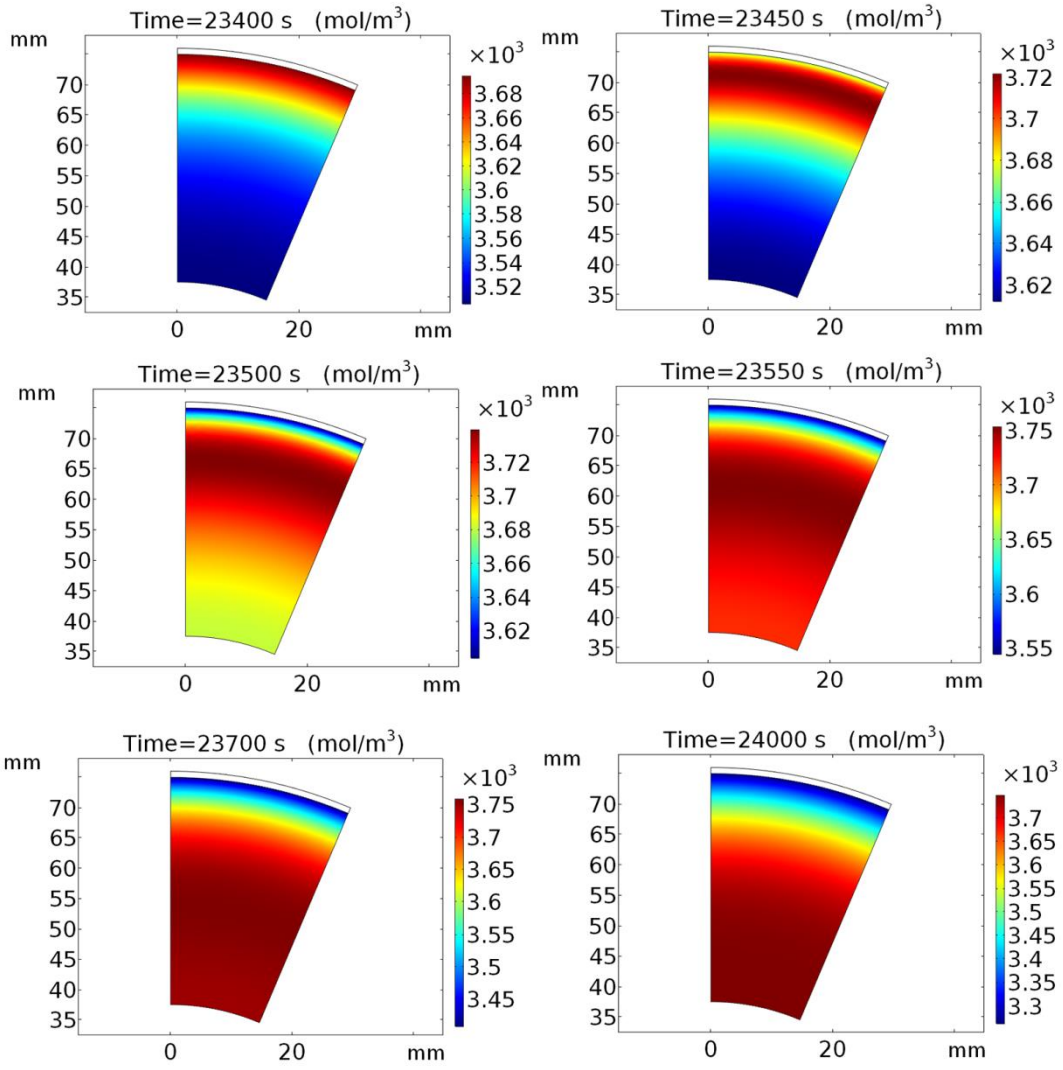

Figure 26. 2D snapshots of concentration profiles of Config. 2 in desorption stage at their specified time.

Temperature profile of this stage is given in Figure 27. As the graph depicts, the outer parts have almost reached the temperature of heating fluid in 50 seconds but for inner parts, the effect is delayed. Finally, temperature profile of the bed gains a uniform distribution but, this phenomenon occurred not because of a good heat transfer. Instead, this form is caused by inner parts that keep adsorbing due to high pressure remained in corresponding places.

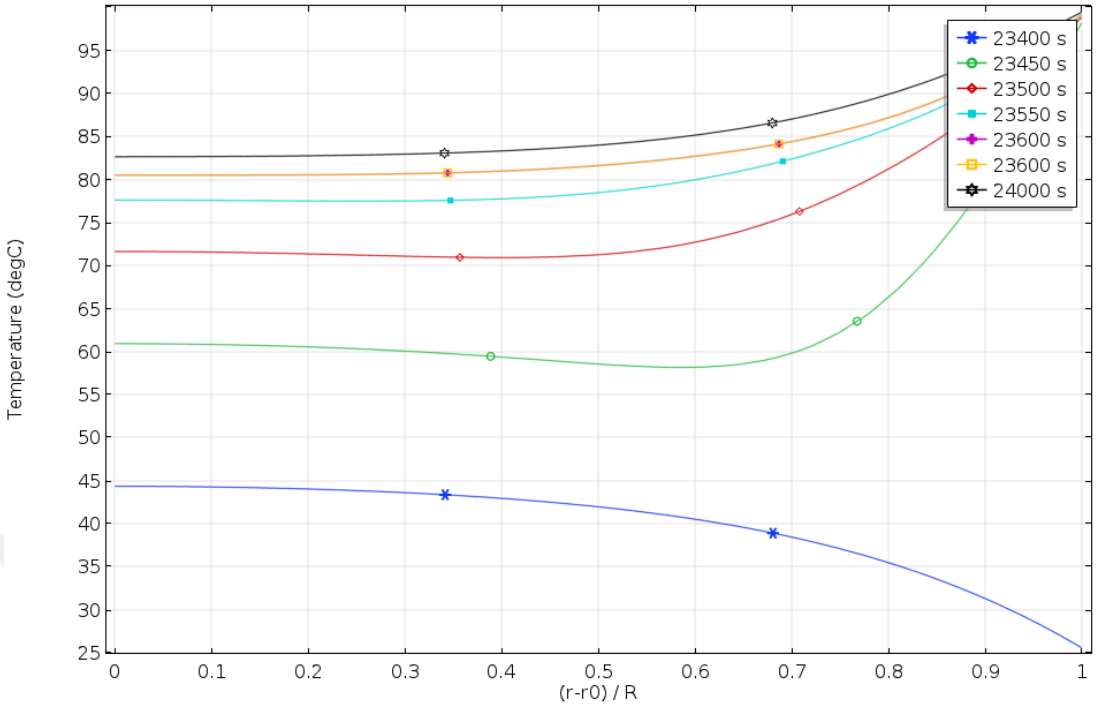

Figure 27. Temperature profile of Config. 2. in desorption stage with respect to radial position in the reactor bed and time.

2D visuals of temperature profiles in given in Figure 28. In illustrations, it is clear that the inner parts where red hue is projected cover most of the bed. Only outer parts almost have reached the temperature of the heating jacket. Even though this distribution changes over time, the change is very small, and a big part of the bed remains unheated.

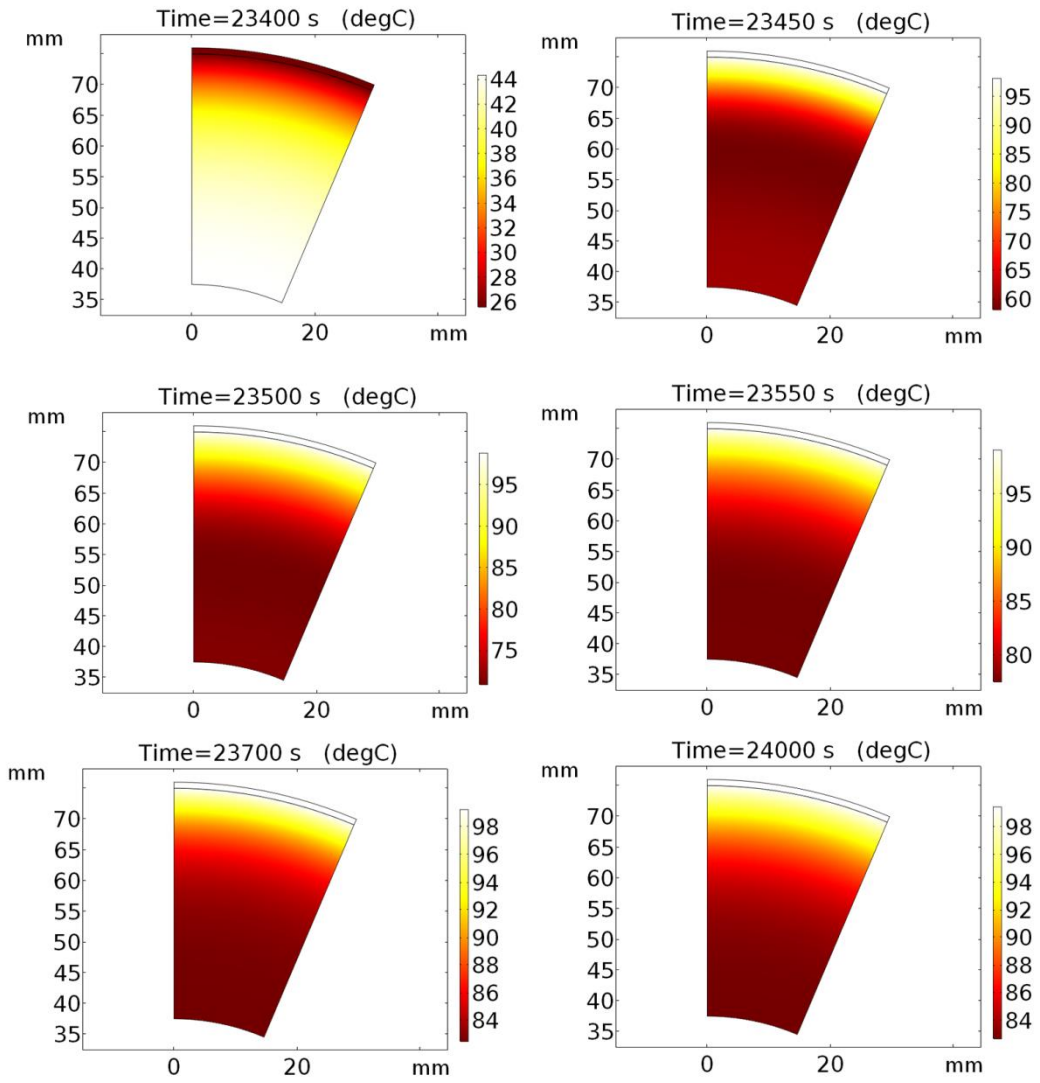

Figure 28. 2D snapshots of temperature profiles of Config. 2 in adsorption stage at their specified time.

The stage of the bed with given parameters was worst-case scenario among other simulations. Expanded geometry with no fins to gain more adsorption capacity decreased the overall performance for the given time. Due to the low heat conductivity of the bed, local temperature differences occurred thus it took more time to remove the initial state that the bed was in.

Compared to previous configuration, the adsorption capacity is increased by utilizing a larger bed size. At the same time, the new large geometry brought the problems of thermal resistance and non-uniform concentration profile mostly caused by dead regions occurred because of low conductivity value of adsorbent material. As a result of this size change, the bed couldn’t even work properly and desorbed in adsorption stage and vice versa. This result emphasizes the vital importance of proper design of geometry of an adsorption bed.

5.2.2 Partly-Finned Configuration (Config. 3)

In this part, the second configuration of designed geometry which has dimensions of 1.25x15mm internal fins has been simulated and the results are analyzed.

Figure 29 shows cycles of finned bed and total adsorbed amount of ethanol during its operation. The bed has reached stability after the 8th cycle and exhibited periodic behavior.

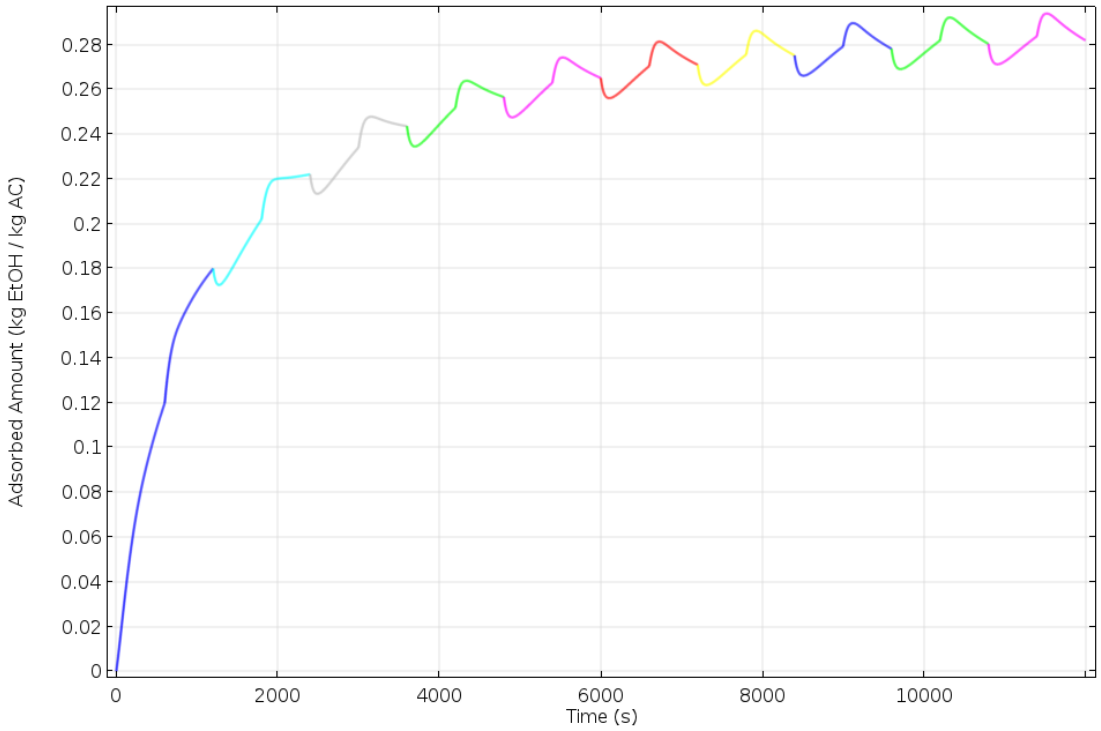

Figure 29. Total adsorbed amount of ethanol(kg/kg) with respect to time for Config. 3. Each color represents a cycle.

Compared to the finless configuration, this one required almost half amount of cycles to reach the stability which shows that the case of better heat exchange helps removal of unwanted remains of concentration in previous cycles.

When the last adsorption cycle is magnified as in Figure 30, it is seen that the bed managed to overcome the pressure change effect and was able to adsorb more vapor than the beginning of the adsorption stage. In addition to this, the time lost during recovery process is decreased from 150 seconds (in the previous configuration) to 120 seconds, resulting in a steeper curve. Also, after the recovery, the accumulation rate went constant, meaning the bed could adsorb more if it is operated in a larger time duration.

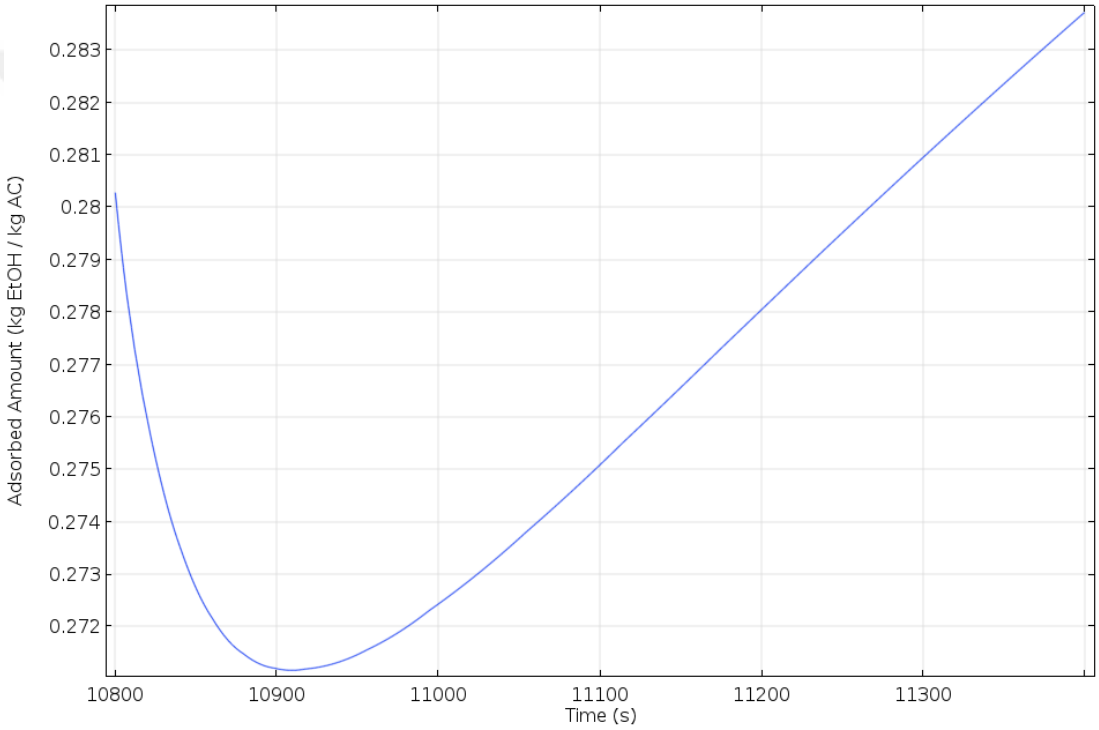

Figure 30. Total adsorbed amount of ethanol(kg/kg) with respect to time in adsorption stage of the last cycle.

Concentration profile for this stage is given in Figure 31. In the first 120 seconds, the bed gradually lost its vapor concentration in all parts due to suddenly being subjected to lower pressure. When the recovery is completed, the vapor concentration in the outer and middle parts that are close to the cooling surfaces increased dramatically

while inner parts remained almost unchanged. The addition of fins reflected its effect by increasing the adsorption amount in the middle parts significantly.

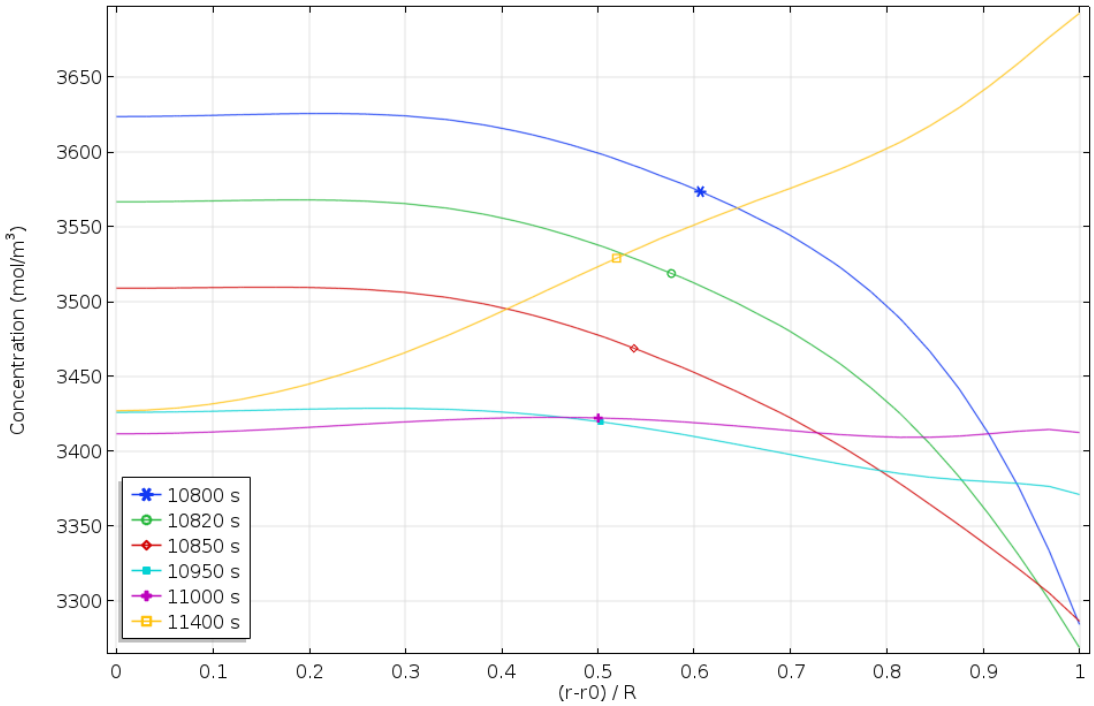

Figure 31. Concentration profile of Config. 3. in adsorption stage with respect to radial position in the reactor bed and time.

For better comprehension, 2D images of the concentration profile of the bed are given in Figure 32. As seen from the 2D visuals, added fins supported the adsorption process and middle parts which were unresponsive in the previous stage are also affected by the altered geometry.

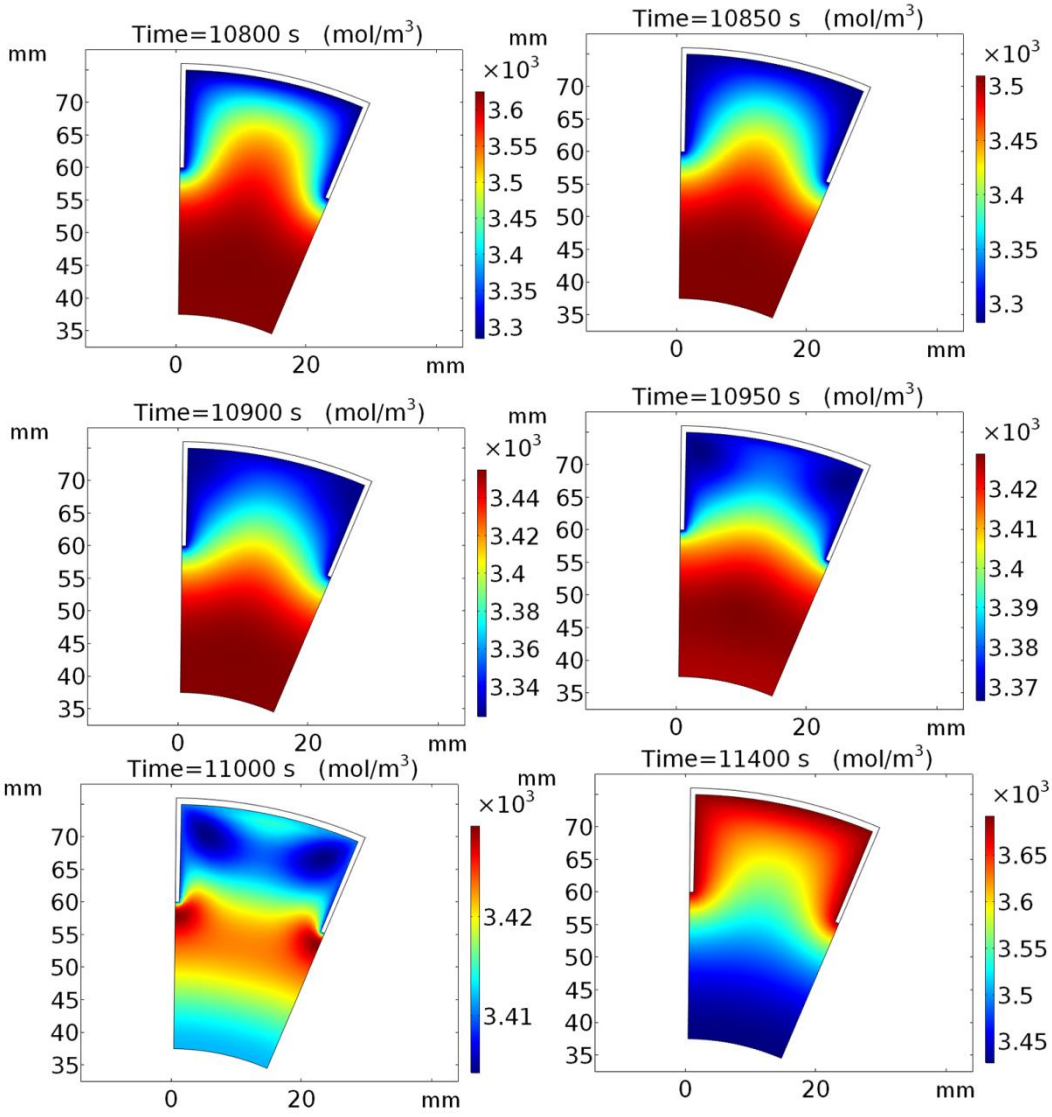

Figure 32. 2D snapshots of concentration profiles of Config. 3 in adsorption stage at their specified time.

The obtained temperature profile for the adsorption stage is given in Figure 33. Started under the influence of desorption process, the bed was initially at the high-temperature stage. As time progressed, the overall temperature at the outer parts have decreased sharply and the trend is followed by middle parts because of the inclusion

of internal fins, causing more homogenous distribution over the bed compared to the finless case of high bed diameter.

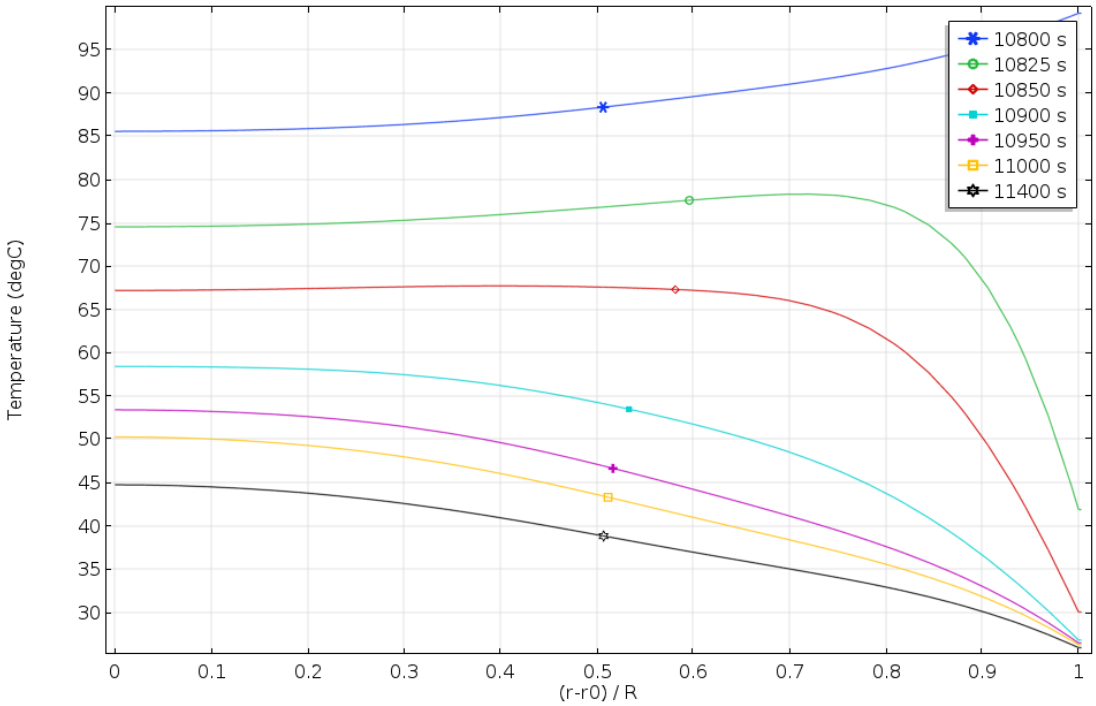

Figure 33. Temperature profile of Config. 3. in adsorption stage with respect to radial position in the reactor bed and time.

2D images of the temperature profile are given in Figure 34. Fins which could reach the middle parts clearly provided a better cooling solution, and as a result of this modification, temperature difference between inner and outer parts decreased rapidly even after 50 seconds.

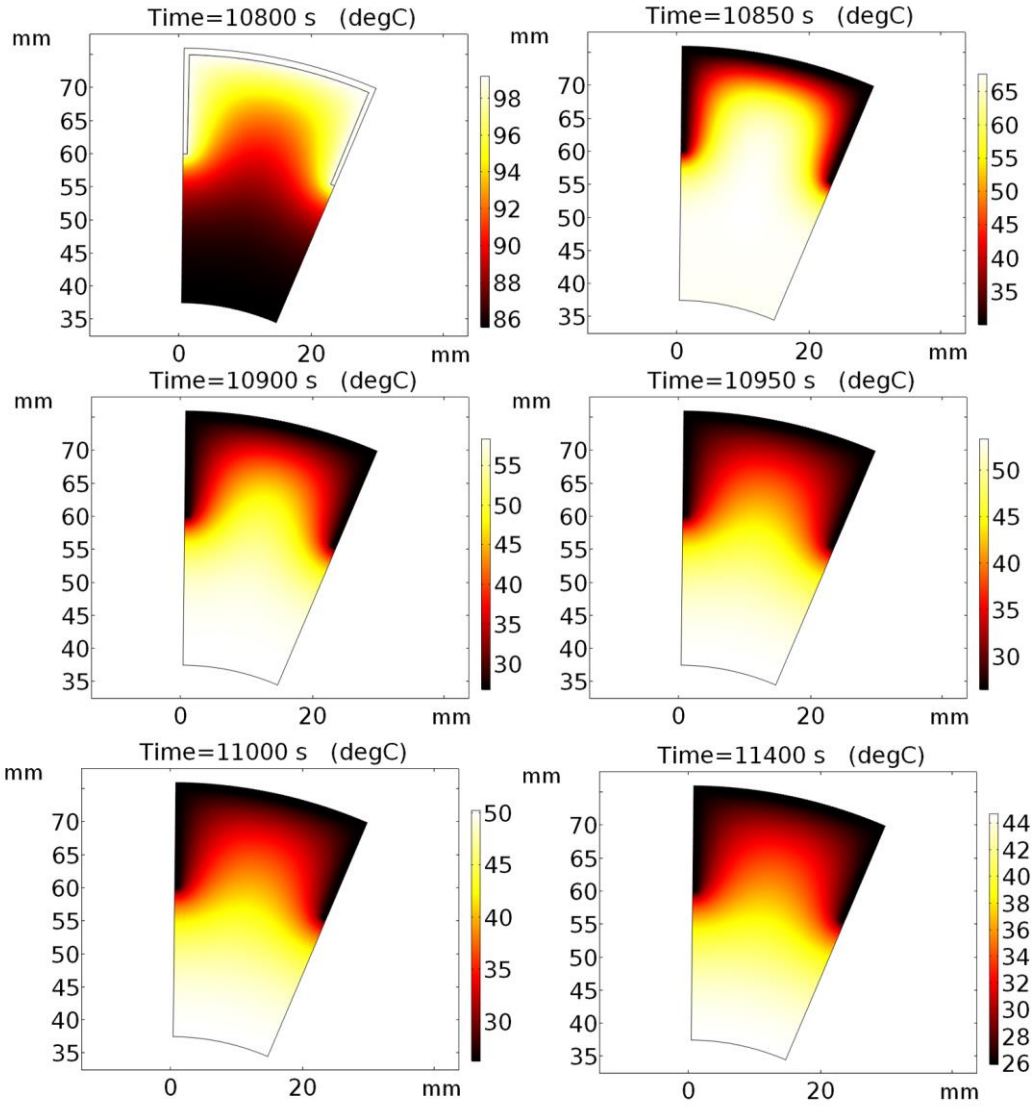

Figure 34. 2D snapshots of temperature profiles of Config. 3 in adsorption stage at their specified time.

Desorption stage of the same cycle is illustrated in Figure 35. The bed started desorbing 30 seconds earlier than the finless case with high bed diameter, therefore, the regeneration process could start earlier, and more efficient desorption occurred for given stage time. After the recovery from the effects of the previous stage, the overall concentration is decreased linearly, meaning the bed could regenerate more with the same rate if more time were allowed during the process.

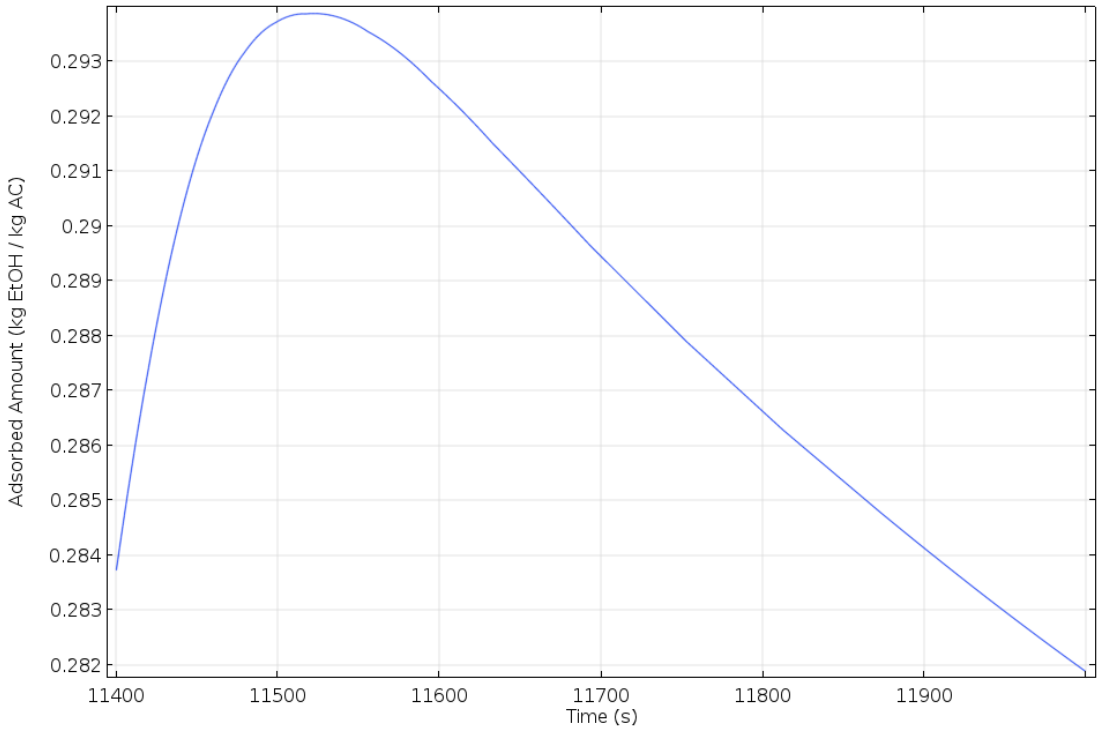

Figure 35. Total adsorbed amount of ethanol(kg/kg) with respect to time in desorption stage of last cycle.

The concentration profile of the aforementioned stage is given in Figure 36. According to the figure, residual vapor remained in the reactor bed is initially higher on the outer parts and lower on inner parts. As the desorption process starts, the overall concentration initially increases due to being exposed to high pressure of adsorbate. Later, with the supplied heat, the outer parts of bed lose concentration sharply and middle parts follow this act. Inner parts are still unresponsive to state change and even the concentration increased because of the exposure of high pressure and delay in supplied heating.

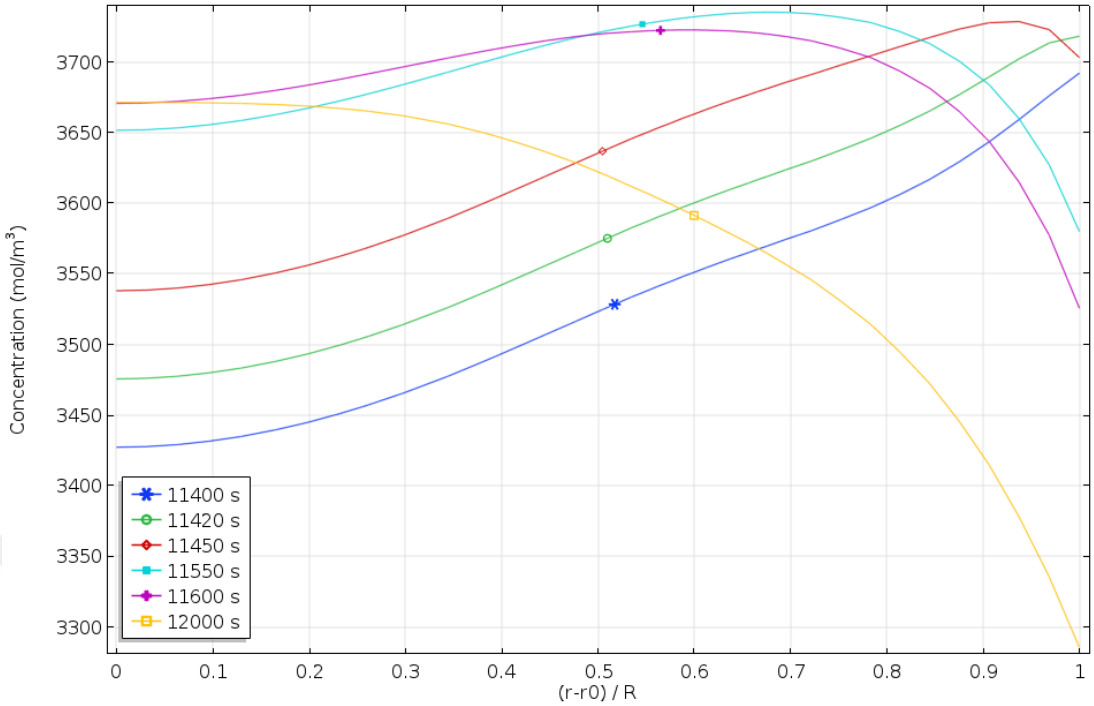

Figure 36. Concentration profile of Config. 3. in desorption stage with respect to radial position in the reactor bed and time.

Concentration profile of desorption stage is visualized in 2D domain as in Figure 37. Exposure of high temperature shows its effect in 3rd visual in below image. Adsorbent material that is close to the fins which is colored in blue hue does have a lower concentration than the adjacent middle parts. Inner parts also have low concentration, but since this area was dead because of its high temperature state in adsorption stage, it could not contain high concentration from the beginning of the stage.

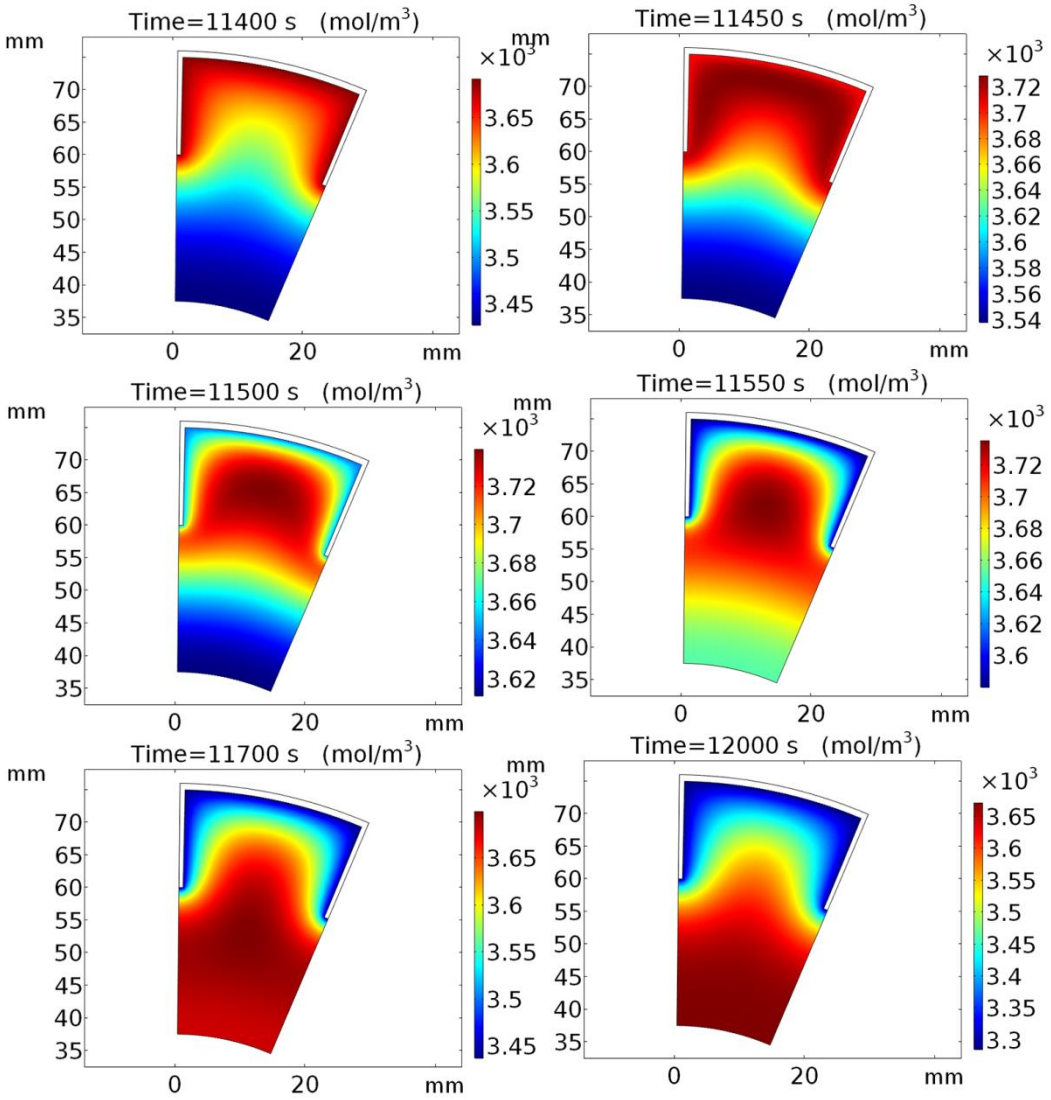

Figure 37. 2D snapshots of concentration profiles of Config. 3 in desorption stage at their specified time.

The temperature profile of the above-named stage of bed is given in Figure 38. As figure depicts, the increase in temperature of outer parts was significantly high and inner parts followed it later. Evidently, placing the rate of heat increment aside, the temperature increment was 5°C more than the unfinned configuration in inner parts.

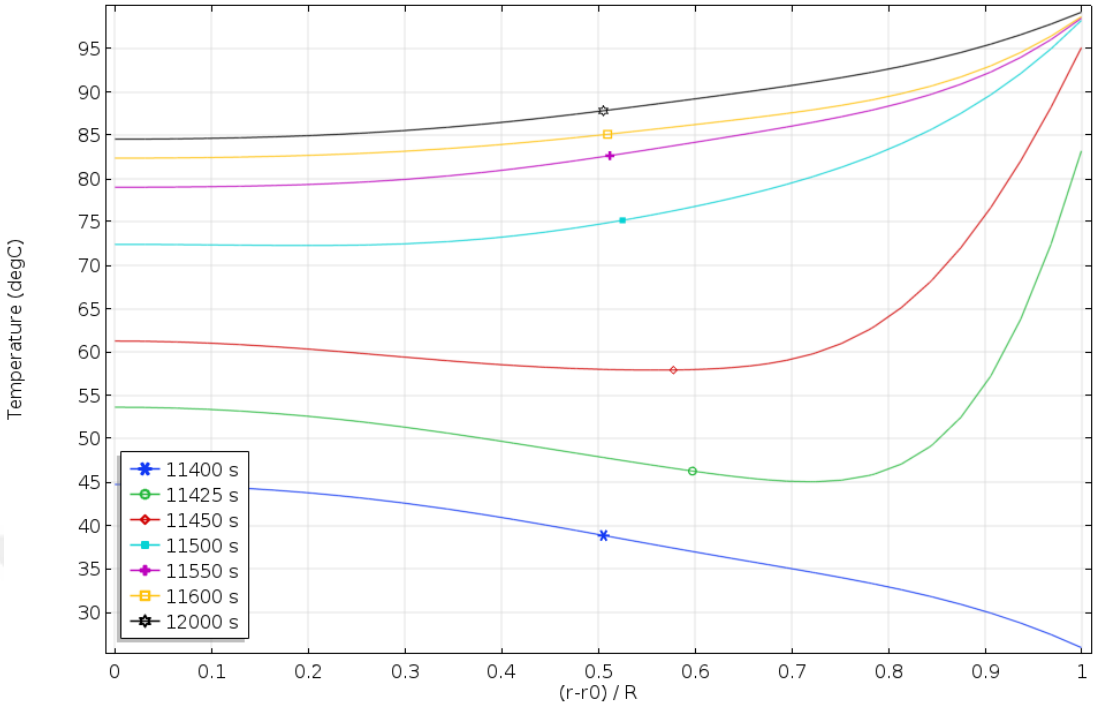

Figure 38. Temperature profile of Config. 3. in desorption stage with respect to radial position in the reactor bed and time.

2D images of temperature profiles in the specified stage are given in Figure 39. According to visuals, while outer parts rapidly reached the temperature of heating fluid, inner parts reacted to change much later. Additionally, the given duration of time in the current stage was not enough for bed to have a uniform temperature distribution.

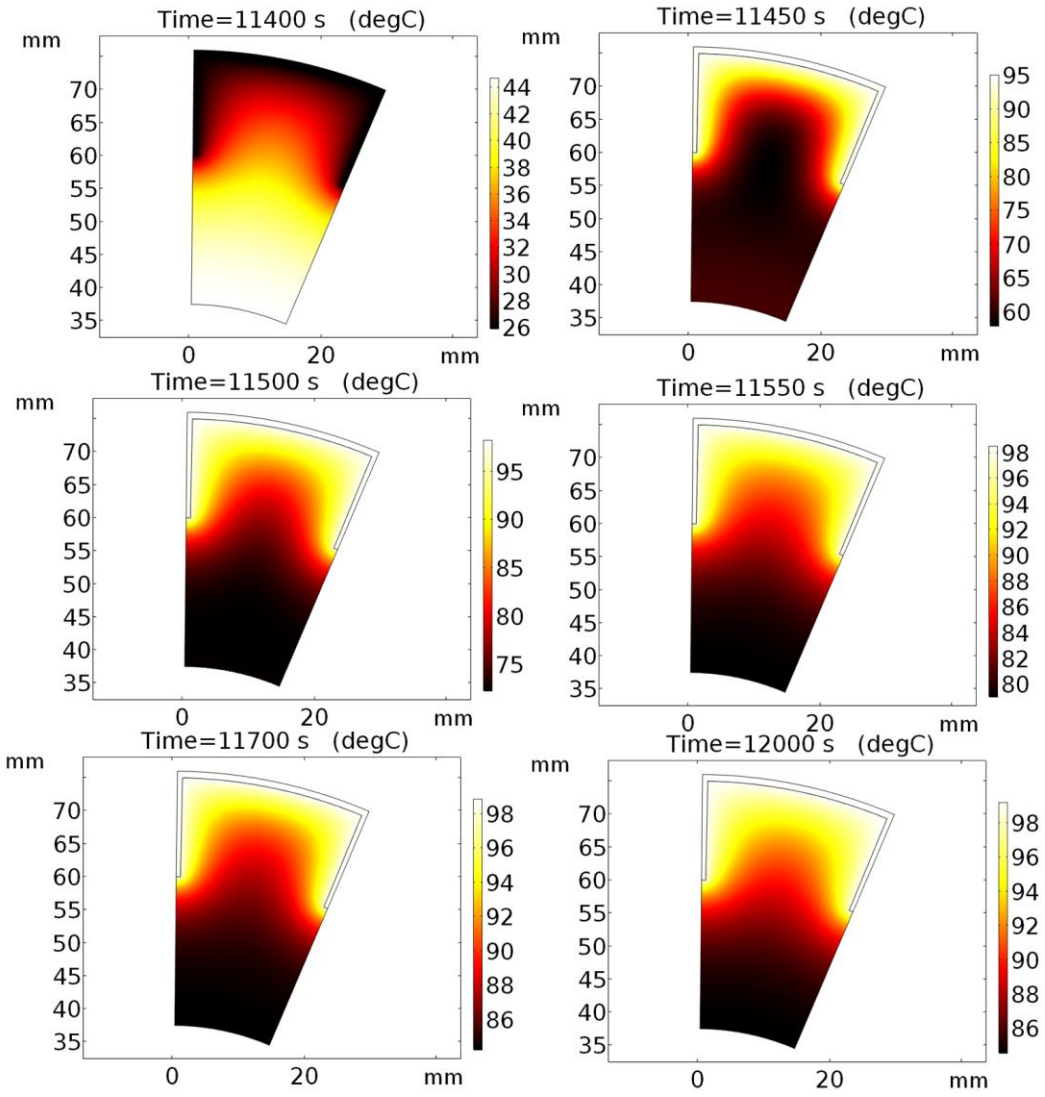

Figure 39. 2D snapshots of temperature profiles of Config. 3 in desorption stage at their specified time.

5.2.3 Fully-finned Configuration (Config. 4)

In order to see maximum possible performance growth, fins are placed in the reactor bed in such a way that the height of fins reaches to inner radius. The graph of the overall adsorption amount is given in Figure 40. As shown in the graph, the bed got steady and exhibited similar behavior after the 4^{th} cycle. Compared to previous configurations, the total time required for the removal of initial conditions is significantly lowered.

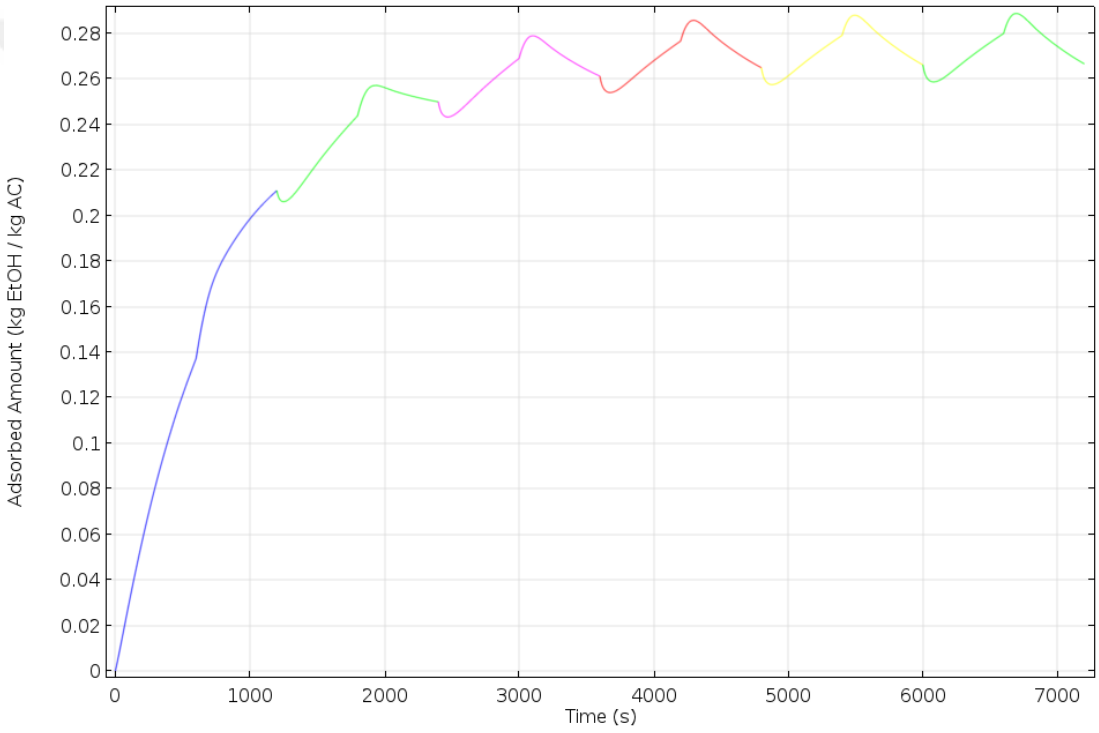

Figure 40. Total adsorbed amount of ethanol(kg/kg) with respect to time for Config. 4. Each color represents a cycle.

Adsorption stage of the last cycle is given in Figure 41. According to the graph, in the first 80 seconds, the bed recovered from exposure of low pressure and started increasing its adsorbed vapor amount steadily. When compared to the finless configuration, total recovery time is decreased by half which strongly increased the

total amount of adsorbed vapor. Total adsorbed amount of vapor is increased from 2.7 to 2.84 during the adsorption process. Surely, the total adsorbed amount could be increased even further if the bed was allowed to operate for more duration of time.

.

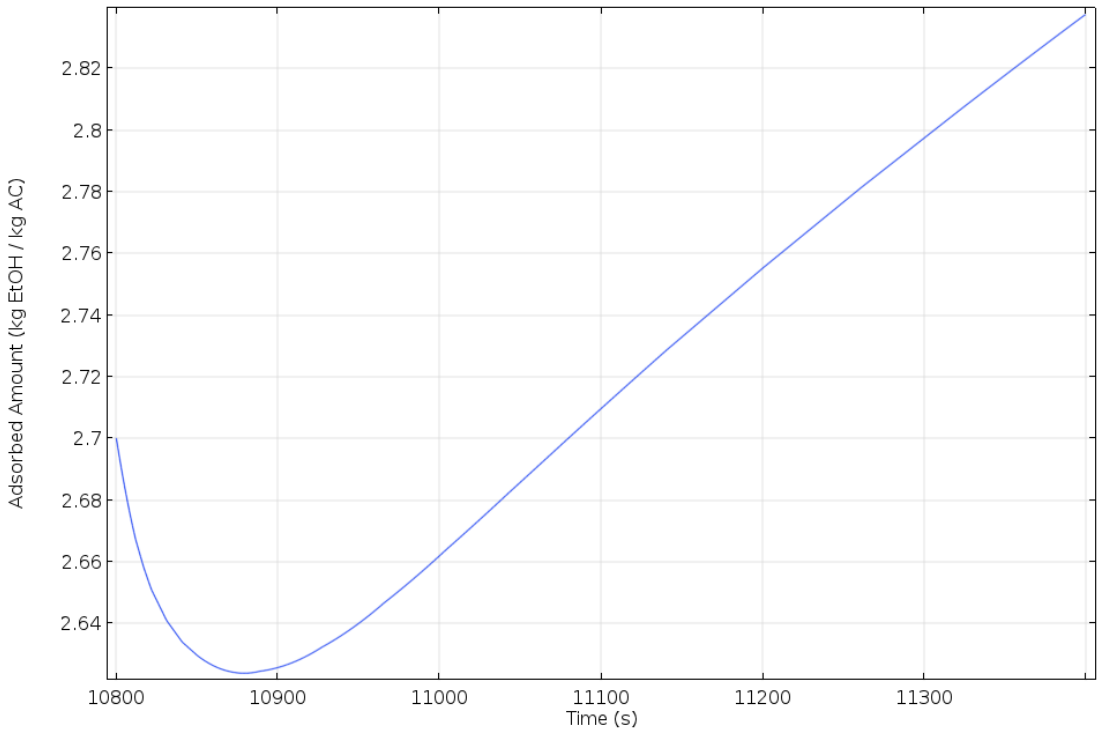

Figure 41. Total adsorbed amount of ethanol(kg/kg) with respect to time in adsorption stage of the last cycle.

Figure 42 shows concentration profile of bed in adsorption stage. The figure gives that, for first 50 seconds, the bed lost dramatically its accumulated vapor mainly in middle and inner regions and for the next 30 seconds, the change amount was minimal. After balance of pressure is obtained and effects of efficient cooling have started, the bed rapidly deposited adsorbate vapor in all parts. Such change evidently shows that having longer fins placed in the bed allows concentration to be accumulated homogenously.

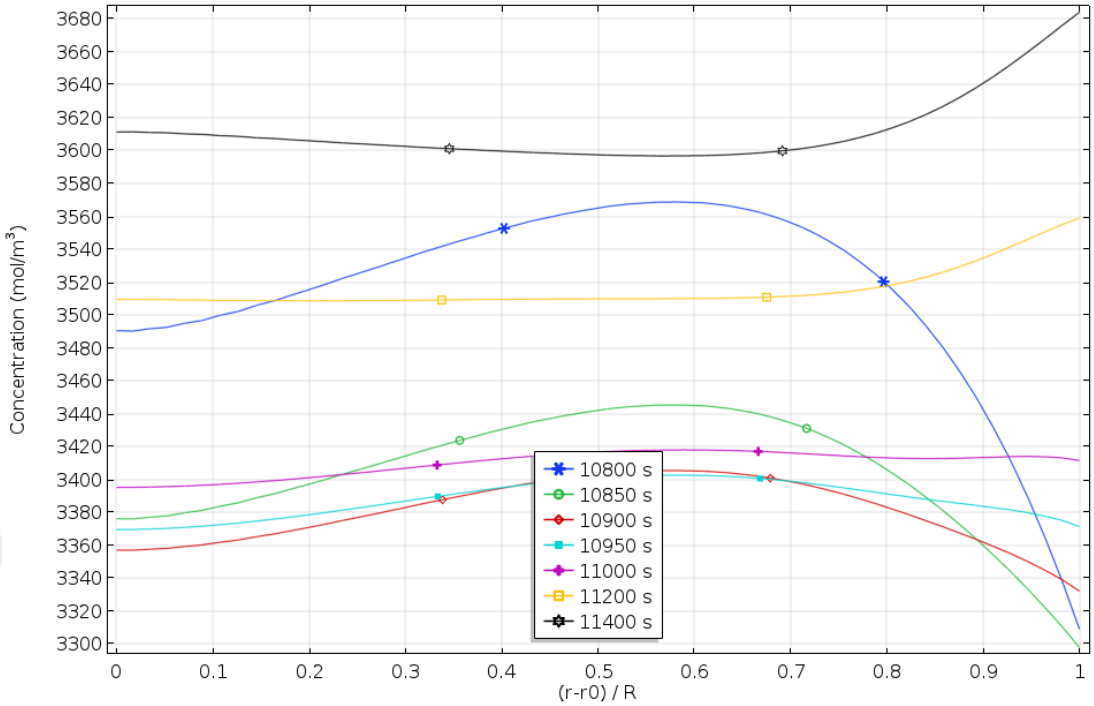

Figure 42. Concentration profile of Config. 4. in adsorption stage with respect to radial position in the reactor bed and time.

Additionally, 2D images of concentration profile of the bed that is in adsorption stage are given in Figure 43. Change in geometry provided a solution to the regions that were unresponsive in previous configurations. Unlike all other geometries, the middle parts that right in between fins has the lowest concentration at the end of the adsorption stage.

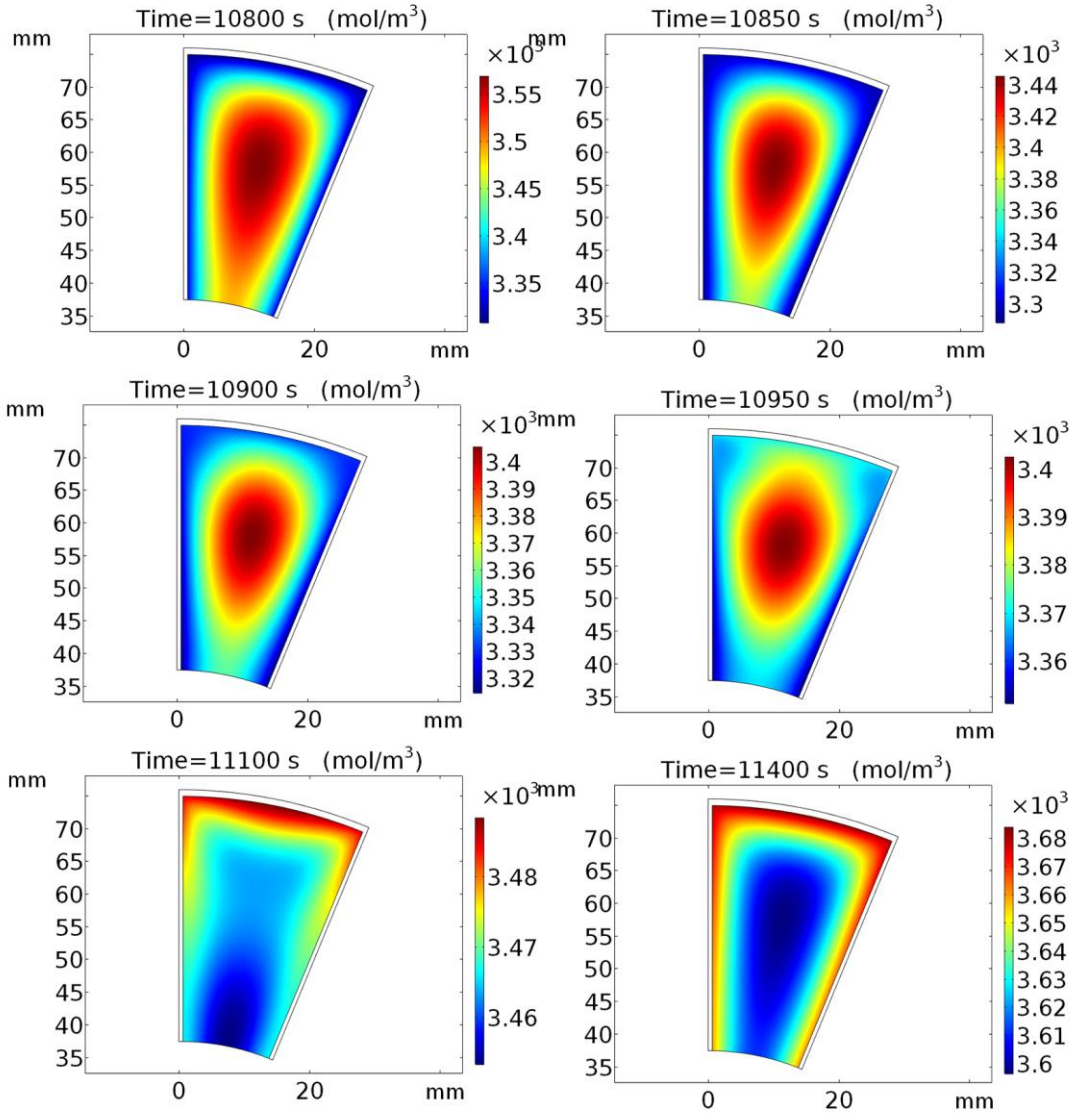

Figure 43. 2D snapshots of concentration profiles of Config. 4 in adsorption stage at their specified time.

When the temperature profile of adsorption stage is inspected in Figure 44, It is seen that allowing fins to reach inner areas granted better overall cooling. Outer parts still give the initial response to this change, but middle and inner parts follow shortly after. Because of the efficient cooling that provided by fins, the bed almost reached its equilibrium temperature heat profile in 200 seconds, therefore last 400 seconds waited mainly for vapor uptake.

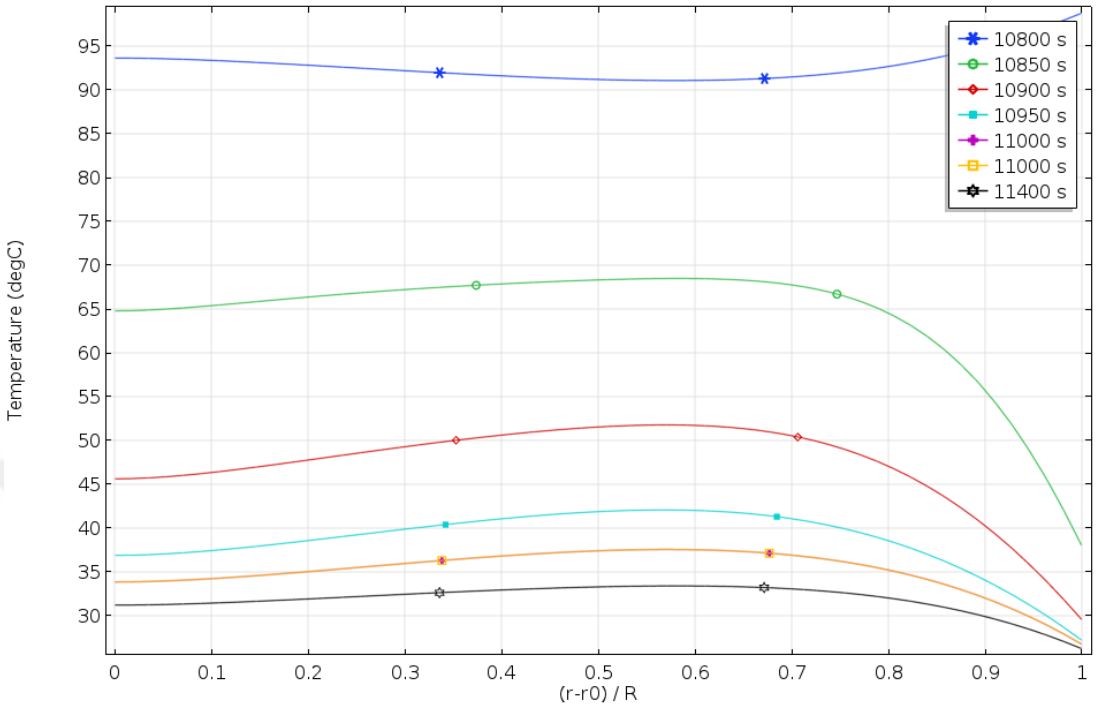

Figure 44. Temperature profile of Config. 4. in adsorption stage with respect to radial position in the reactor bed and time.

Temperature profile of the currently mentioned bed is also given as 2D images in Figure 45. Even though temperature distribution range was so narrow, the middle parts had the highest temperature values at the end of adsorption stage.

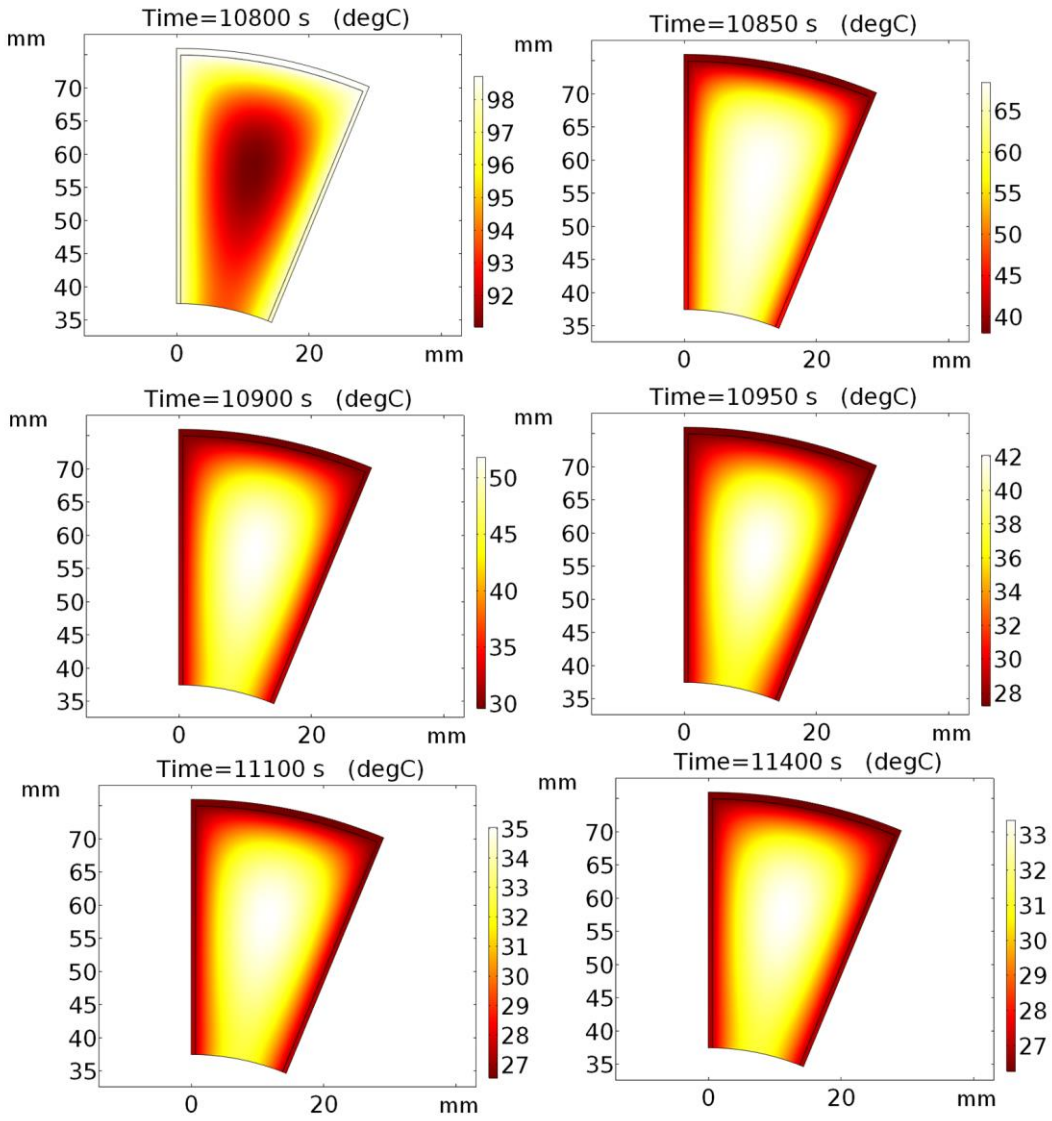

Figure 45. 2D snapshots of temperature profiles of Config. 4 in adsorption stage at their specified time.

Vapor uptake graph of the last cycle in desorption stage is given in Figure 46. As demonstrated in the figure, being suddenly subjected to high pressure has increased overall uptake in desorption stage. After 90 seconds, applied heating took part and reduced the uptake amount as intended.

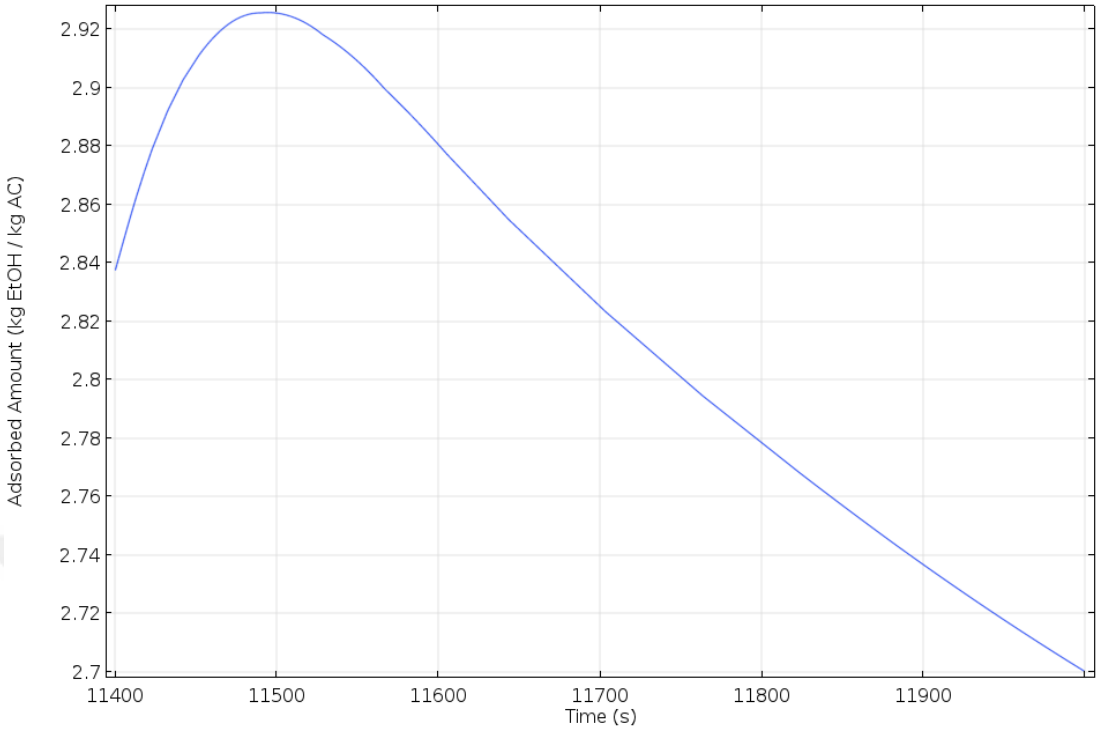

Figure 46. Total adsorbed amount of ethanol(kg/kg) with respect to time in desorption stage of the last cycle.

Concentration profile that was observed in this stage is given in Figure 47. According to the figure, the concentration of adsorbed vapor increased mainly in middle and inner parts of the bed, and after the pressure effects are balanced, outer parts quickly released the contained vapor and this trend is followed by middle and inner parts. Having full length fins in designed bed clearly supported temperature alteration to reach inner parts.

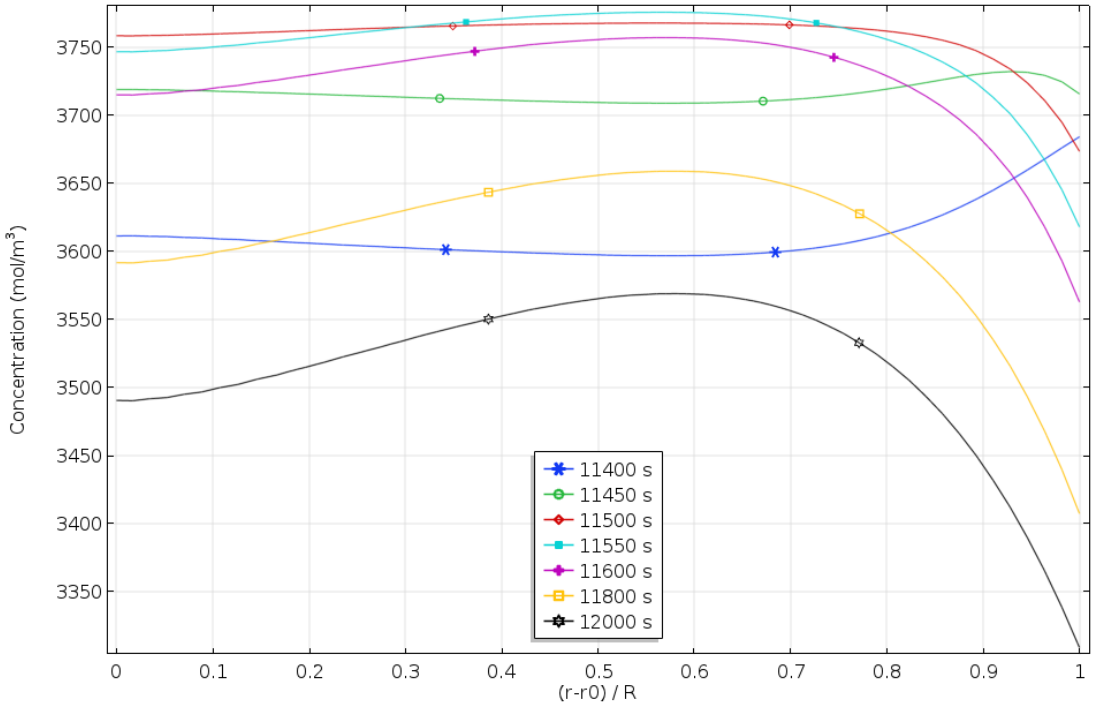

Figure 47. Concentration profile of Config. 4. in desorption stage with respect to radial position in the reactor bed and time.

Two dimensional images of concentration profile of reactor bed in desorption stage is given in Figure 48. Contrary to the previous stage, areas that are close to fins rapidly switched to desorption process but the middle part that is away from fins had the reaction delayed.

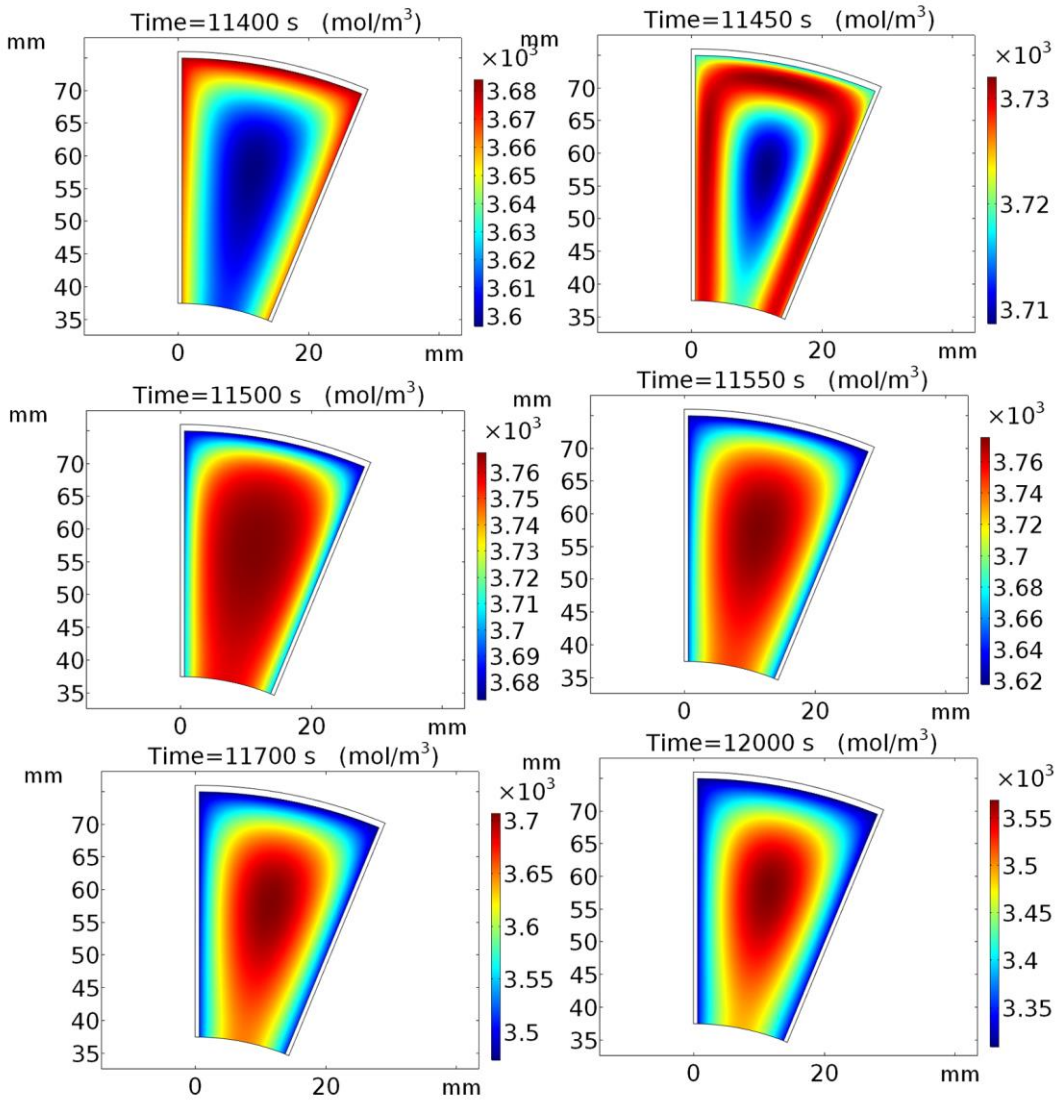

Figure 48. 2D snapshots of concentration profiles of Config. 4 in desorption stage at their specified time.

Temperature profile of the aforementioned stage is given in Figure 49. Fast temperature increments in middle and inner parts which led by drastically change in outer parts provided more efficient heating over the bed.

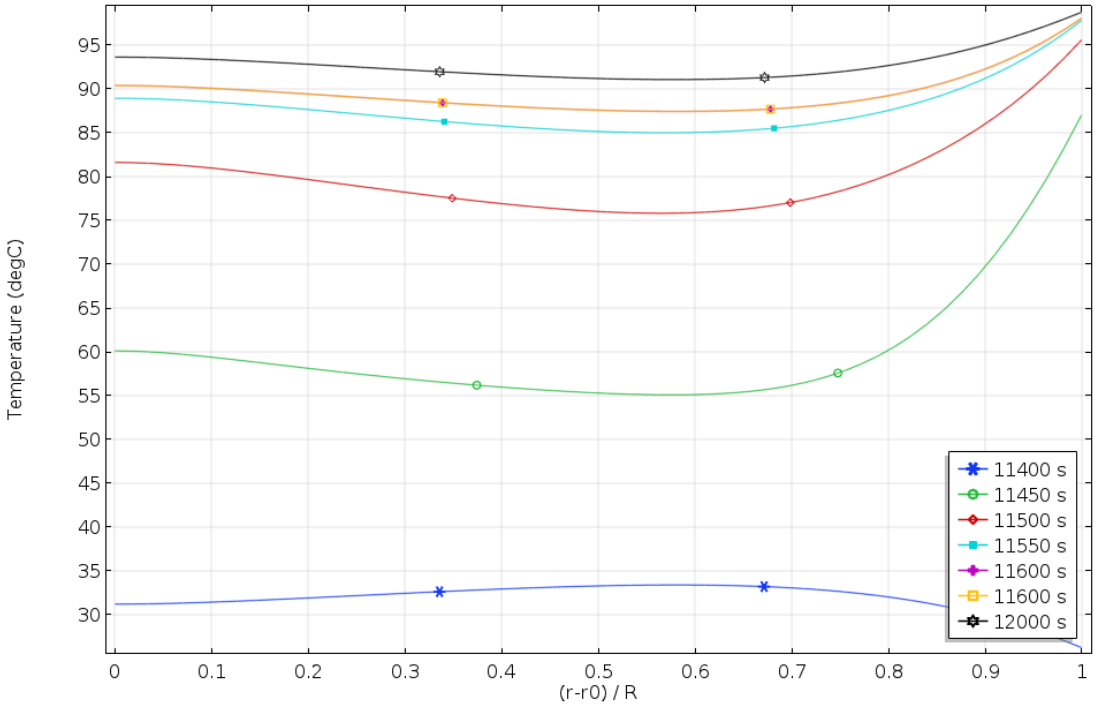

Figure 49. Temperature profile of Config. 4. in desorption stage with respect to radial position in the reactor bed and time.

Temperature profile of the reactor bed in desorption stage was visualized in 2D images in Figure 50.

Increased bed geometry with the purpose of having higher adsorption capacity had failed in the initial design but added internal fins provided better heating/cooling according to the stage, turned a non-operational design into a responsive one. In addition to this, dead and unresponsive regions that reside in inner parts of the bed got activated and caught up the similar behavior as the outer parts with modified geometry. The approach of adding internal fins to cylindrical geometry with intentions of eliminating thermal resistance was acknowledged. This result also shows that even larger beds for industrial purposes could be built, and heat transfer problem could be eliminated by losing a bit amount of packed bed area.

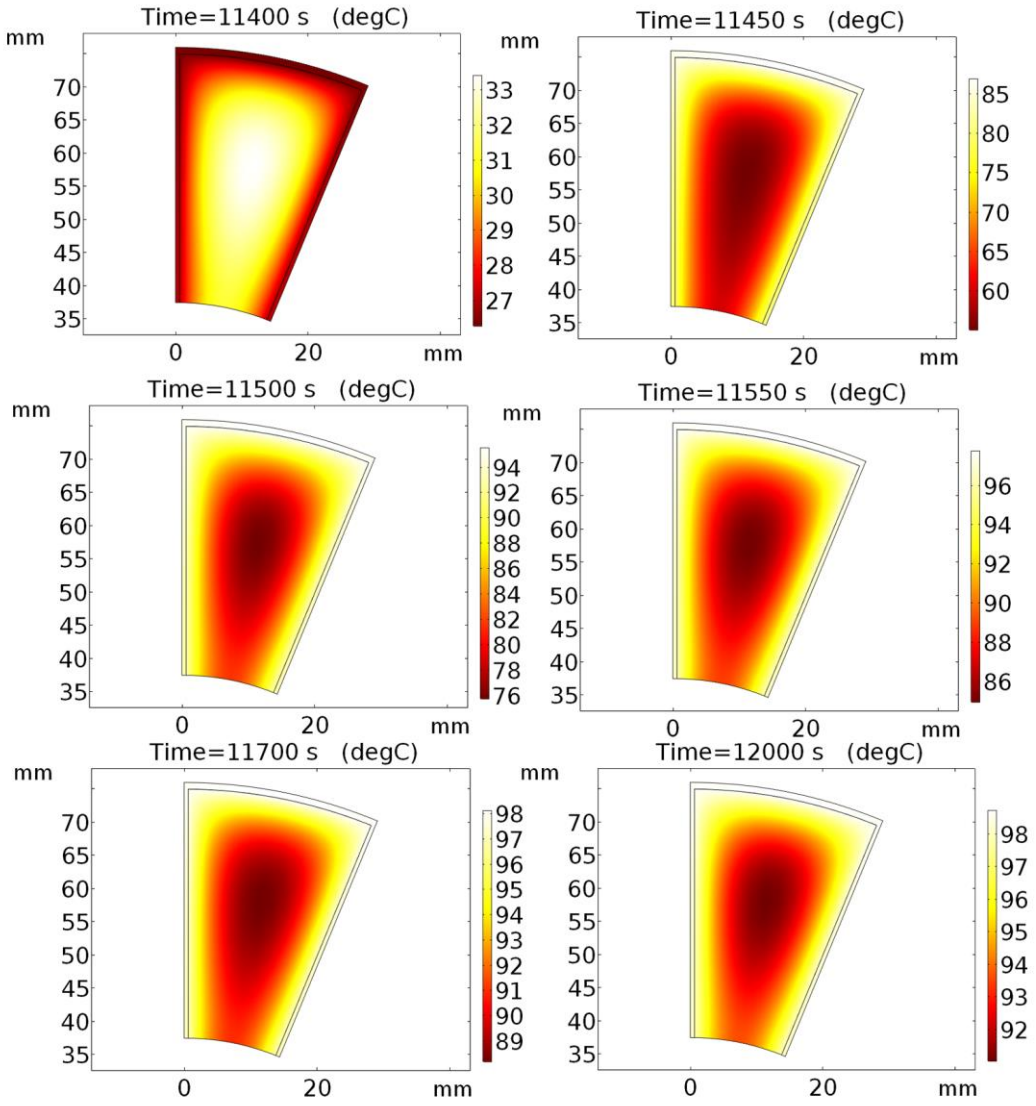

Figure 50. 2D snapshots of temperature profiles of Config. 4 in desorption stage at their specified time.

5.3 COP & Power Values of Designed Systems

5.3.1 COP Values

The COP values are calculated for each system and the results are given in Table 3. The '-' symbol is used when the system failed because of total number of adsorbed vapor decreased in adsorption stage.

Table 3. COP values of four different configurations with respect to different cycle operation times. NI: Not Inspected.

COP	600s	900s	1200s
Config. 1	0.3845	NI	NI
Config. 2	–	–	–
Config. 3	–	0.2661	0.3477
Config. 4	0.2821	0.3963	0.4613

Config. 2 has failed in all three cycle operation times due to its thermal incapability caused by its increased volume whereas config. 3 only failed in 600 seconds of operation time and config. 4 achieved good COP values in all three cases. Only 3.4% fin volume difference allowed the latest bed to achieve 49% increment in COP value in 900 seconds cycle and 33% increment in 1200 seconds of operation time.

As cycle time increases, the amount of vapor adsorbed and desorbed also increases since more time is allowed for the bed to come closer to the equilibrium. Therefore, there is a consistent increase in COP values with respect to cycle times.

5.3.2 Power Values

Operating the bed at high cycle times results in higher COP values as shown earlier. On the other hand, as the bed gets closer and closer to the equilibrium, rate of adsorption or desorption decreases. Therefore, an increase in the amount of energy upgraded associated with the long cycle times may be overshadowed by the long cycle times giving rise to the limited cooling power gains.

Calculated cooling power values are given in Table 4. As in COP calculation, the unfinned geometry of Config. 2 failed to bring up a value due to negative value of adsorbed amount of vapor as the adsorption or desorption processes in the bed could not keep up with the respective cycles.

Table 4. Cooling power values of four different configurations with respect to different cycle operation times. NI: Not Inspected.

Power (W)	600s	900s	1200s
Config. 1	11.26	NI	NI
Config. 2	–	–	–
Config. 3	–	39.46	48.89
Config. 4	72.05	92.64	95.21

The thermal resistance has been eliminated and more uniform temperature distribution is obtained with modified geometries, which promoted higher overall concentration difference between adsorption and desorption stages. This difference provided better performance with a forfeiting a negligible area of packed domain.

In 600 seconds of stage time, 9 times increased geometry with added internal fins of config. 4 results in almost 7 times more cooling power in spite of its larger diameter than that of config. 1. This value increased by 28% when stage times are changed to 900 seconds. For config. 4 higher than 900 second cycle time gives rise to a negligible increase in the power outcome. The results also show that a bed which was unable to operate in the unmodified case were able to work as intended after heat transfer limitations are lifted via added internal fins.

Additionally, while config. 2 in each case gives no power/kg value due to low adsorption amount, config. 3 in 900 seconds of stage time has 5.32 W/kg and this value is equal to 6.6 W/kg for 1200 seconds of stage time. In config. 4, power per kg values are 9.96, 12.81 and 13.20 for 600, 900 and 1200 seconds of stage times, respectively.

For 1 kilowatt of power, eleven tubes of config. 4 or twenty-one tubes of config. 3 should be operated in 1200 seconds of stage time. For same power value, 900 seconds of stage operation time should be preferred with eleven tubes of config. 4 and 25 tubes of config. 3.

CHAPTER 6

CONCLUSIONS

This study deals with having more COP and power values by increasing adsorption uptake of the pre-defined adsorbent-adsorbate pair by changing several parameters such as reactor bed size, internal fin volume and cycle time. The analysis of results leads to the following conclusions:

1. As described previously, heat transfer limitations have an important role on the performance of the system as well as reaction kinetics of selected pair. For optimum result, both reaction kinetics and heat transfer characteristics should be considered while designing such adsorption heat pump systems.
2. Having high bed diameter with the intention of increasing adsorbent amount should increase adsorption uptake intuitively, but such case brings up heat transfer limitations because of low thermal conductivity values of adsorbent material which will result in non-homogenous thermal profile in reactor bed. Even though heat removal can be completed by having more operation time, the added time will decrease the power outcome of the bed which will destroy its main purpose of usage.
3. 10 distinct geometries are thoroughly modeled and simulated in COMSOL Multiphysics software. Among these simulations;
    a. Config. 1 has low bed thickness which promotes better heat transfer that results in a good COP value of 0.38 for 600 seconds of stage time. Since thermal performance was good, other stage time variations were skipped.

b. Config. 2 with high bed diameter but no fins resulted in almost no vapor to be contained in reactor bed. The designed bed failed to bring a COP value of each stage time.
c. In config. 3, the internal fins reach up to middle parts of reactor bed and grants better thermal performance. This bed underperformed in 600 seconds of stage time, but it delivered COP value of 0.2661 and 0.3477, with power per kg values of 5.32 and 6.6 for 900 seconds and 1200 seconds of stage times, respectively.
d. In the case of config. 4, where fins could reach the inner bed performed well for all 3 stage times. This bed attained COP values of 72.05, 92.64 and 95.21 and power/kg values of 9.96, 12.81 and 13.20 for 600, 900 and 1200 seconds of stage times, respectively.

4. Usage of internal fins works well for such systems. The long fins that penetrate the adsorbent material could reach dead areas in terms of heat transfer, which will aid accessing those places and will turn them into operational zones. Uniform concentration profile could be achieved by this method and thus will result in increased COP and power values.
5. Allowing more adsorbate to be accumulated in reactor bed by increasing the cycle time will result in higher COP value, but this act will lower cooling power because of consumption of more time. Since the first necessity of chemical heat pumps systems is cooling power, the cycle time should be selected optimally for this requirement.
6. Adsorption heat pumps with modified geometries for higher adsorption capacities and better heat transfer domain could be used in industry where waste or unused energy is available. Requiring inexpensive materials to build and lacking maintenance in short operation times, this type of heat pumps are perfect for re-evaluating waste energy.

REFERENCES

Ahmed, M. S., Abd, A., & Shehata, E.-K. (n.d.). A REVIEW: FUTURE OF THE ADSORPTION WORKING PAIRS IN COOLING. Retrieved from http://ultracrib.com/wp-content/uploads/2014/04/1337695528.4453A-Rewiew-Future-of-the-Adsorpt.pdf

Ambrose, D., Sprake, C. H. ., & Townsend, R. (1975). Thermodynamic properties of organic oxygen compounds XXXVII. Vapour pressures of methanol, ethanol, pentan-1-ol, and octan-1-ol from the normal boiling temperature to the critical temperature. *The Journal of Chemical Thermodynamics*, *7*(2), 185–190. https://doi.org/10.1016/0021-9614(75)90267-0

Anyanwu, E. E., & Ezekwe, C. I. (2003). Design, construction and test run of a solid adsorption solar refrigerator using activated carbon/methanol, as adsorbent/adsorbate pair. *Energy Conversion and Management*, *44*(18), 2879–2892. https://doi.org/10.1016/S0196-8904(03)00072-4

Anyanwu, E. E., & Ogueke, N. V. (2005). Thermodynamic design procedure for solid adsorption solar refrigerator. *Renewable Energy*, *30*(1), 81–96. https://doi.org/10.1016/J.RENENE.2004.05.005

Askalany, A. A., Henninger, S. K., Ghazy, M., & Saha, B. B. (2017). Effect of improving thermal conductivity of the adsorbent on performance of adsorption cooling system. *Applied Thermal Engineering*, *110*, 695–702. https://doi.org/10.1016/J.APPLTHERMALENG.2016.08.075

Bidyut Baran Saha, *,†, Ibrahim I. El-Sharkawy, †, Anutosh Chakraborty, †, Shigeru Koyama, †, Seong-Ho Yoon, ‡ and, & Ng§, K. C. (2006). Adsorption Rate of Ethanol on Activated Carbon Fiber. https://doi.org/10.1021/JE060071Z

Chekirou, W., Boukheit, N., & Karaali, A. (2016). Heat recovery process in an adsorption refrigeration machine. *International Journal of Hydrogen Energy*, *41*(17), 7146–7157. https://doi.org/10.1016/J.IJHYDENE.2016.02.070

Douss, N., Meunier, F. E., & Sun, L. M. (1988). Predictive model and experimental results for a two-adsorber solid adsorption heat pump. *Industrial & Engineering Chemistry Research*, *27*(2), 310–316. https://doi.org/10.1021/ie00074a017

González, M. I., & Rodríguez, L. R. (2007). Solar powered adsorption refrigerator with CPC collection system: Collector design and experimental test. *Energy Conversion and Management*, *48*(9), 2587–2594. https://doi.org/10.1016/J.ENCONMAN.2007.03.016

Jribi, S., Miyazaki, T., Saha, B. B., Koyama, S., Maeda, S., & Maruyama, T. (2016). Corrected adsorption rate model of activated carbon–ethanol pair by means of

CFD simulation. *International Journal of Refrigeration*, *71*, 60–68. https://doi.org/10.1016/J.IJREFRIG.2016.08.004

Kawasaki, H., Kanzawa, A., & Watanabe, T. (1998). Characteristics of Chemical Heat Pump through Kinetic Analysis of Paraldehyde Depolymerization. *JOURNAL OF CHEMICAL ENGINEERING OF JAPAN*, *31*(3), 374–380. https://doi.org/10.1252/jcej.31.374

Li, Z. F., & Sumathy, K. (1999). A solar-powered ice-maker with the solid adsorption pair of activated carbon and methanol. *International Journal of Energy Research*, *23*(6), 517–527. https://doi.org/10.1002/(SICI)1099-114X(199905)23:6<517::AID-ER495>3.0.CO;2-B

Menard, D., Py, X., & Mazet, N. (2005). Activated carbon monolith of high thermal conductivity for adsorption processes improvement: Part A: Adsorption step. *Chemical Engineering and Processing: Process Intensification*, *44*(9), 1029–1038. https://doi.org/10.1016/J.CEP.2005.02.002

Miltkau, T., & Dawoud, B. (2002). Dynamic modeling of the combined heat and mass transfer during the adsorption/desorption of water vapor into/from a zeolite layer of an adsorption heat pump. *International Journal of Thermal Sciences*, *41*(8), 753–762. https://doi.org/10.1016/S1290-0729(02)01369-8

San, J.-Y. (2006). Analysis of the performance of a multi-bed adsorption heat pump using a solid-side resistance model. *Applied Thermal Engineering*, *26*(17–18), 2219–2227. https://doi.org/10.1016/J.APPLTHERMALENG.2006.03.013

San, J.-Y., & Lin, W.-M. (2008). Comparison among three adsorption pairs for using as the working substances in a multi-bed adsorption heat pump. *Applied Thermal Engineering*, *28*(8–9), 988–997. https://doi.org/10.1016/J.APPLTHERMALENG.2007.06.026

TeGrotenhuis, W. E., Humble, P. H., & Sweeney, J. B. (2012). Simulation of a high efficiency multi-bed adsorption heat pump. *Applied Thermal Engineering*, *37*, 176–182. https://doi.org/10.1016/J.APPLTHERMALENG.2011.11.012

Tso, C. Y., Chao, C. Y. H., & Fu, S. C. (2012). Performance analysis of a waste heat driven activated carbon based composite adsorbent – Water adsorption chiller using simulation model. *International Journal of Heat and Mass Transfer*, *55*(25–26), 7596–7610. https://doi.org/10.1016/J.IJHEATMASSTRANSFER.2012.07.064

Wang, L. W., Wang, R. Z., Lu, Z. S., Chen, C. J., Wang, K., & Wu, J. Y. (2006). The performance of two adsorption ice making test units using activated carbon and a carbon composite as adsorbents. *Carbon*, *44*(13), 2671–2680. https://doi.org/10.1016/J.CARBON.2006.04.013

Wang, L. W., Wang, R. Z., Wu, J. Y., Wang, K., & Wang, S. G. (2004). Adsorption ice makers for fishing boats driven by the exhaust heat from diesel engine:

choice of adsorption pair. *Energy Conversion and Management*, *45*(13–14), 2043–2057. https://doi.org/10.1016/J.ENCONMAN.2003.10.021

Wang, R. ., Wu, J. ., Xu, Y. ., & Wang, W. (2001). Performance researches and improvements on heat regenerative adsorption refrigerator and heat pump. *Energy Conversion and Management*, *42*(2), 233–249. https://doi.org/10.1016/S0196-8904(99)00189-2

Yurtsever, A. O., Karakas, G., & Uludag, Y. (2013). Modeling and computational simulation of adsorption based chemical heat pumps. *Applied Thermal Engineering*, *50*(1), 401–407. https://doi.org/10.1016/j.applthermaleng.2012.07.009

Ziegler, E. N. (1971). Chemical engineering kinetics, second edition. J. M. Smith, McGraw-hill, book Co., New York, 1970. 612 pp. *Journal of Polymer Science Part B: Polymer Letters*, *9*(3), 229–230. https://doi.org/10.1002/pol.1971.110090314

APPENDICES

APPENDIX A

A.A Program Code for Wmax Values

```
In[5]:= Clear["Global`*"]
c = 0.35 * 550000 / 46;
a =
  ((0.3955 * Exp[-0.0006049 * (T * (Log[(10^(5.24667 - (1598.673 / (T - 46.424))) / P)]))^
        1.156])) - (c * 46 / 550000);
For[T = 293, T <= 363 , T = T + 5, Print[T, NSolve[a == 0, P, Reals]]]
(*NSolve[a==0,{P},Reals]*)
293{{P→0.0413883}}
298{{P→0.0560003}}
303{{P→0.0748857}}
308{{P→0.0990369}}
313{{P→0.129614}}
318{{P→0.167965}}
323{{P→0.215638}}
328{{P→0.274403}}
333{{P→0.346267}}
338{{P→0.433488}}
343{{P→0.538594}}
348{{P→0.664398}}
353{{P→0.814009}}
358{{P→0.990846}}
363{{P→1.19865}}
```

A.B Calculation of COP and Power Values

COP VALUES

Formulation:

$$COP = \frac{\Delta H_v \, n_{ads}}{\Delta H_{ads} \, n_{ads} + C_{peff} \, m_{bed} \, \Delta T}$$

600 *s*

- CONFIG1

```
COP = (38600 * 0.305) / (49000 * 0.305 + 553 * 550 * 1472 * 10^-6 * 35)
0.384552
```

- CONFIG4

```
COP2 = (38600 * 0.138 * 16) / (49000 * 0.138 * 16 + 553 * 550 * 781 * 10^-6 * 16 * 51)
0.282191
```

900 s

- CONFIG3

```
COP3 = (38600 * 0.115 * 16) / (49000 * 0.115 * 16 + 553 * 550 * 807 * 16 * 10^-6 * 45)
0.266124
```

- CONFIG4

```
COP4 = (38600 * 0.27 * 16) / (49000 * 0.27 * 16 + 553 * 550 * 781 * 16 * 10^-6 * 55)
0.396353
```

1200 s

- CONFIG3

```
COP5 = (38600*0.19*16) / (49000*0.19*16 + 553*550*807*16*10^-6*48)
0.347722
```

- CONFIG4

```
COP6 = (38600*0.37*16) / (49000*0.37*16 + 553*550*781*16*10^-6*54)
0.461346
```

POWER VALUES

Formulation:

$$W_t = \frac{(n_{ads,final} - n_{ads,beginning}) * \Delta H_v}{TotalCycleTime}$$

600 *s*

■ CONFIG1

```
In[4]:= Wt = ((0.35) * 38600) / 1200
Out[4]= 11.2583
```

■ CONFIG4

```
In[5]:= Wt = ((0.14*16) * 38600) / 1200
Out[5]= 72.0533
```

900 s

■ CONFIG3

```
In[6]:= Wt = ((0.115*16) * 38600) / 1800
Out[6]= 39.4578
```

■ CONFIG4

```
In[7]:= Wt = ((0.27*16) * 38600) / 1800
Out[7]= 92.64
```

1200 s

- CONFIG3

```
In[8]:= Wt = ((0.19*16) * 38600) / 2400
Out[8]= 48.8933
```

- CONFIG4

```
In[9]:= Wt = ((0.37*16) * 38600) / 2400
Out[9]= 95.2133
```

APPENDIX B

B.A 900 Seconds of Cycle Operation Time.

B.A.A Config. 2

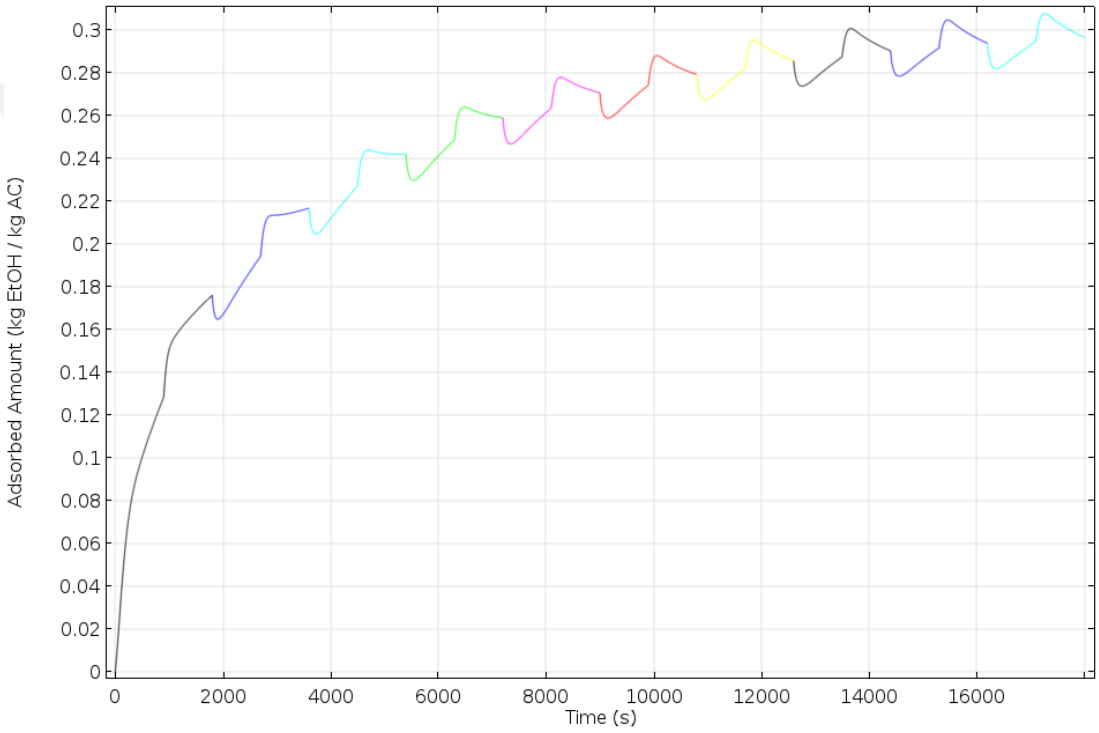

Figure 51. Total adsorbed amount of ethanol(kg/kg) with respect to time for Config. 2. Each color represents a cycle.

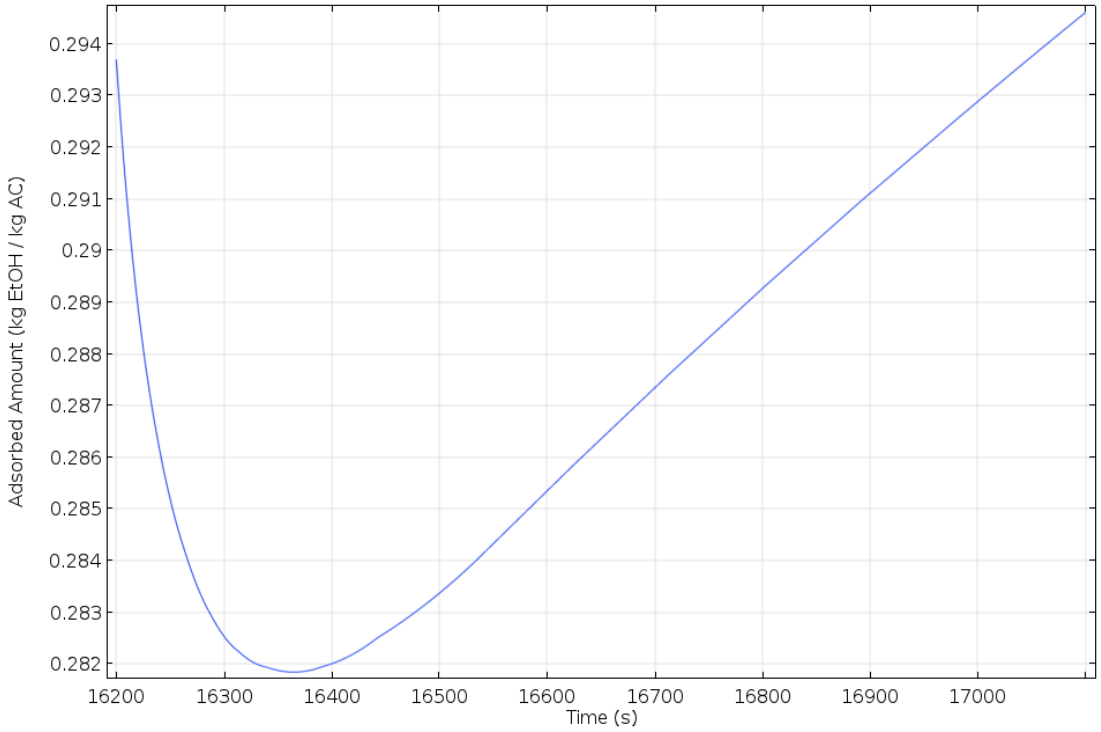

Figure 52. Total adsorbed amount of ethanol(kg/kg) with respect to time in adsorption stage of the last cycle.

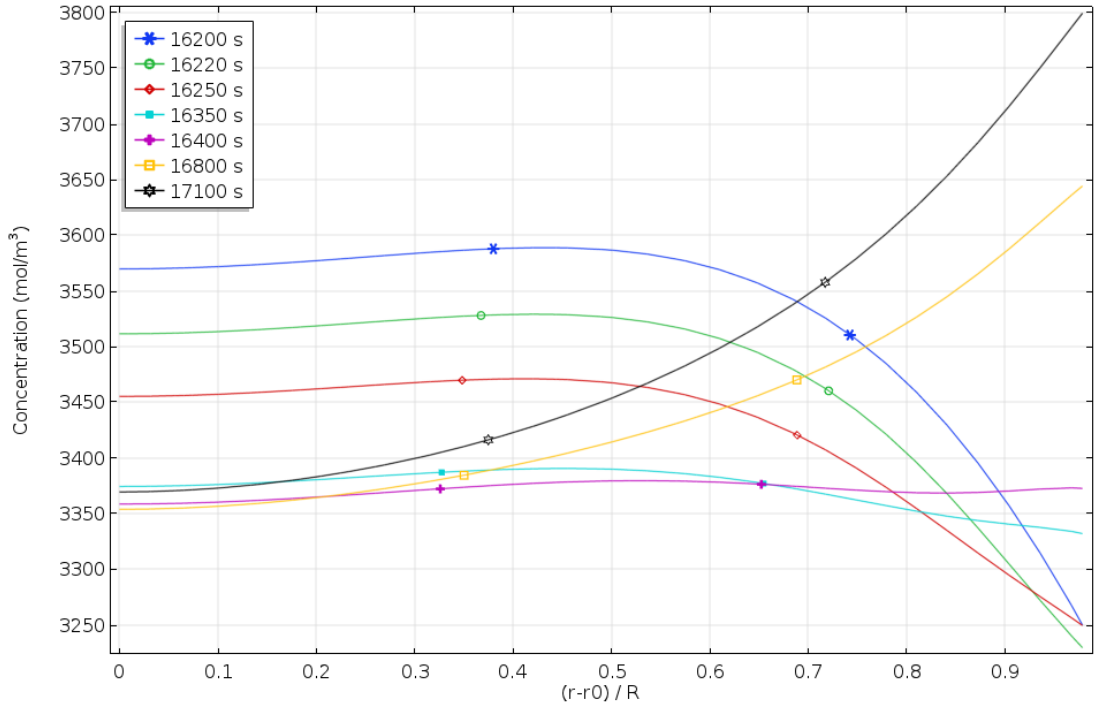

Figure 53. Concentration profile of Config. 2. in adsorption stage with respect to radial position in the reactor bed and time.

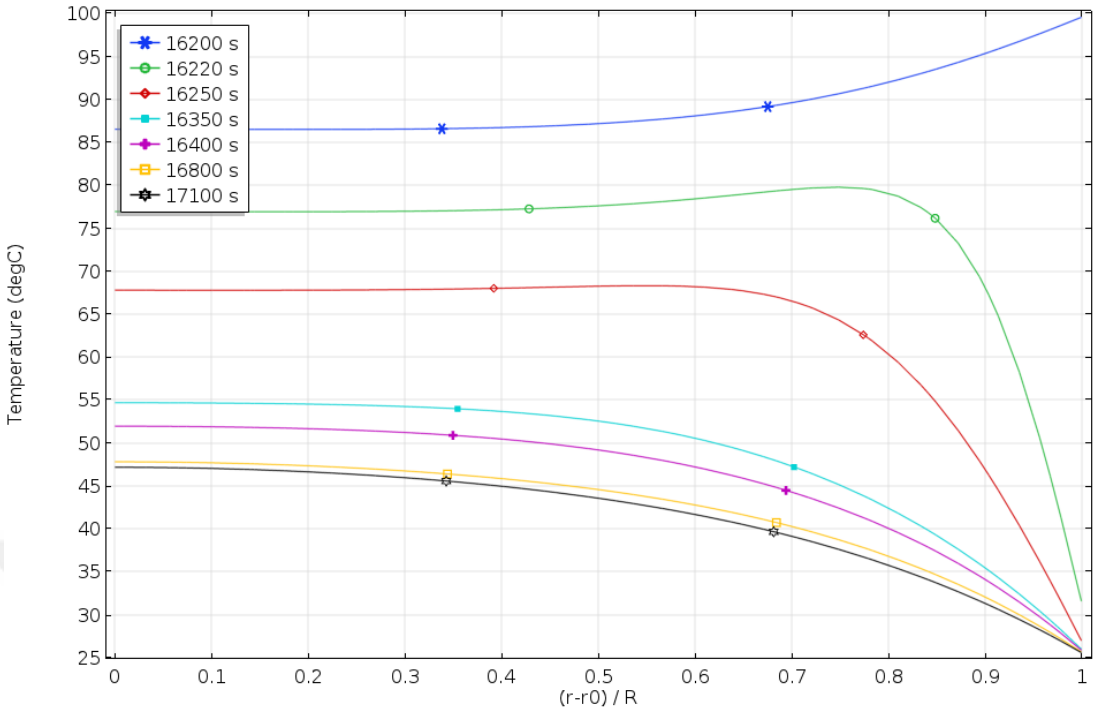

Figure 54. Temperature profile of Config. 4. in desorption stage with respect to radial position in the reactor bed and time.

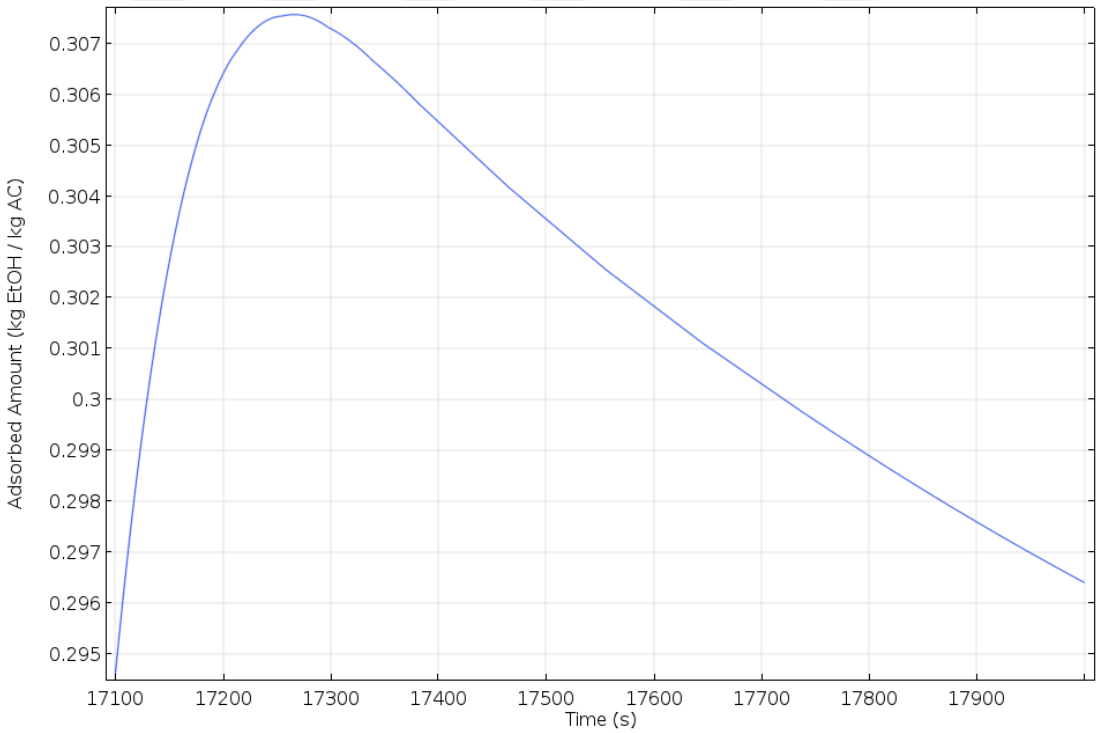

Figure 55. Total adsorbed amount of ethanol(kg/kg) with respect to time in desorption stage of the last cycle.

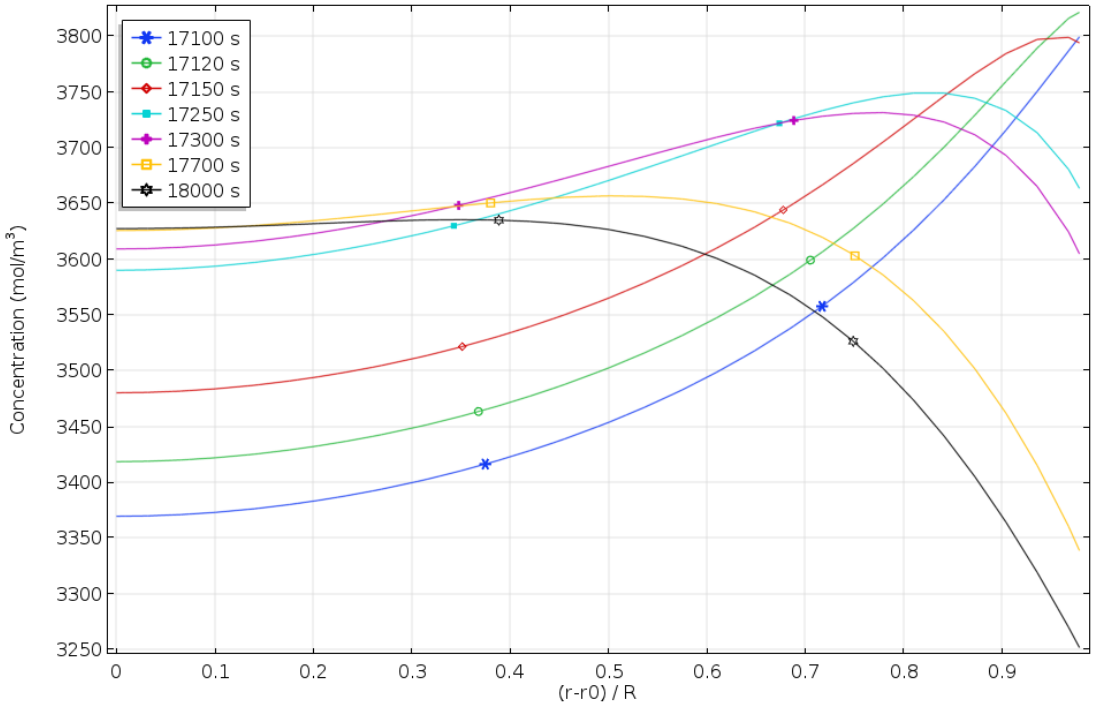

Figure 56. Concentration profile of Config. 2. in desorption stage with respect to radial position in the reactor bed and time.

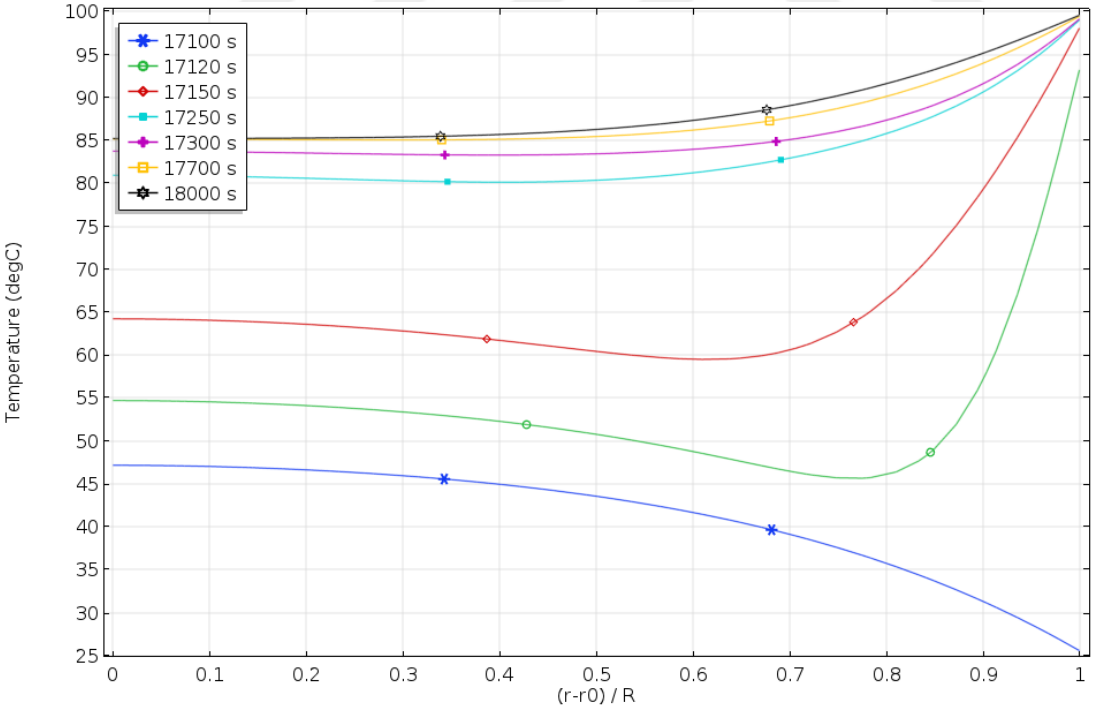

Figure 57. Temperature profile of Config. 2. in desorption stage with respect to radial position in the reactor bed and time.

B.A.B Config. 3

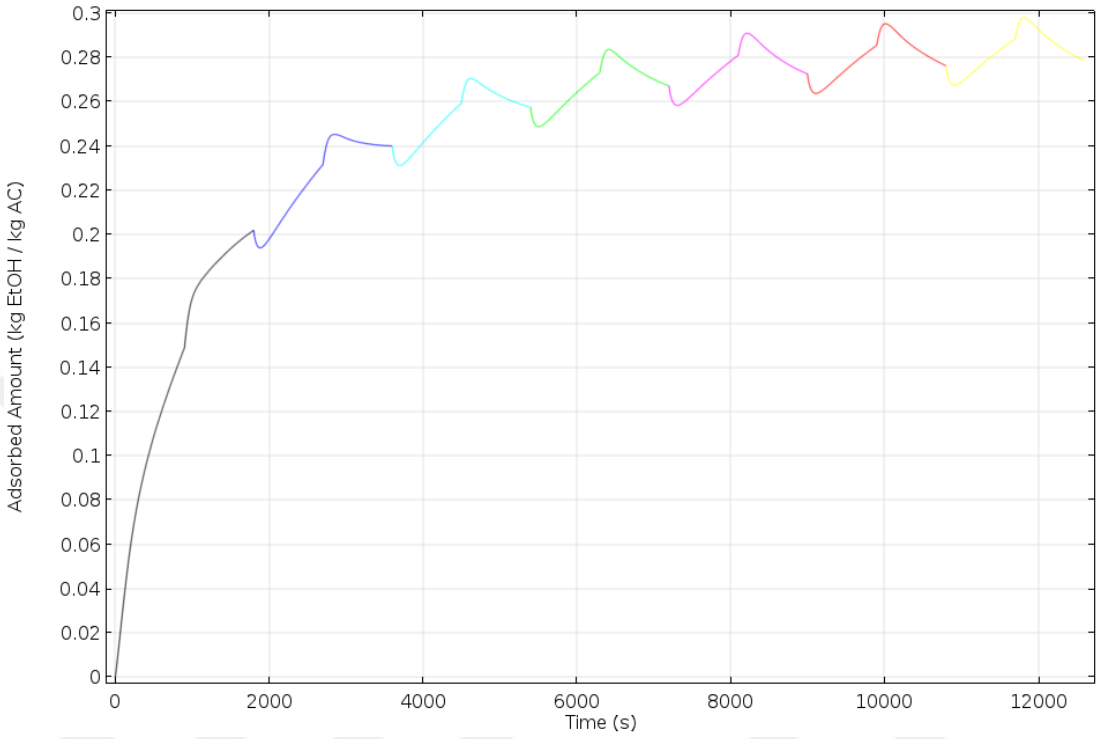

Figure 58. Total adsorbed amount of ethanol(kg/kg) with respect to time for Config. 3. Each color represents a cycle.

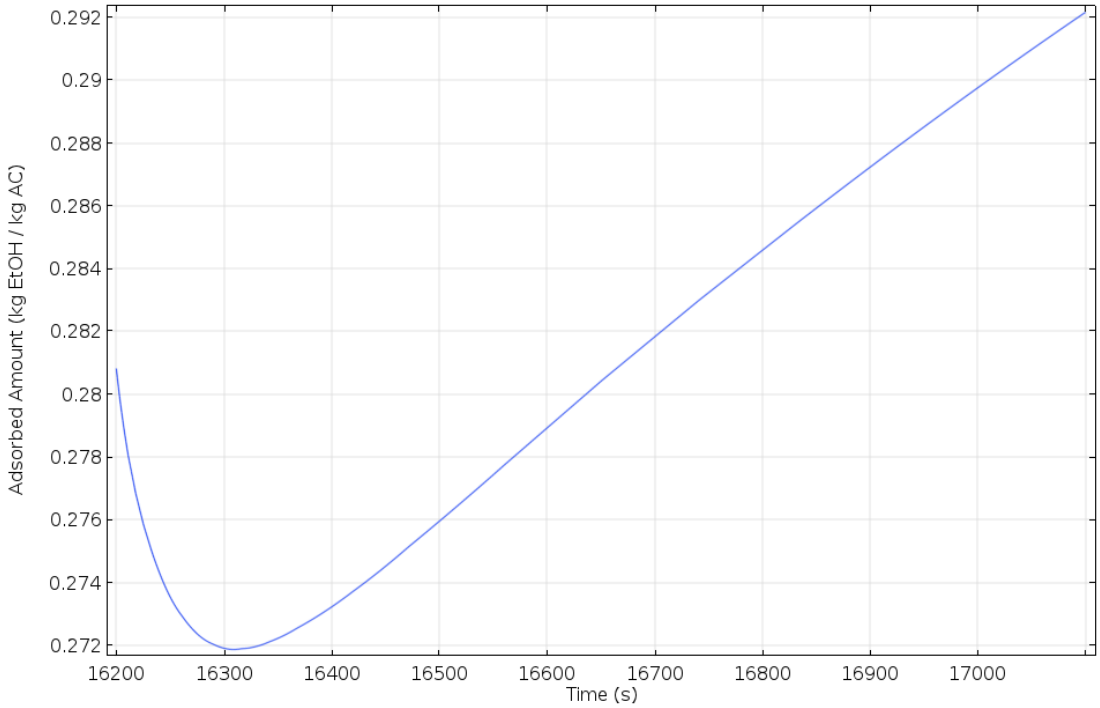

Figure 59. Total adsorbed amount of ethanol(kg/kg) with respect to time in adsorption stage of the last cycle.

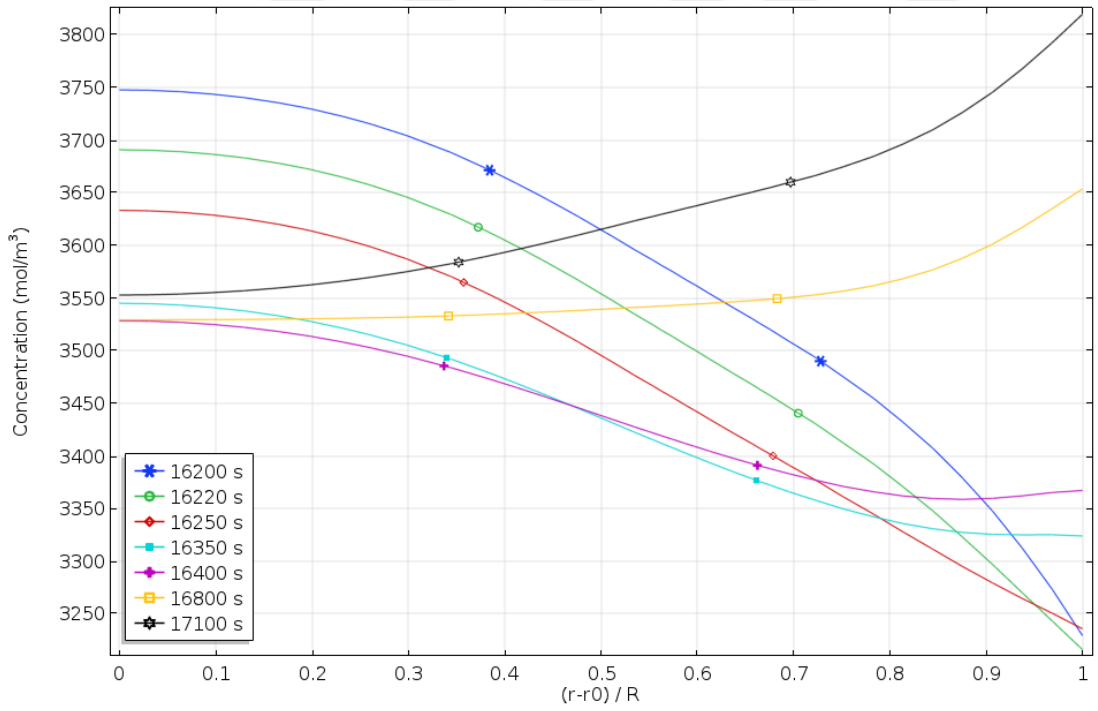

Figure 60. Concentration profile of Config. 3. in adsorption stage with respect to radial position in the reactor bed and time.

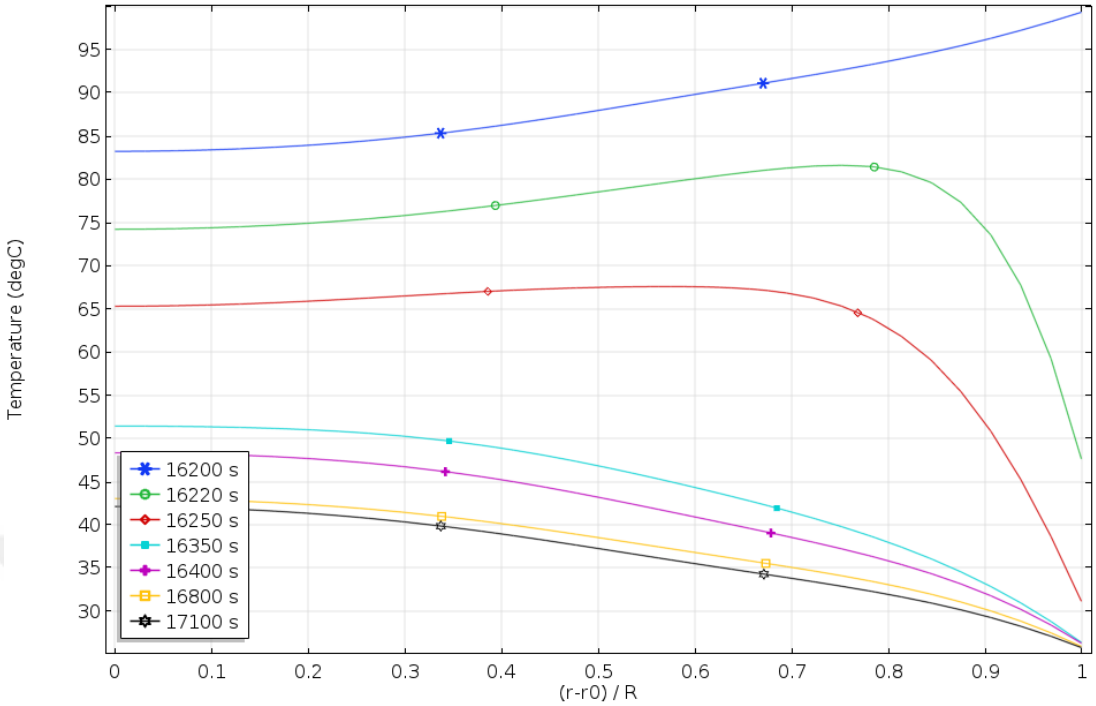

Figure 61. Temperature profile of Config. 2. in adsorption stage with respect to radial position in the reactor bed and time.

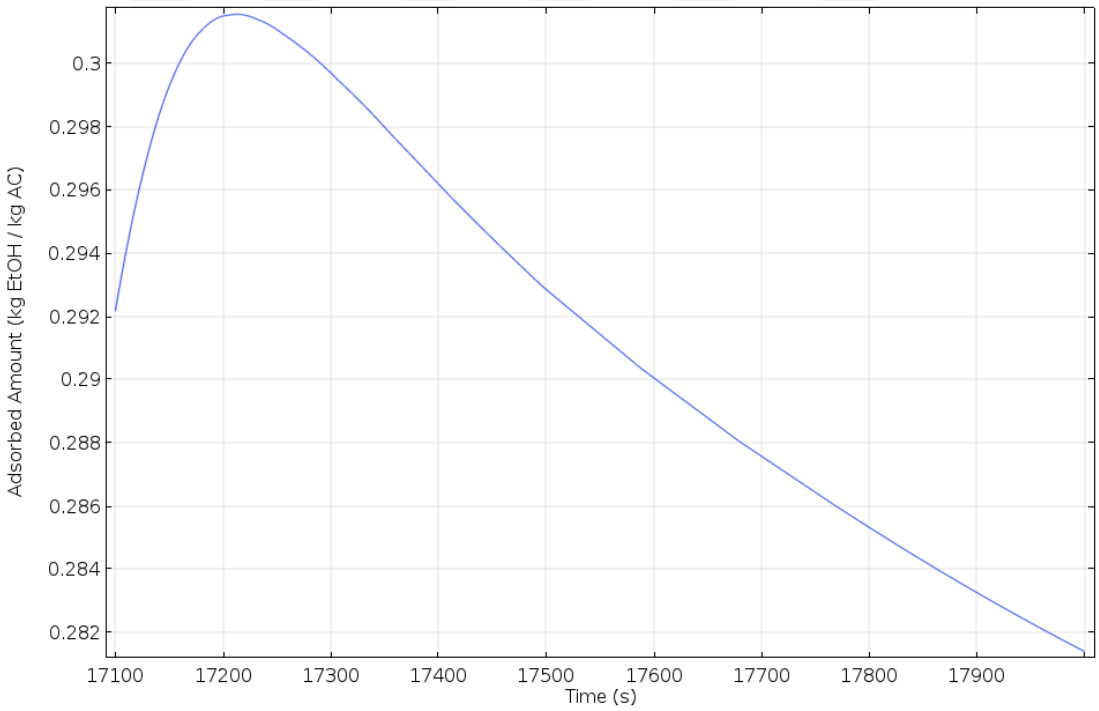

Figure 62. Total adsorbed amount of ethanol(kg/kg) with respect to time in adsorption stage of the last cycle.

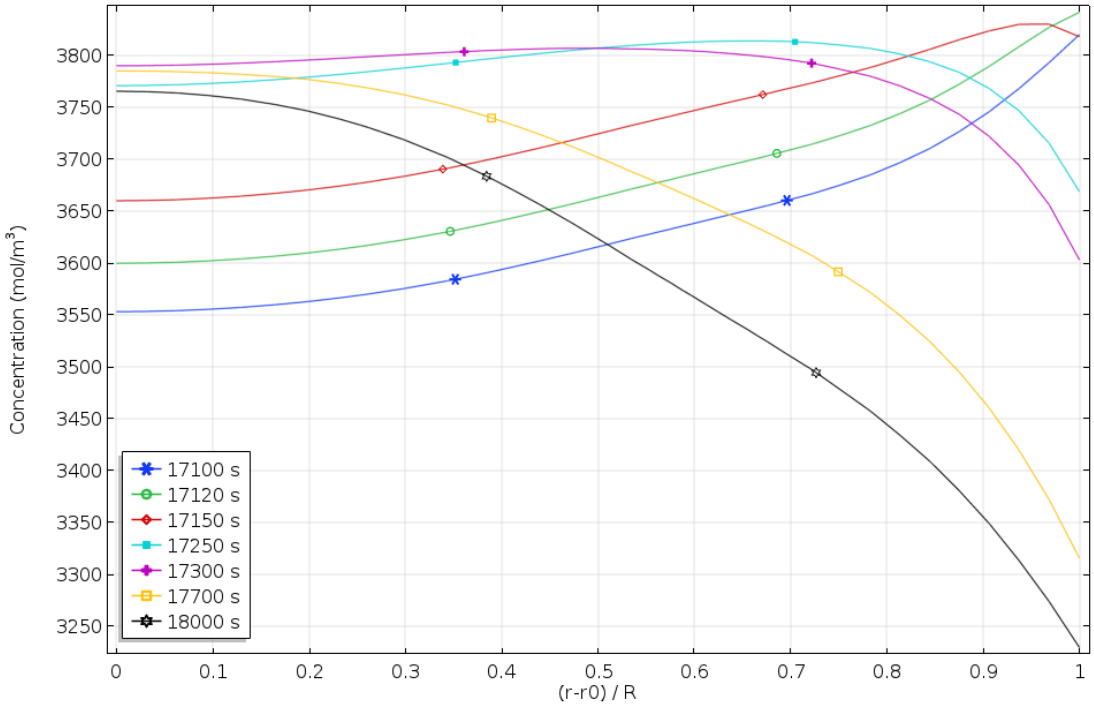

Figure 63. Concentration profile of Config. 3. in desorption stage with respect to radial position in the reactor bed and time.

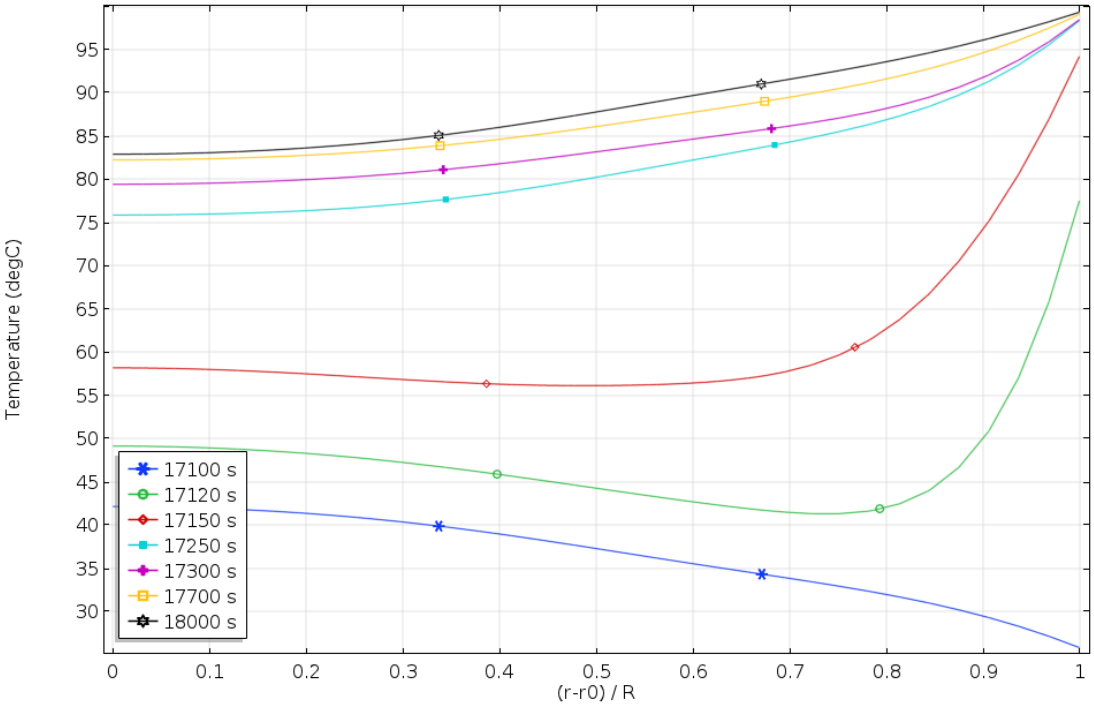

Figure 64. Temperature profile of Config. 3. in desorption stage with respect to radial position in the reactor bed and time.

B.A.C Config. 4

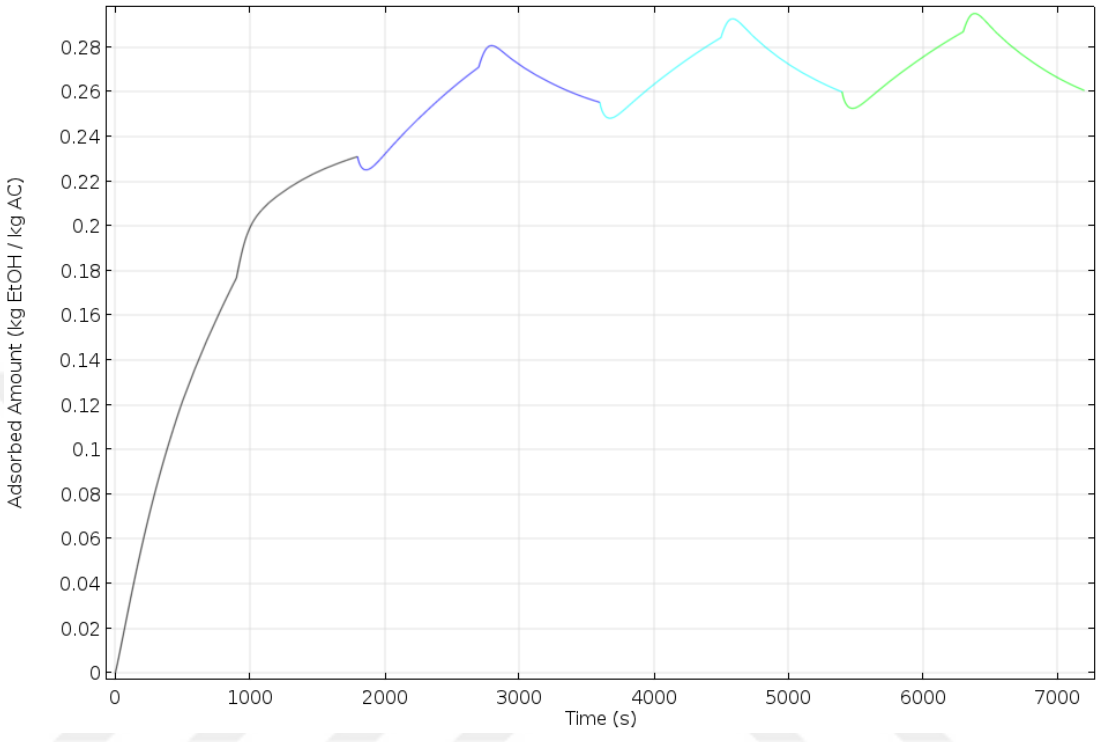

Figure 65. Total adsorbed amount of ethanol(kg/kg) with respect to time for Config. 4. Each color represents a cycle.

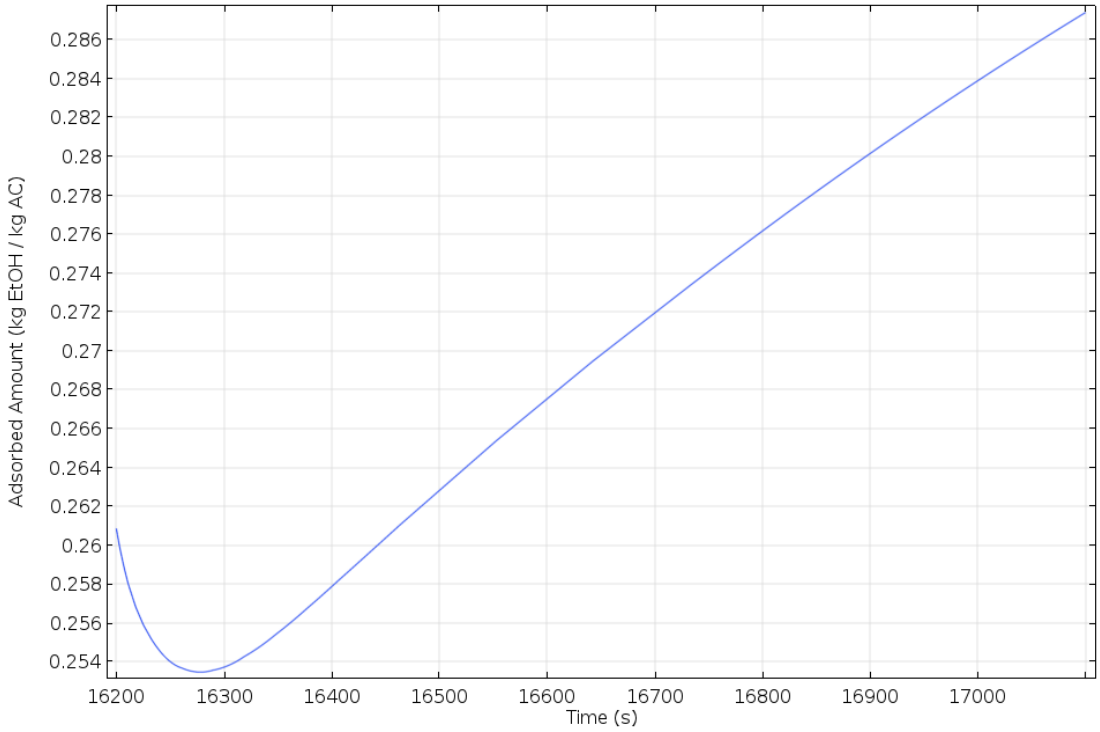

Figure 66. Total adsorbed amount of ethanol(kg/kg) with respect to time in adsorption stage of the last cycle.

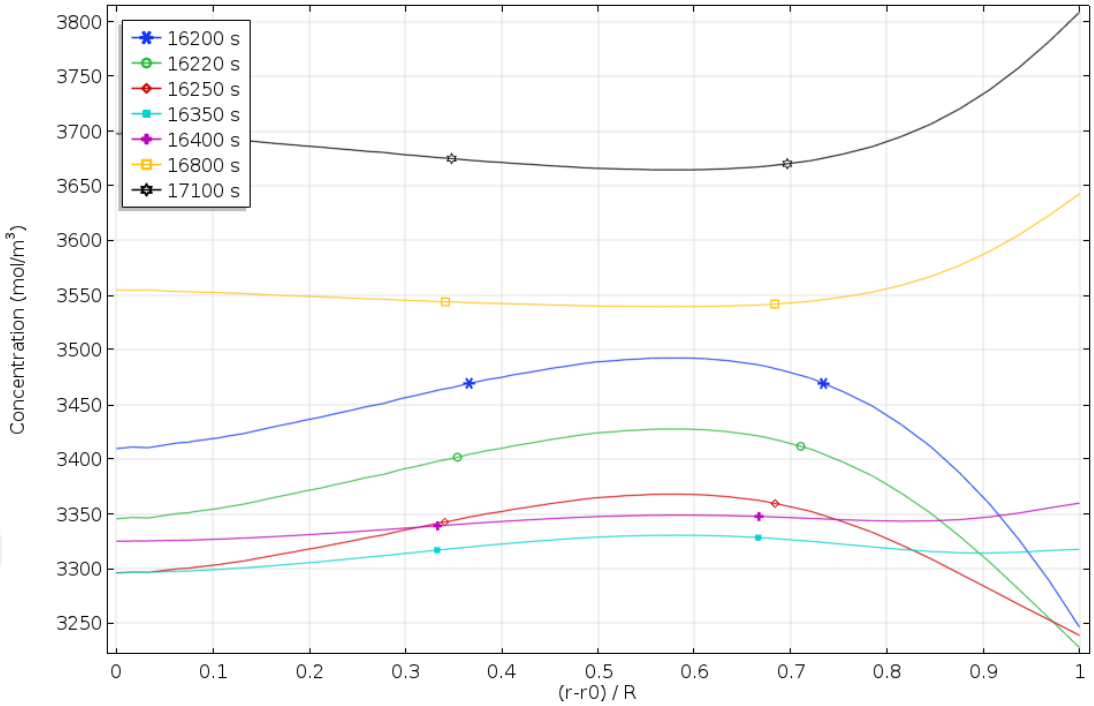

Figure 67. Concentration profile of Config. 4. in adsorption stage with respect to radial position in the reactor bed and time.

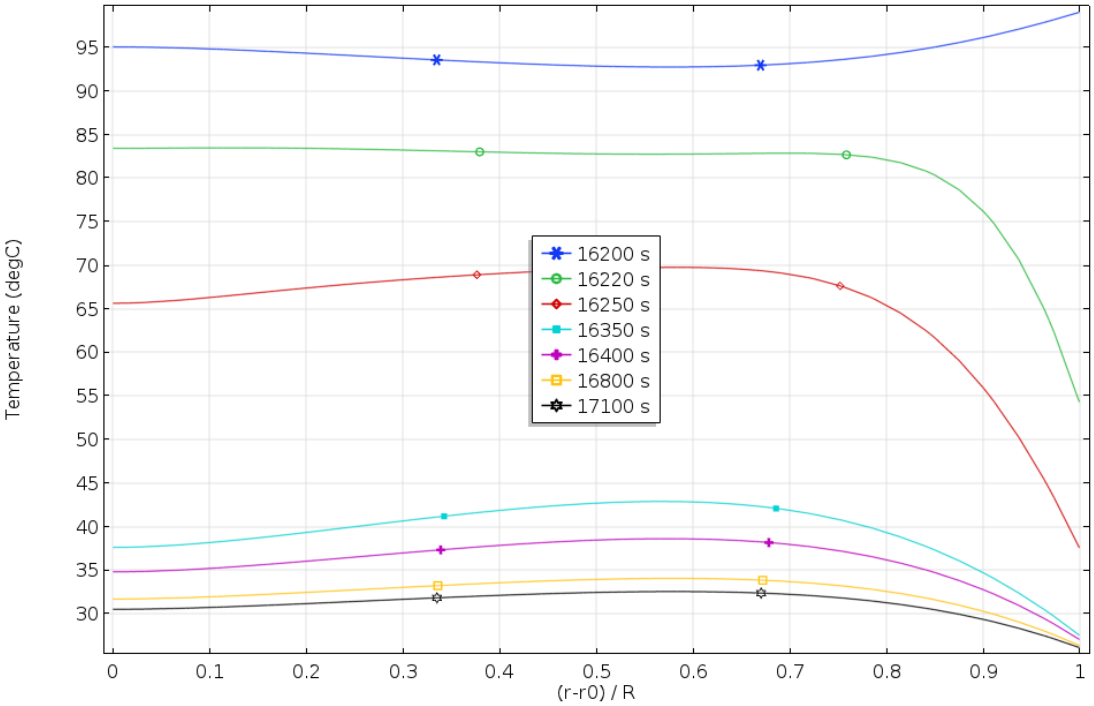

Figure 68. Temperature profile of Config. 4. in adsorption stage with respect to radial position in the reactor bed and time.

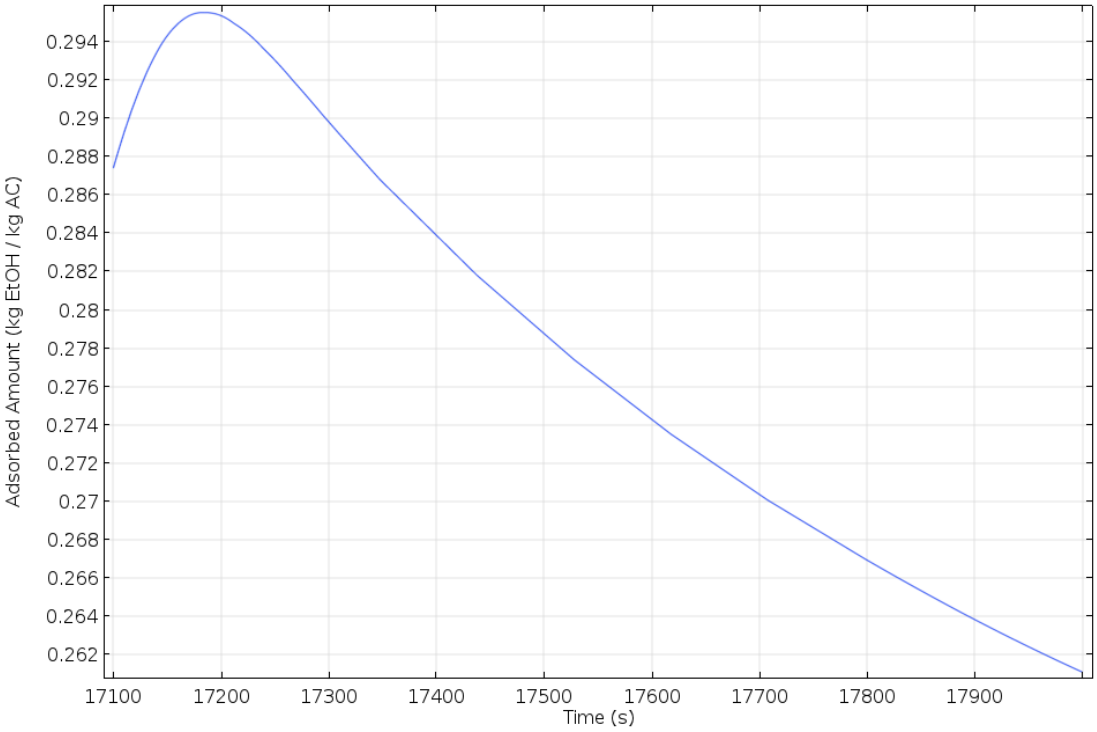

Figure 69. Total adsorbed amount of ethanol(kg/kg) with respect to time in desorption stage of the last cycle.

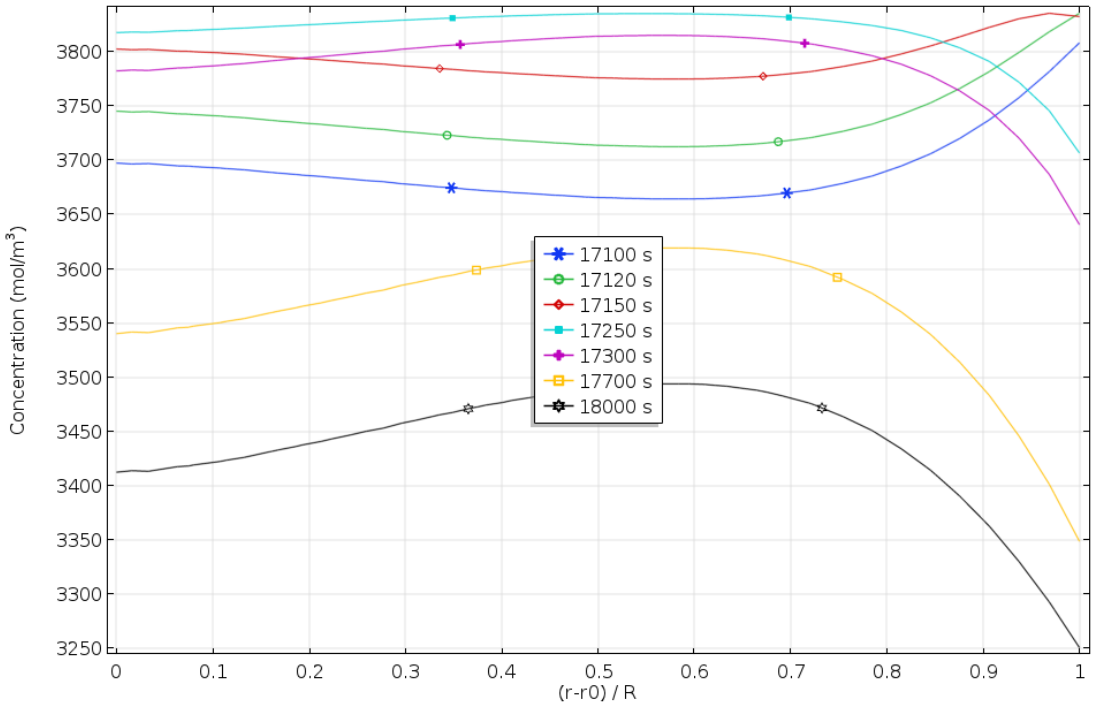

Figure 70. Concentration profile of Config. 4. in desorption stage with respect to radial position in the reactor bed and time.

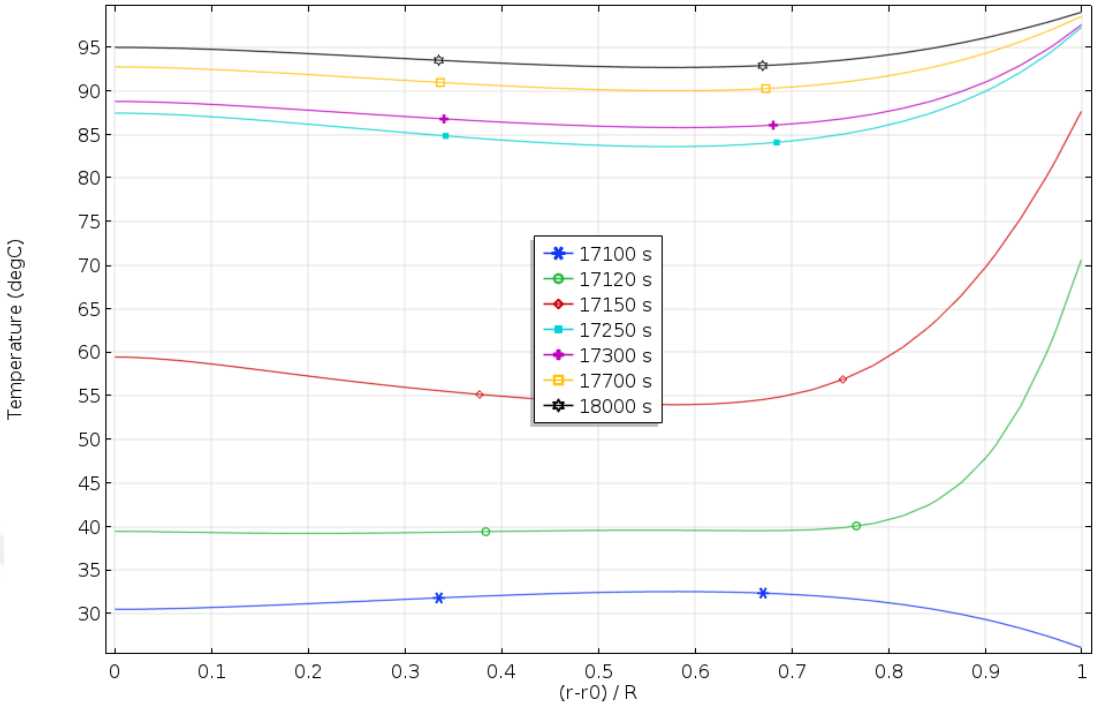

Figure 71. Temperature profile of Config. 4. in adsorption stage with respect to radial position in the reactor bed and time.

B.B 1200 Seconds of Cycle Operation Time

B.B.A Config. 2

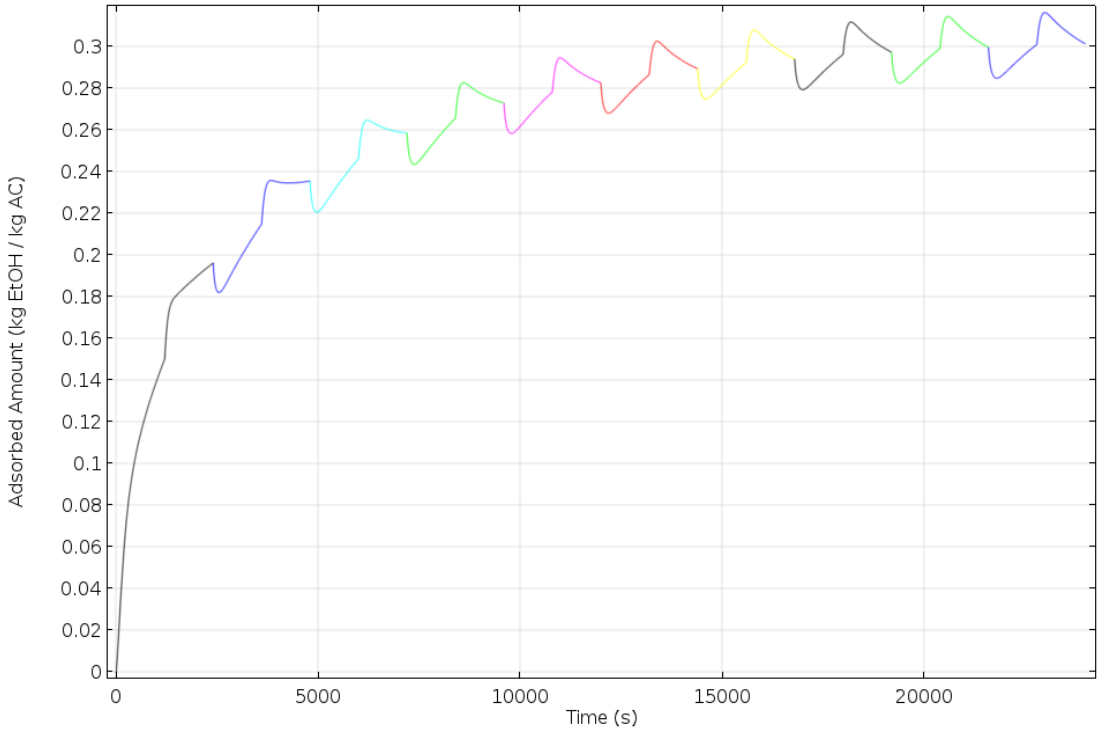

Figure 72. Total adsorbed amount of ethanol(kg/kg) with respect to time for Config. 2. Each color represents a cycle.

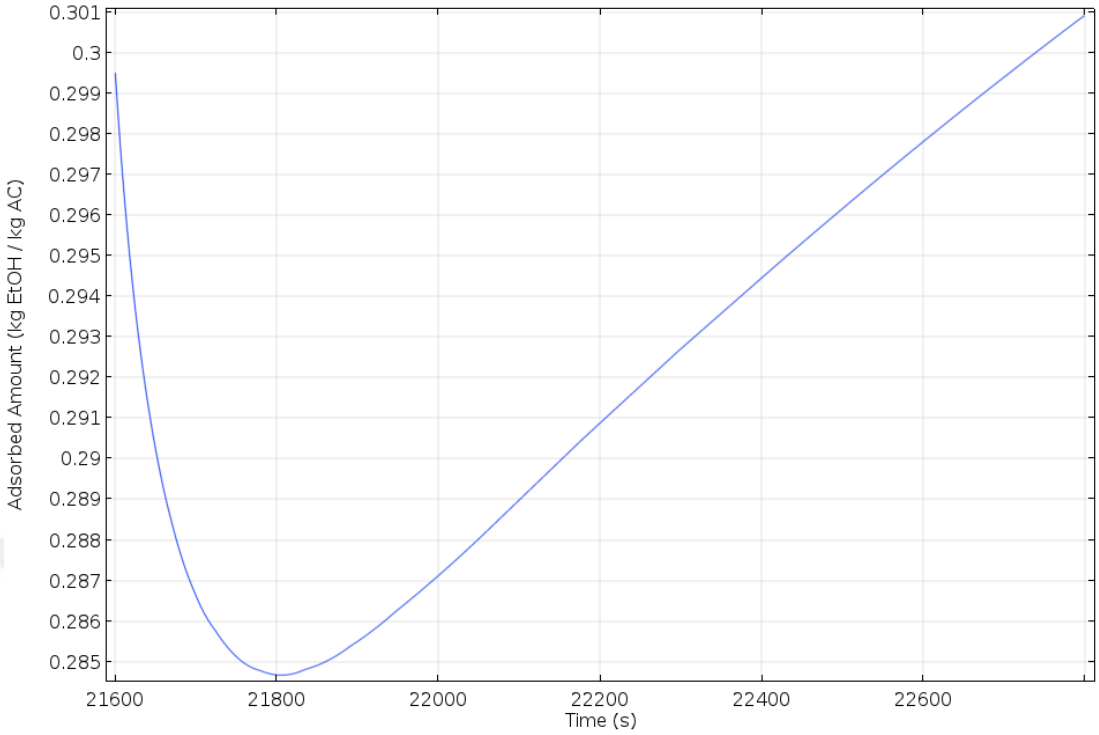

Figure 73. Total adsorbed amount of ethanol(kg/kg) with respect to time in adsorption stage of the last cycle.

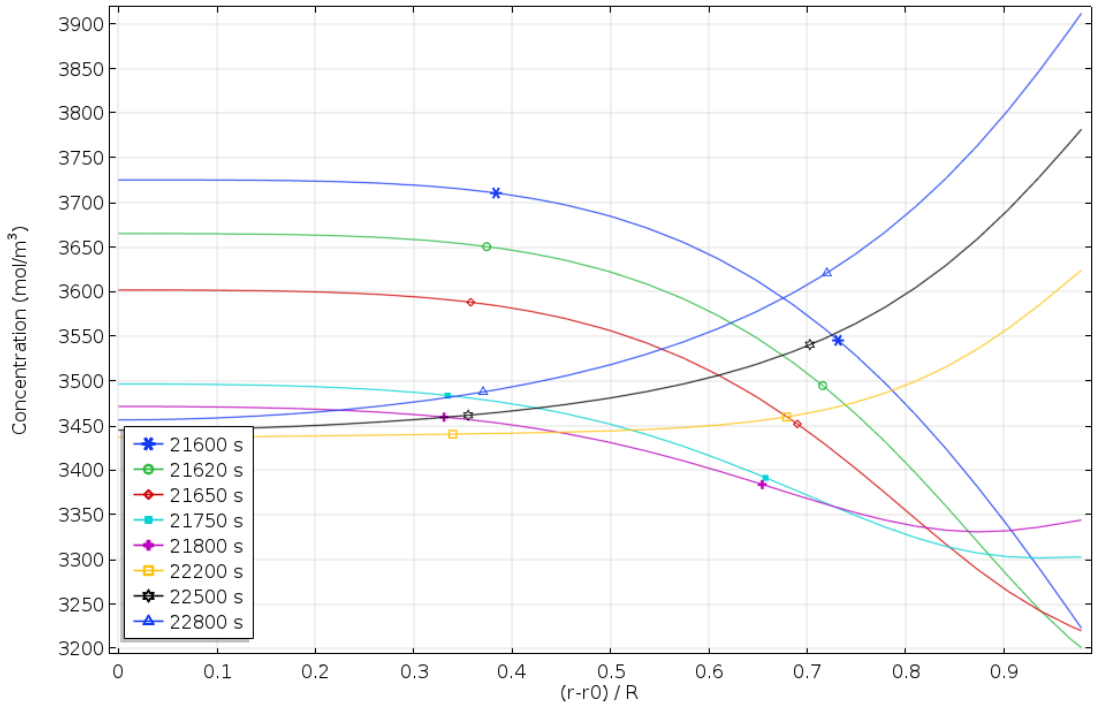

Figure 74. Concentration profile of Config. 2. in adsorption stage with respect to radial position in the reactor bed and time.

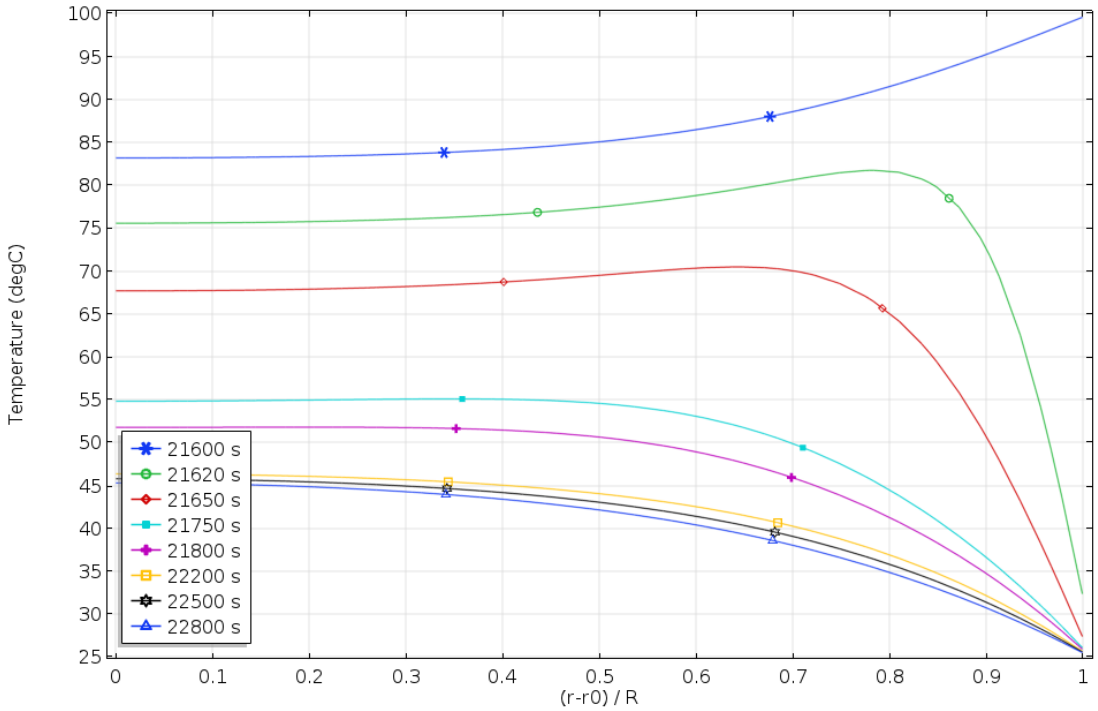

Figure 75. Temperature profile of Config. 2. in adsorption stage with respect to radial position in the reactor bed and time.

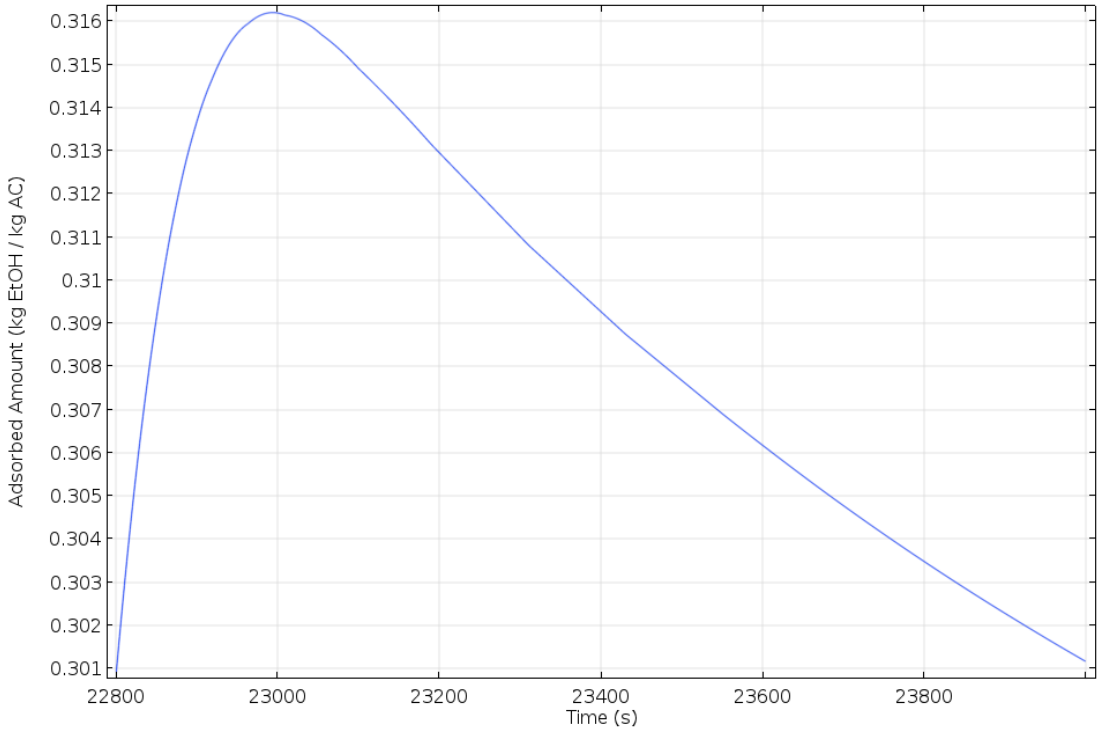

Figure 76. Total adsorbed amount of ethanol(kg/kg) with respect to time in adsorption stage of the last cycle.

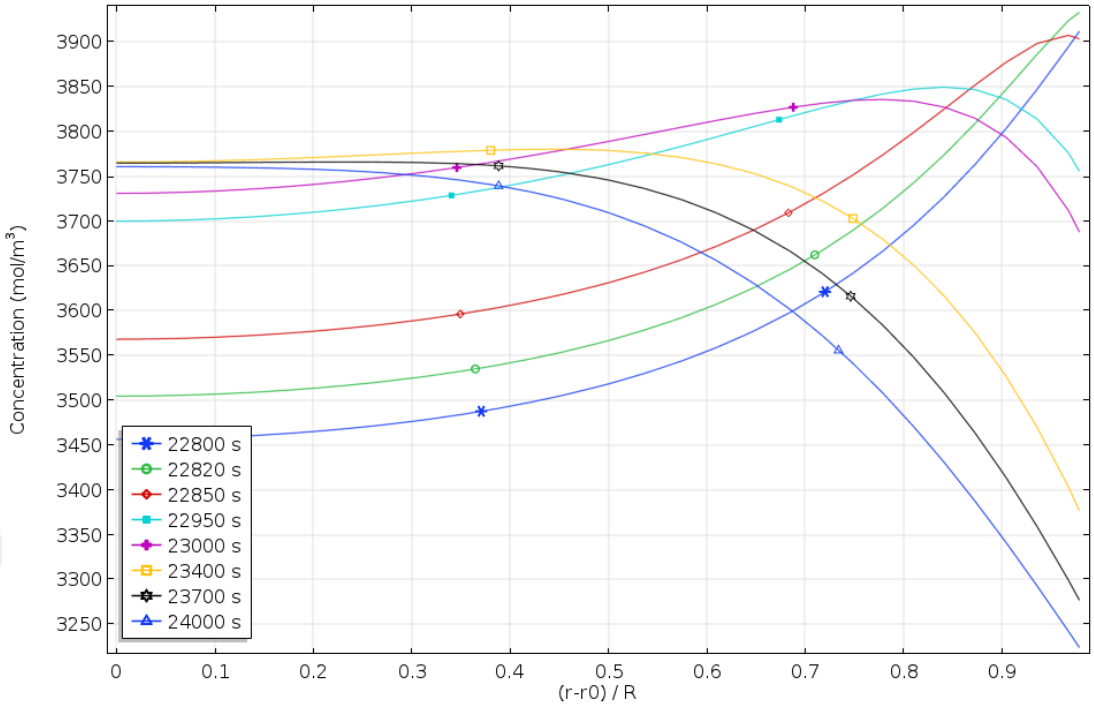

Figure 77. Concentration profile of Config. 2. in desorption stage with respect to radial position in the reactor bed and time.

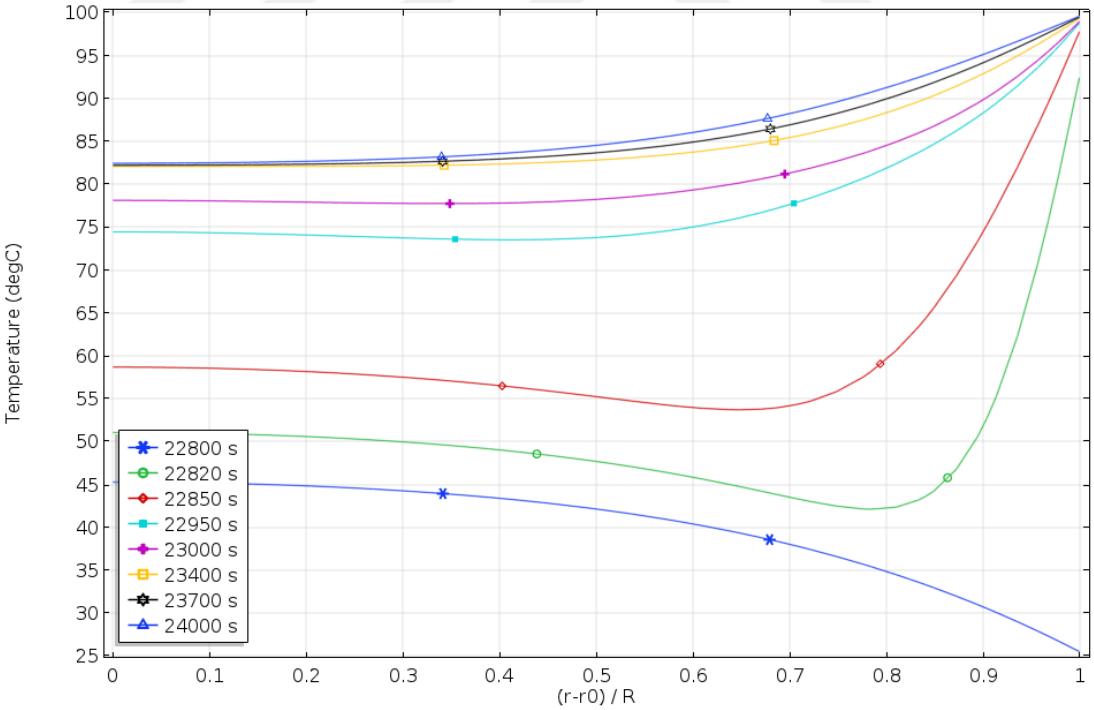

Figure 78. Temperature profile of Config. 2. in desorption stage with respect to radial position in the reactor bed and time.

B.B.B Config. 3

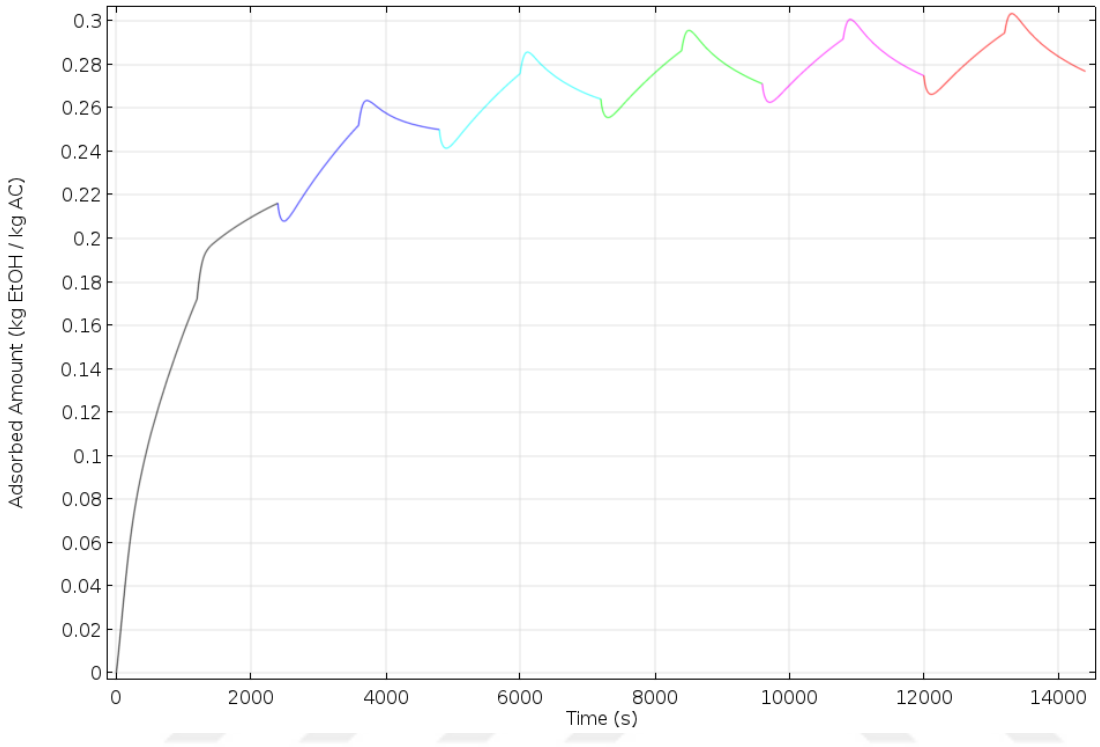

Figure 79. Total adsorbed amount of ethanol(kg/kg) with respect to time for Config. 3. Each color represents a cycle.

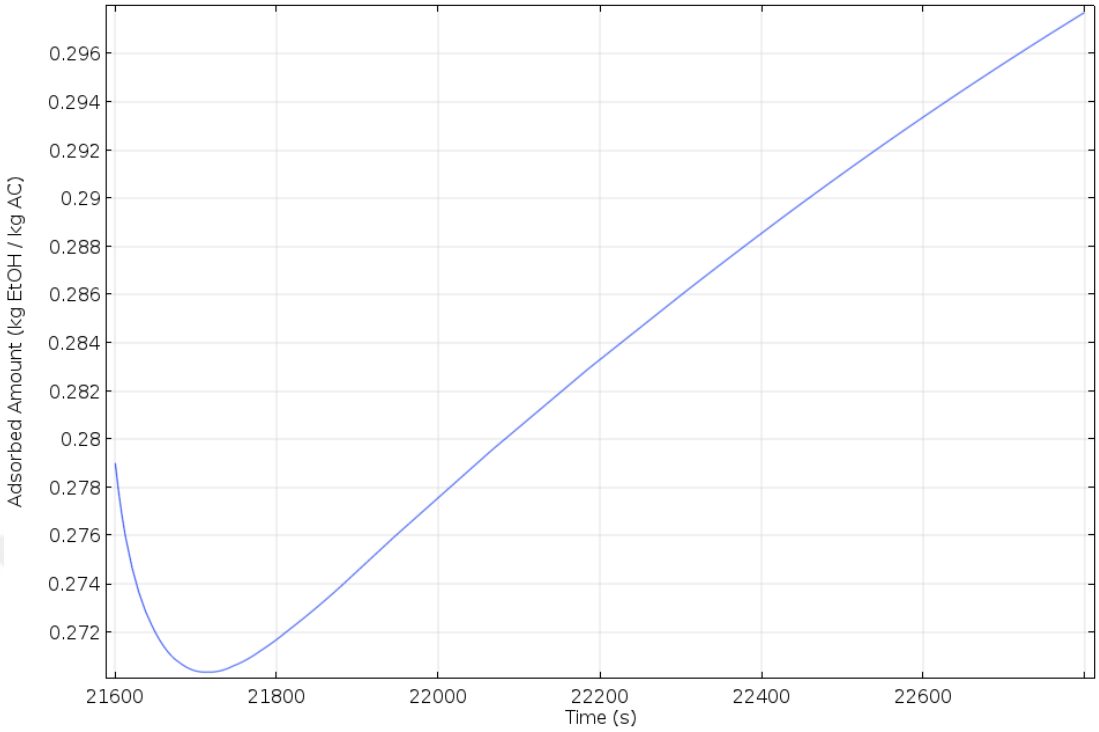

Figure 80. Total adsorbed amount of ethanol(kg/kg) with respect to time in adsorption stage of the last cycle.

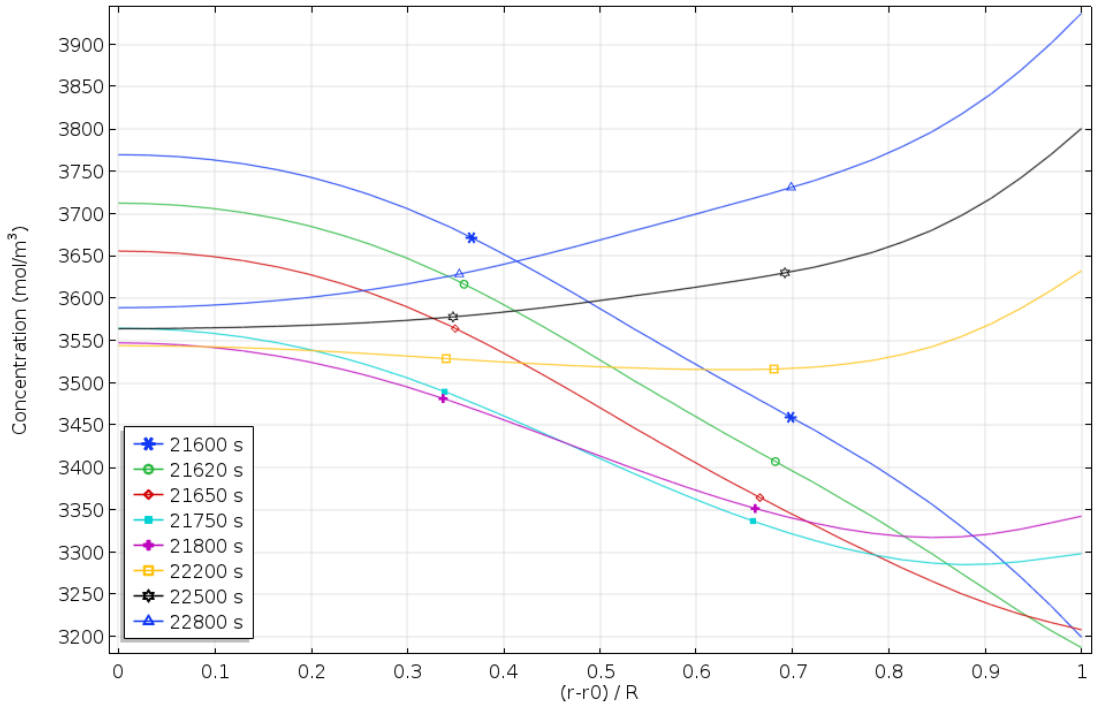

Figure 81. Concentration profile of Config. 3. in adsorption stage with respect to radial position in the reactor bed and time.

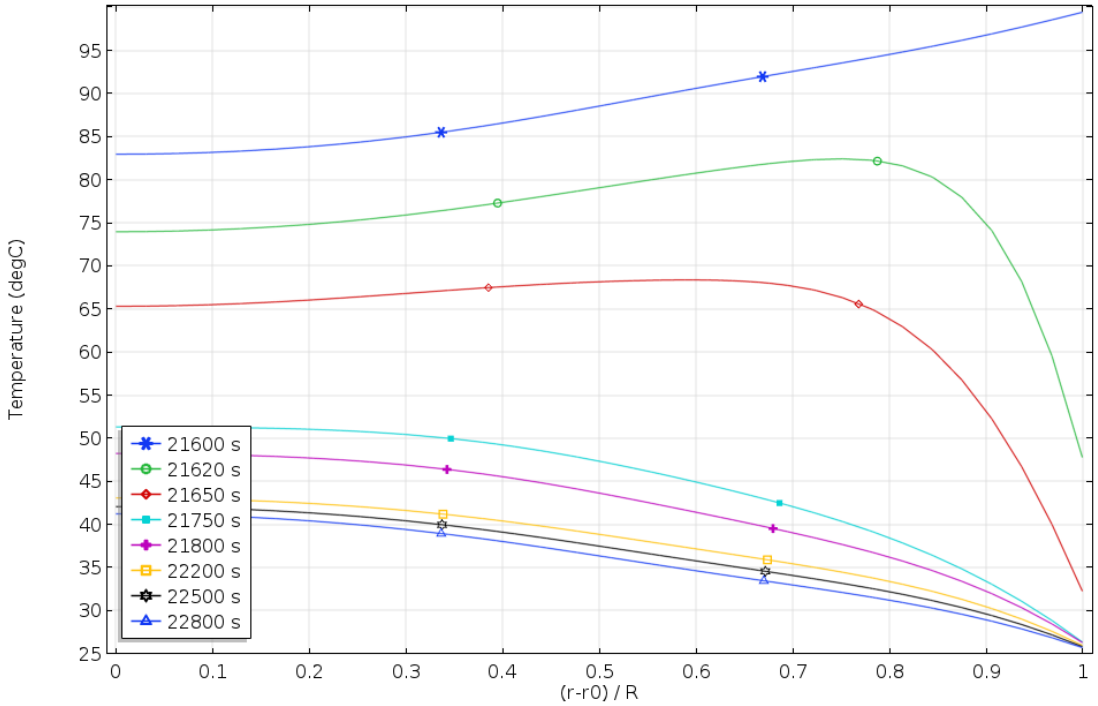

Figure 82. Temperature profile of Config. 3. in adsorption stage with respect to radial position in the reactor bed and time.

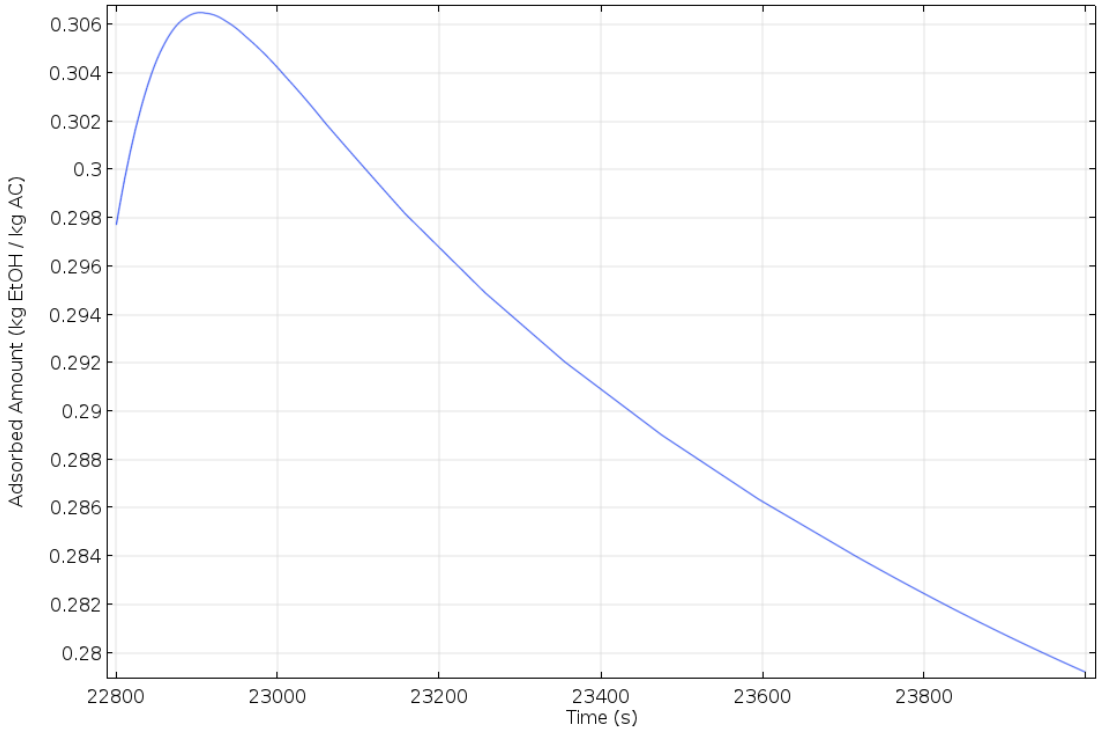

Figure 83. Total adsorbed amount of ethanol(kg/kg) with respect to time in desorption stage of the last cycle.

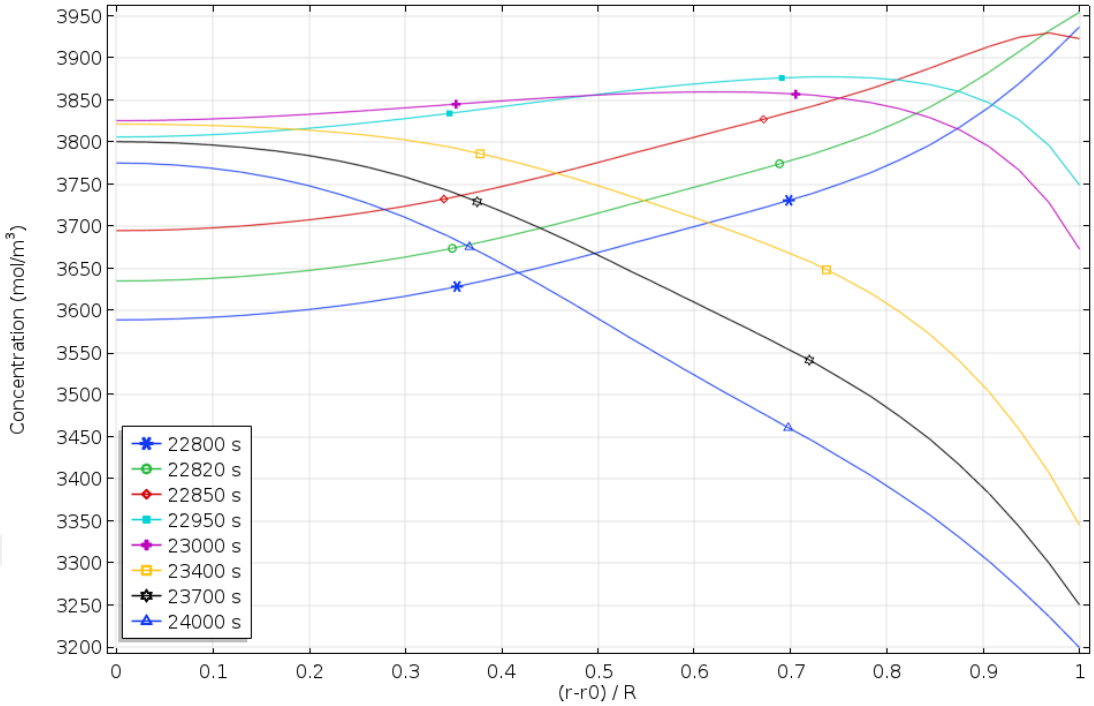

Figure 84. Concentration profile of Config. 3. in desorption stage with respect to radial position in the reactor bed and time.

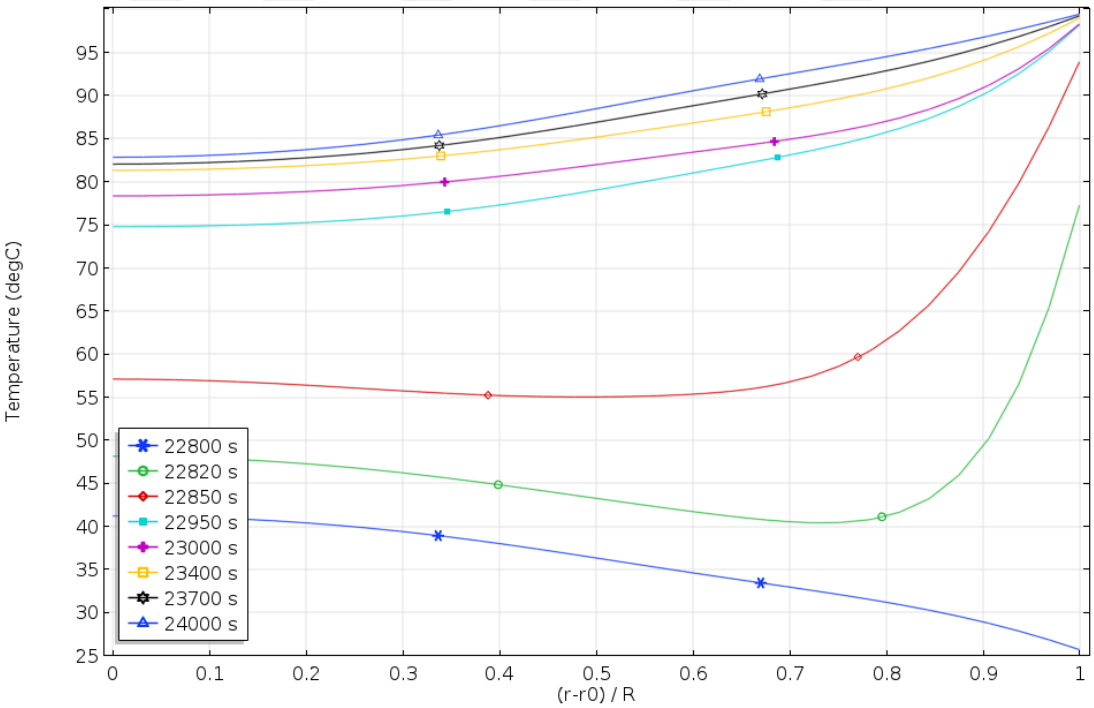

Figure 85. Temperature profile of Config. 3. in adsorption stage with respect to radial position in the reactor bed and time.

B.B.C Config. 4

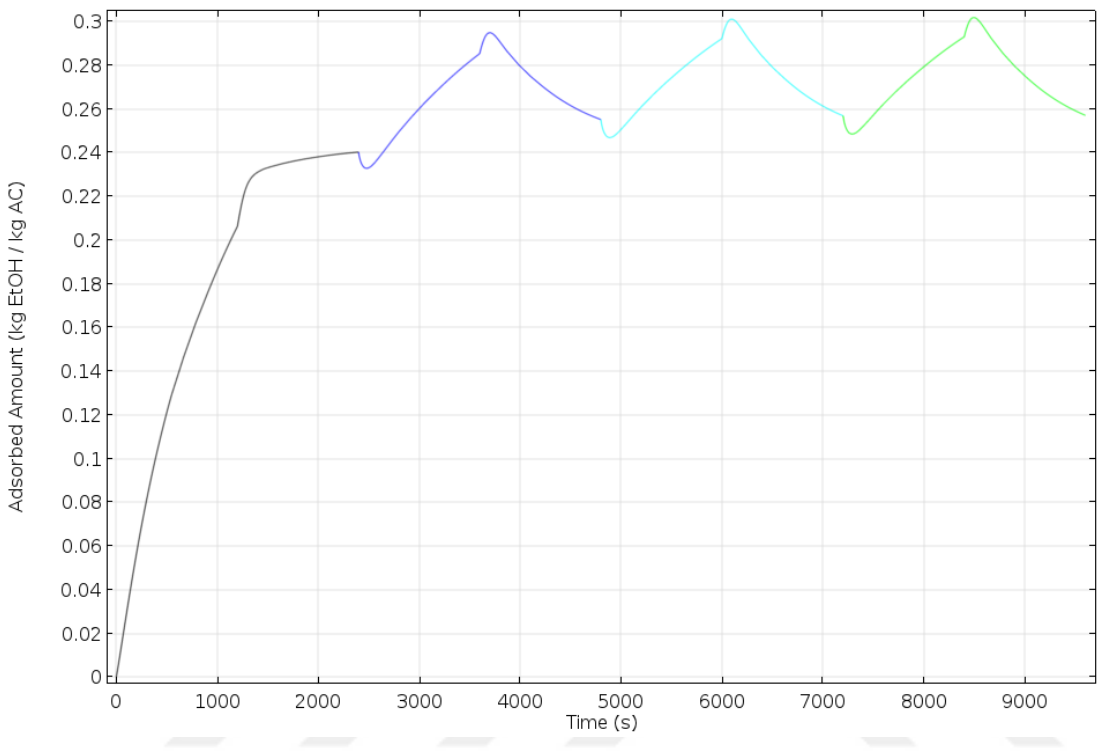

Figure 86. Total adsorbed amount of ethanol(kg/kg) with respect to time for Config. 4. Each color represents a cycle.

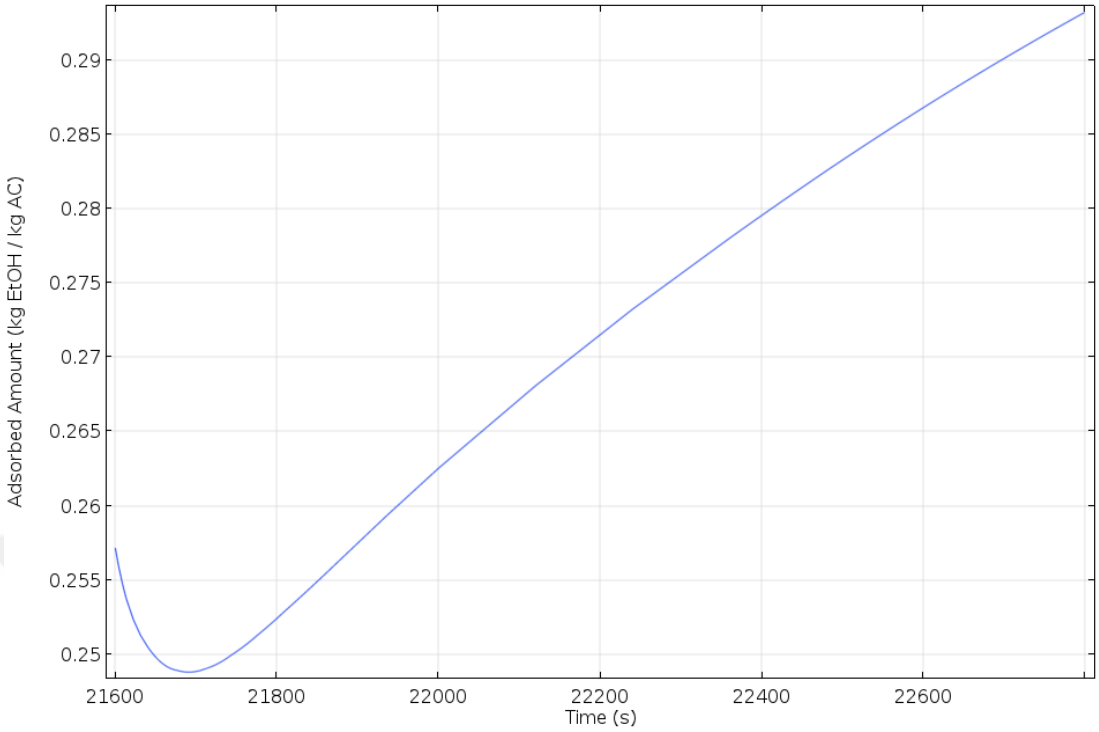

Figure 87. Total adsorbed amount of ethanol(kg/kg) with respect to time in adsorption stage of the last cycle.

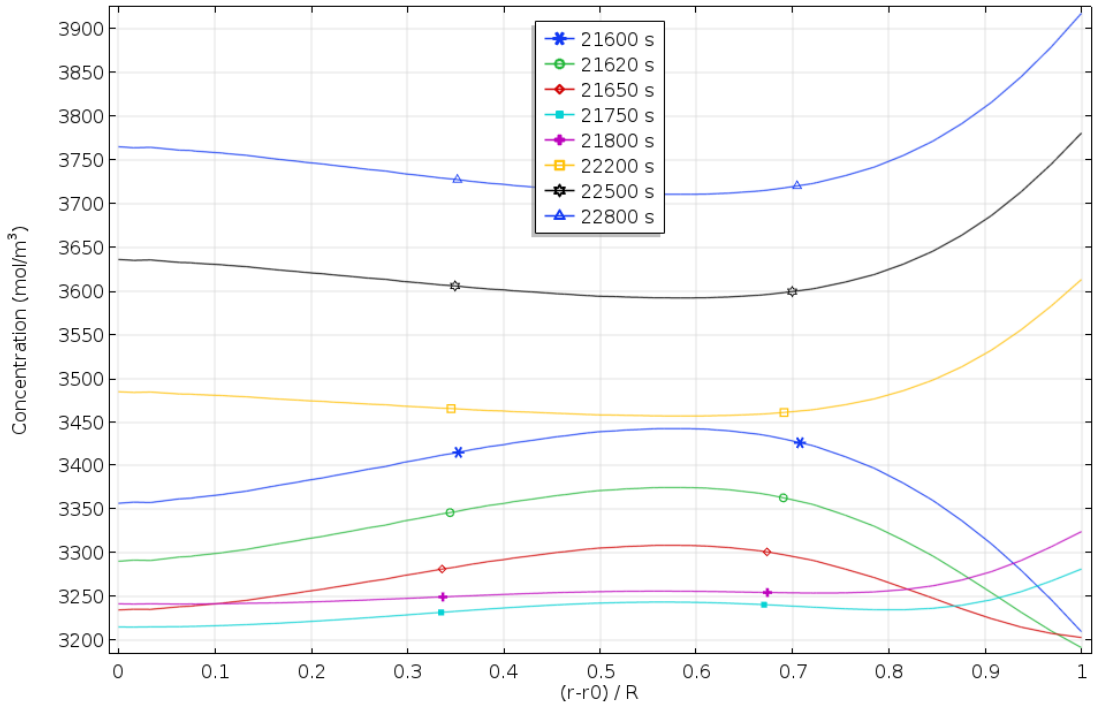

Figure 88. Concentration profile of Config. 4. in adsorption stage with respect to radial position in the reactor bed and time.

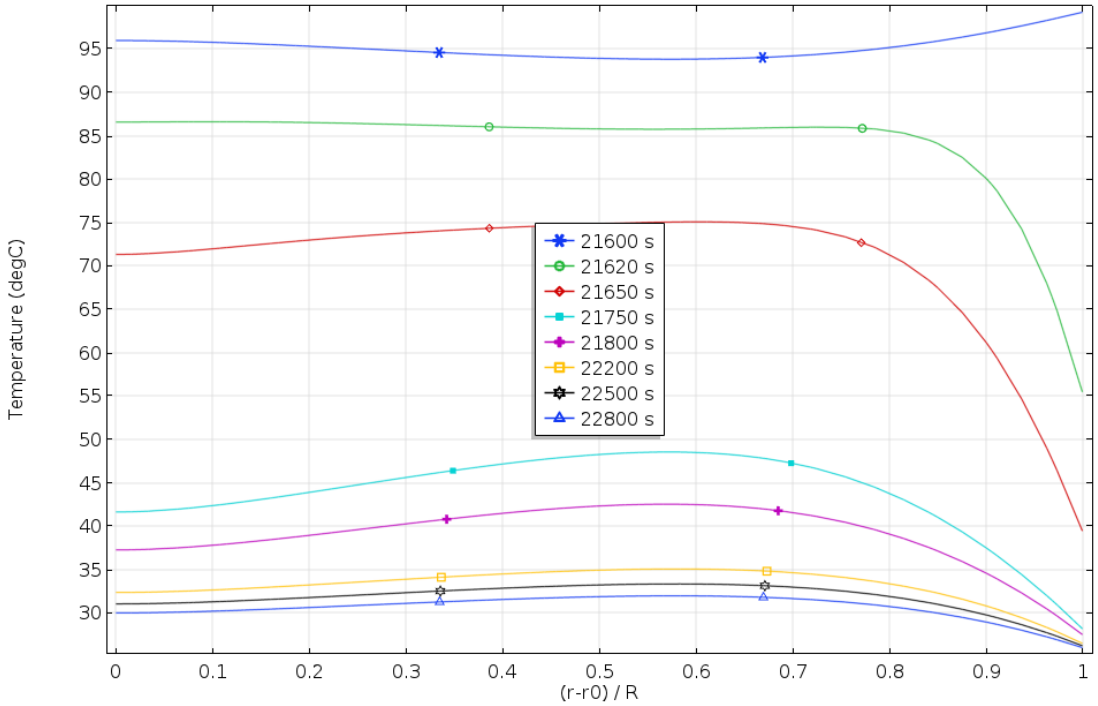

Figure 89. Temperature profile of Config. 4. in adsorption stage with respect to radial position in the reactor bed and time.

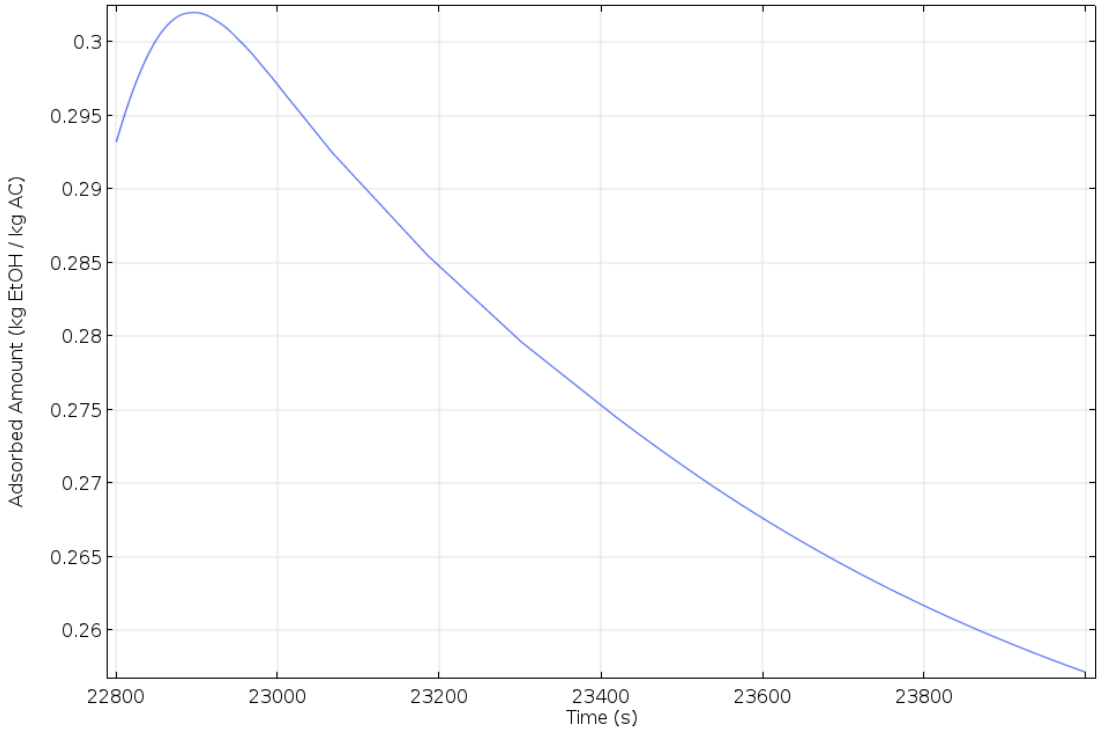

Figure 90. Total adsorbed amount of ethanol(kg/kg) with respect to time in desorption stage of the last cycle.

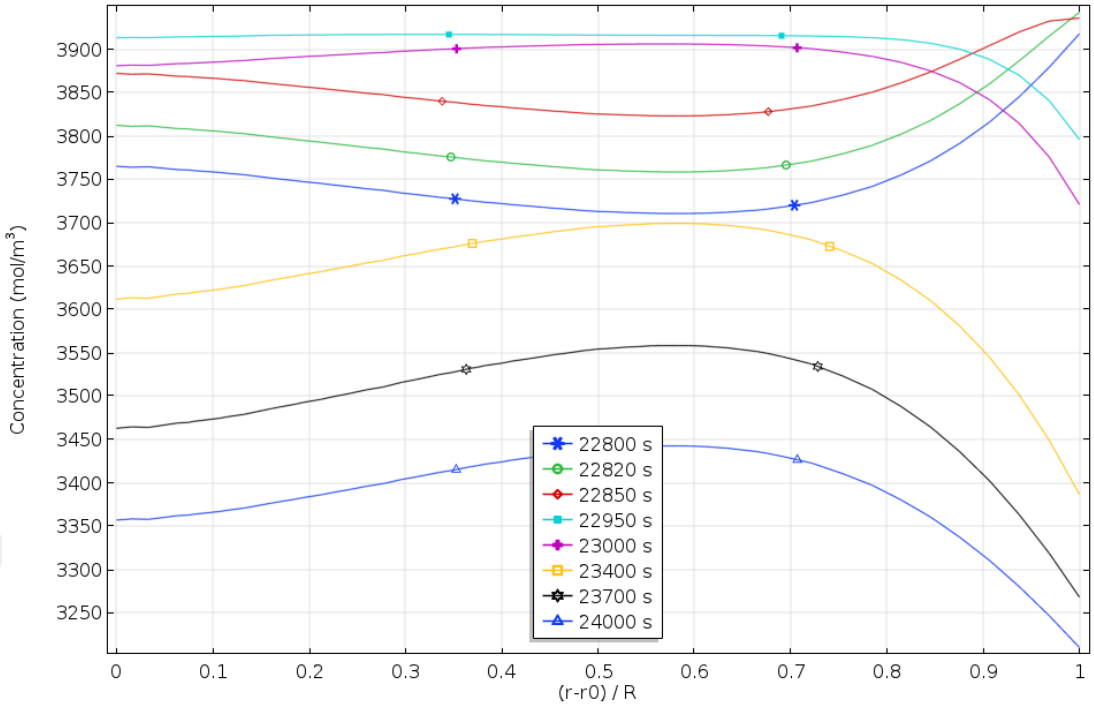

Figure 91. Concentration profile of Config. 4. in desorption stage with respect to radial position in the reactor bed and time.

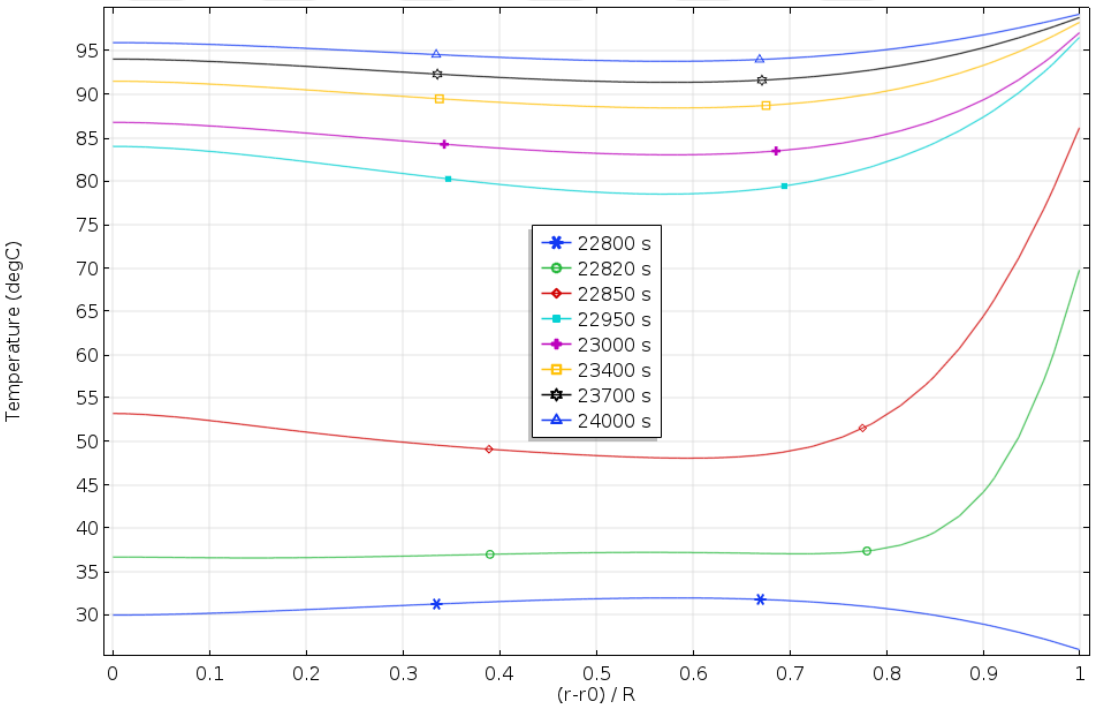

Figure 92. Temperature profile of Config. 4. in desorption stage with respect to radial position in the reactor bed and time